

UC Office of the President

Recent Work

Title

STELLAR WEAK INTERACTION RATES FOR INTERMEDIATE MASS NUCLEI .3. RATE TABLES FOR THE FREE NUCLEONS AND NUCLEI WITH $A = 21$ TO $A = 60$

Permalink

<https://escholarship.org/uc/item/8b214033>

Journal

ASTROPHYSICAL JOURNAL SUPPLEMENT SERIES, 48(3)

ISSN

0067-0049

Authors

FULLER, GM
FOWLER, WA
NEWMAN, MJ

Publication Date

1982

DOI

10.1086/190779

Peer reviewed

STELLAR WEAK INTERACTION RATES¹ FOR INTERMEDIATE MASS NUCLEI. III. RATE TABLES FOR THE FREE NUCLEONS AND NUCLEI WITH $A = 21$ TO $A = 60$

GEORGE M. FULLER² AND WILLIAM A. FOWLER

W. K. Kellogg Radiation Laboratory, California Institute of Technology

AND

MICHAEL J. NEWMAN

Applied Theoretical Physics Division, Los Alamos National Laboratory, University of California, Los Alamos

Received 1981 June 12; accepted 1981 August 24

ABSTRACT

Stellar electron and positron emission rates and continuum electron and positron capture rates, as well as the associated neutrino energy loss rates, are tabulated for the free nucleons and 226 nuclei with masses between $A = 21$ and 60. These rates were calculated in accordance with the procedure described in Papers I and II of this series and are presented here in tabular form on an abbreviated temperature and density grid. Results of these calculations on a detailed temperature and density grid are available in computer readable form on magnetic tape upon request to MJN. The stellar weak rate calculation procedure is reviewed, and the results are discussed. Comparison of the stellar weak rates to terrestrial decay rates are made where possible.

Subject headings: equation of state — neutrinos — nuclear reactions — stars: collapsed — stars: interiors — stars: supernovae

I. INTRODUCTION

In this work, electron and positron emission rates in stars, continuum electron and positron capture rates in stars, and the associated neutrino energy loss rates are tabulated for free protons and neutrons as well as 226 nuclei with masses between $A = 21$ and 60. The rate computations were performed following the procedures discussed in Papers I and II of this series (Fuller, Fowler, and Newman 1980, hereafter F²NI; Fuller, Fowler, and Newman 1982, hereafter F²NII). The previous papers are concerned with the details of stellar weak rate calculations and the nuclear physics of the Gamow-Teller strength distribution.

The purpose of this paper is to discuss the results of the stellar rate computations in comparison with other work and with known terrestrial decay rates and provide ready access to printed rates for active investigations in the fields of stellar evolution and nucleosynthesis. The rates presented here in tabular form are reproduced, by necessity, on an abbreviated temperature and density grid which will allow a fair estimate of stellar rates to be made for most astrophysical environments. Where more accurate stellar rates are required, as in stellar evolution and nucleosynthesis calculations, the reader is urged to

write to MJN and request the stellar rate magnetic tape. This tape presents the computation results on a far more detailed temperature and density grid in a computer readable form suitable for interpolation in temperature and density.

The temperature and density grid employed in these calculations covers conditions ranging from the relatively mild environments characteristic of hydrostatic carbon and oxygen burning through the more extreme conditions characteristic of silicon burning and the onset of core collapse. The temperatures cover the range $0.01 \leq T_9 \leq 100$. ($0.862 \text{ keV} \leq kT \leq 8.617 \text{ MeV}$), while the densities cover the range $10 \leq \rho/\mu_e \text{ (g cm}^{-3}\text{)} \leq 10^{11}$; thus, the electron gas ranges from nondegenerate to degenerate conditions, with electron Fermi energies approaching 25 MeV for the highest densities.

The nuclear weak rates computed here are important in determining the neutronization and neutrino energy loss rates during stellar evolution and collapse (Weaver and Woosley 1981; Arnett and Thielemann 1982). The outcome of stellar core collapse and bounce calculations depends on the previous neutronization history of the star and on electron capture during the collapse phase (Van Riper and Lattimer 1981; Baym, Bethe, and Brown 1981). Ultimately, the nuclear weak rates presented here will be important in determinations of the nucleosynthesis yields of the elements and their isotopes, both during hydrostatic burning regimes and the subsequent collapse and explosive burning phases.

¹Supported in part by the National Science Foundation (PHY79-23638) at California Institute of Technology and in part by the US Department of Energy.

²Fannie and John Hertz Foundation Fellow.

The nuclei whose stellar weak rates are computed here range in mass from $A = 21$ up to $A = 60$. These include many nuclei of astrophysical interest in the stellar conditions discussed above. Subsequent work will extend the rate survey presented here to include neutron-rich nuclei in the $A = 60$ to $A = 75$ mass range for use in the supernova problem. Concomitant with this extension in mass range will come an extension in the density range to include $\rho/\mu_e = 10^{12} \text{ g cm}^{-3}$. Of interest in the r -process and s -process are the weak transition rates of heavy neutron-rich nuclei at temperatures and densities which are relatively low compared to those encountered in the late stages of stellar evolution discussed above. In these less extreme conditions unmeasured forbidden transitions and bound state electron capture may be important. The reader is referred to Cosner and Truran (1981) for the most up-to-date treatment of the problem.

II. REVIEW OF STELLAR RATE COMPUTATION PROCEDURE

The stellar rate computation problem is shown schematically in Figure 1 for $T^<$ and $T^>$ nuclei. The $T^< \rightleftharpoons T^>$ stellar transition rates must be computed. Some 20 discrete states are typically included in each nucleus for many of the cases considered here. The discrete state excitation energies, spins, and parities are taken from the experimental tabulations of Lederer *et al.* (1978) and Endt and van der Leun (1978) wherever possible. Isospin symmetry is used to obtain excitation energies, spins, and parities in unmeasured nuclei whose mirror nuclei are well studied. For very neutron-rich unmeasured nuclei, discrete state energies, spins, and parities are inferred from isotopes with similar shell structure. The discrete states in the $T^<$ ($T^>$) nucleus are denoted by $E^<$ ($E^>$) in Figure 1, while the resonant states are denoted by $R^<$ ($R^>$). The symbols also designate the energies of the discrete and resonant states.

The weak transition rate from the i th state of the parent to the j th state of the daughter nucleus is given by

$$\lambda_{ij} = \ln 2 \frac{f_{ij}(T, \rho, U_F)}{(ft)_{ij}}, \quad (1)$$

where $(ft)_{ij}$ is the comparative half-life, which is related to the allowed weak interaction matrix elements by equations (I-2a) and (I-2b) (I and II denote equations in Papers I and II of this series, respectively). The $f_{ij}(T, \rho, U_F)$ are the phase space factors for either electron or positron emission (eq. [I-3a]), continuum electron or positron capture (eq. [I-3b]), or the associated neutrino energy loss rates for these processes (eqs. [I-6a] and [I-6b]).

In principle, weak transition matrix elements are required between all $E^<$ and $E^>$ discrete states. Experi-

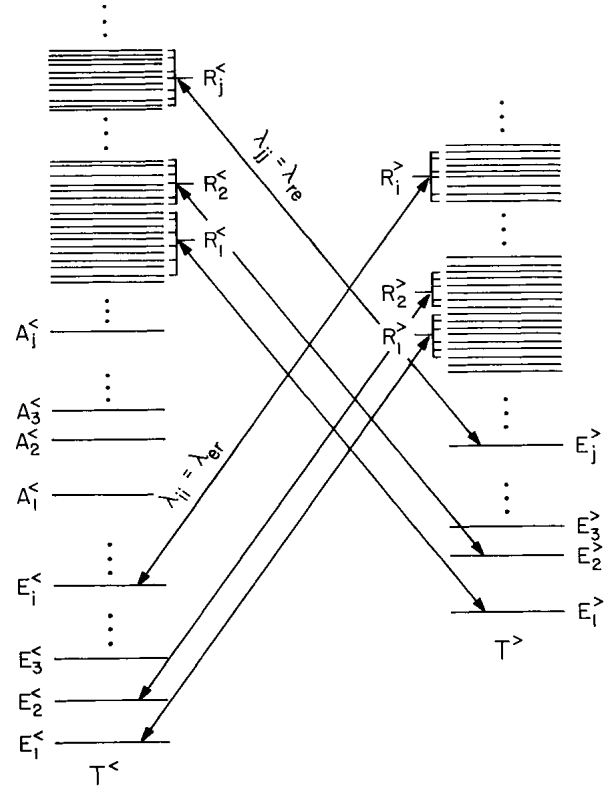


FIG. 1.—A schematic representation of a typical excited state problem is shown. $E_1^<, E_2^<, \dots, E_i^<$ are the discrete states of the $T^<$ nucleus. $E_1^>, E_2^>, \dots, E_j^>$ are the discrete states in the $T^>$ nucleus. $A_1^<, A_2^<, \dots, A_j^<$ are the analogs of $E_1^>, E_2^>, \dots, E_j^>$. Transitions from the discrete states of the $T^<$ nucleus to Gamow-Teller collective resonances ($R_1^>, R_2^>, \dots, R_j^>$) in the $T^>$ nucleus, and the reverse transitions, are shown with rates $\lambda_{ij} = \lambda_{er}$. Similarly, transitions from the discrete states of the $T^>$ nucleus to collective Gamow-Teller resonances in the $T^<$ nucleus ($R_1^<, R_2^<, \dots, R_j^<$), and the reverse transitions are shown with rates $\lambda_{jj} = \lambda_{er}$. For clarity the Fermi transitions λ_{jj}^F between $E_j^> \rightleftharpoons A_j^<$ are not illustrated.

mentally determined transition matrix elements are employed where known, whether or not they correspond to allowed transitions. Unmeasured Gamow-Teller allowed transitions are assigned $\log ft = 5.0$ ($F^2\text{NI}$; Gleit, Tang, and Coryell 1968), unless experiment gives an indication of $\log ft \gg 5$ despite satisfaction of the allowed selection rules. Such cases of hindered allowed transitions were assigned $\log ft = 99.9$ where they might otherwise be important in the determination of low temperature, low density rates. More discussion of the low temperature, low density rates and the adjustment of experimental $\log ft$ values follows in the next section. Fermi transitions are assigned appropriate matrix elements according to equation (I-11). Unmeasured forbidden transitions are neglected because of the dominant effect of the large number of allowed transitions which contribute in most stellar environments. Some $\log ft$ values between the parent ground state and low-lying

daughter states have been adjusted to reproduce measured laboratory decay rates using accurately computed f -values; this procedure is discussed further in § III.

In order to simulate transitions into and from the continuum, appropriately placed Gamow-Teller resonances are included in each stellar weak rate calculation with the procedure discussed in F²NII. The excitation energies of the Gamow-Teller resonances are calculated on the basis of a simple shell model employing the tabulated single particle energies of Seeger and Howard (1975). The procedure for computing the resonance excitation energy differs for $T^< \rightarrow T^>$ and $T^> \rightarrow T^<$ transitions; the reader is referred to §§ III and IV of F²NII for an exhaustive discussion. The sum rules for $T^< \rightleftharpoons T^>$ transitions are estimated by constructing a zero-order shell model configuration for the parent nucleus ground state and applying equation (II-16). The observed discrete state strength for transitions from the parent ground state is summed and subtracted from the equation (II-16) sum rule strength. The remaining strength is lumped into the ground state \rightleftharpoons resonance state transition.

Resonances corresponding to excited states are taken into account here with a special treatment of the population index for ground state \rightleftharpoons resonance transitions. This procedure is based on the assumptions of constant Q -value and sum rule for each discrete state \rightleftharpoons corresponding state transition and is discussed in detail in § V of F²NII. In summary, the contribution of the $E^< \rightarrow R^>$ transitions to the total $T^< \rightarrow T^>$ transition rate can be calculated by including only the $E_1^< \rightarrow R_1^>$ transition and setting the occupation index for the $E_1^<$ state in this transition equal to unity (cf. eqs. [II-43] and [II-44]). The $R^<$ to $E^>$ transitions proceed through the thermal population of the $R^<$ resonances. In the special procedure used in this calculation, the contribution of the $R^< \rightarrow E^>$ transitions to the total $T^< \rightarrow T^>$ transition rate can be calculated by including only the $R_1^< \rightarrow E_1^>$ transition. In addition, the occupation index for the $R_1^<$ state in this transition must be set equal to $P = (G^>/G^<) \exp(-R_1^</kT)$, where $G^<$ and $G^>$ are the nuclear partition functions at the ambient temperature for the $T^<$ and $T^>$ nuclei, respectively (cf. eqs. [II-52] and [II-53]). The generalization for the contribution of the $E^> \rightarrow R^<$ and $R^> \rightarrow E^<$ transitions to the total $T^> \rightarrow T^<$ transition rate is obvious.

Fermi transitions involving excited states in the $T^>$ nucleus explicitly obey the constant Q -value and sum rule assumptions discussed above. Thus, the contributions of these excited states plus that of the ground state to the $T^> \rightarrow T^<$ rate can be taken into account by calculating $E_1^> \rightarrow A_1^<$, where $A_1^<$ designates the analog state in the $T^<$ nucleus corresponding to the ground state of the $T^>$ nucleus. In addition, the occupation index for the $E_1^>$ state in this transition must be set equal to unity. In the $T^< \rightarrow T^>$ transition the contribu-

tion of the analog states can be calculated for $A_1^< \rightarrow E_1^>$, setting the population index for the $A_1^<$ state equal to $P = (G^>/G^<) \exp(-A_1^</kT)$.

The total weak transition rate λ is given by

$$\lambda = \sum_i \sum_j P_i \lambda_{ij}, \quad (2)$$

where the sum on i is over parent states, the sum on j is over daughter states, and P_i is the occupation index defined by equation (I-9a) and modified in the manner discussed above for transitions involving resonances and analog states.

The phase space factors in equation (1) were computed numerically and checked for electron and positron emission at low temperature and density against the tables of $\log ft$ by Gove and Martin (1971). A number of low temperature, high density and high temperature, low density results were checked against easily performed analytic calculations. The definite integrals for the electron and positron emission phase space factors were done by 64 point Gaussian quadrature. The integrands of the electron and positron capture phase space integrals are modulated strongly by the electron or positron distribution function, so that the integrand has a characteristically slowly varying part and an exponentially decaying part, corresponding to the shape of the Fermi-Dirac distribution function. The portion of the improper integrals containing the slowly varying part of the integrand was done with 64 point Gaussian quadrature, and the exponential tail was treated with 32 point Gauss-Laguerre quadrature. For each nuclear transition a table of appropriate phase space factors as a function of q_n (eq. [I-3c]) was prepared at each temperature and density grid point, and the f_{ij} and f_{ij}^v (eqs. [I-3a], [I-3b], [I-6a], [I-6b]) were obtained by cubic spline interpolation in q_n . This procedure was checked for electron and positron capture in nondegenerate conditions against the analytic phase space factors in Fowler and Hoyle (1964).

The free nucleons are unique "nuclei" in that they have no excited states. As a result the interpolation procedure described above for calculating weak phase space factors was not used; free nucleon phase space factors were performed by direct numerical integration at each temperature and density point. The matrix elements for the free nucleon transitions are $|M_F|^2 = 1$ ($\log ft = 3.791$ from I-2b) and $|M_{GT}|^2 = 3$ ($\log ft = 3.596 - \log 3 = 3.118$ from I-2a) to give an overall $\log ft = 3.035$. (In F²NI the value $[G_A/G_V]^2 = 1.567$ was used, and the half-life of the neutron was taken to be 936 s.) Nucleon recoil effects (forbidden transitions) are small at the temperatures and densities considered here and are therefore neglected. For a discussion of forbidden transitions see Fuller (1982).

III. RESULTS AND DISCUSSION

In this section the results of the stellar weak interaction rate calculations are discussed. The terrestrial decay rates of the nuclear species considered in this survey are tabulated in Table 1 based on experimental measurements when available. These rates can be compared with the lowest temperature and density rates calculated in this work. The stellar rates are tabulated on the very abbreviated temperature and density grid shown in Table 2. As noted previously, the rates can be obtained by request on a detailed grid of temperature and density on magnetic tape.

The stellar rate magnetic tape has electron and positron emission rates, continuum electron and positron

capture rates (in s^{-1}), and the associated ν and $\bar{\nu}$ energy loss rates (in $MeV s^{-1}$) for the free nucleons and 226 nuclei with masses between $A=21$ and $A=60$ on a temperature-density grid which includes $0.01 \leq T_9 \leq 100$ and $10 \leq \rho/\mu_e$ ($g cm^{-3}$) $\leq 10^{11}$. In particular, the rates are calculated at $T_9 = 0.01, 0.1, 0.2, 0.4, 0.7, 1.0, 1.5, 2.0, 3.0, 5.0, 10.0, 30,$ and 100 for each density point at $\log(\rho/\mu_e) = 1$ to 11 by unit increment; thus, there are 143 temperature-density points at which are computed the rates in s^{-1} of the four weak processes and the sum of continuum electron capture plus positron emission and continuum positron capture plus electron emission. In addition, the total ν -energy loss rate and the total $\bar{\nu}$ -energy loss rate in $MeV s^{-1}$ are given.

At higher temperatures or at higher densities nuclei are completely ionized in astrophysical environments, and continuum electron capture predominates over

TABLE 1A
TERRESTRIAL WEAK INTERACTION RATES (s^{-1})

Parent (1)	Daughter (2)	Decay (3)	Q_n (MeV) (4)	Log Rate (5)
n	p	β^-	1.293	-2.972
^{21}O	^{21}F	β^-	8.678	(+0 EST)
^{21}F	^{21}Ne	β^-	6.197	-0.795
^{21}Na	^{21}Ne	β^+	3.036	-1.511
^{21}Mg	$^{21}Na^{20}Ne$	$\beta^+ p$	12.587	+0.751
^{22}F	^{22}Ne	β^-	11.364	-0.786
^{22}Na	^{22}Ne	β^+	2.331	-8.117
		ϵ^-	2.331	-9.096
		SUM		-8.074
^{22}Mg	^{22}Na	β^+	4.279	-0.746
^{23}F	^{23}Ne	β^-	9.021	-0.502
^{23}Ne	^{23}Na	β^-	4.886	-1.734
^{23}Mg	^{23}Na	β^+	3.548	-1.212
^{23}Al	$^{23}Mg^{22}Na$	$\beta^+ p$	11.727	+0.169
^{24}Ne	^{24}Na	β^-	2.979	-2.466
^{24}Na	^{24}Mg	β^-	6.024	-4.892
$^{24}Na^m$	^{24}Na	IT	0.472	+1.535
	^{24}Mg	β^-	6.496	(-2 EST)
^{24}Al	$^{24}Mg^{20}Ne$	$\beta^+ \alpha$	13.367	-0.475
$^{24}Al^m$	^{24}Al	IT	0.439	+0.695
	$^{24}Mg^{20}Ne$	$\beta^+ \alpha$	13.806	-0.428
		SUM		+0.727
^{24}Si	^{24}Al	β^+	10.281	(+0.560)
^{25}Ne	^{25}Na	β^-	7.711	+0.0627
^{25}Na	^{25}Mg	β^-	4.344	-1.937
^{25}Al	^{25}Mg	β^+	3.767	-1.015
^{25}Si	$^{25}Al^{24}Mg$	$\beta^+ p$	12.226	+0.498
^{26}Na	^{26}Mg	β^-	9.836	-0.189
^{26}Al	^{26}Mg	β^+	3.494	-13.602
		ϵ^-	3.494	-14.260
		SUM		-13.516
$^{26}Al^m$	^{26}Mg	β^+	3.722	-0.963
^{26}Si	^{26}Al	β^+	4.553	-0.504
^{27}Na	$^{27}Mg^{26}Mg$	$\beta^- n$	9.466	+0.364
^{27}Mg	^{27}Al	β^-	3.120	-2.913
^{27}Si	^{27}Al	β^+	4.298	-0.775
^{27}P	^{27}Si	β^+	11.284	(+0.454)
^{28}Na	$^{28}Mg^{27}Mg$	$\beta^- n$	14.397	+1.349
^{28}Mg	^{28}Al	β^-	2.343	-5.038
^{28}Al	^{28}Si	β^-	5.154	-2.288
^{28}P	^{28}Si	β^+	13.821	+0.409
^{28}S	^{28}P	β^+	10.839	(+0.491)

TABLE 1B
TERRESTRIAL WEAK INTERACTION RATES (s^{-1})

Parent (1)	Daughter (2)	Decay (3)	Q_n (MeV) (4)	Log Rate (5)
^{29}Na	$^{29}Mg^{28}Mg$	$\beta^- n$	13.921	+1.207
^{29}Mg	^{29}Al	β^-	7.973	-0.305
^{29}Al	^{29}Si	β^-	4.192	-2.757
^{29}P	^{29}Si	β^+	4.433	-0.772
^{29}S	$^{29}P^{29}Si$	$\beta^+ p$	13.278	+0.562
^{30}Na	$^{30}Mg^{29}Mg$	$\beta^- n$	18.681	+1.108
^{30}Mg	^{30}Al	β^-	6.611	-0.238
^{30}Al	^{30}Si	β^-	9.050	-0.726
^{30}P	^{30}Si	β^+	3.716	-2.335
		ϵ^-	3.716	-5.241
		SUM		-2.335
^{30}S	^{30}P	β^+	5.631	-0.238
^{31}Na	$^{31}Mg^{30}Mg$	$\beta^- n$	15.021	+1.610
^{31}Mg	^{31}Al	β^-	11.711	(+1 EST)
^{31}Al	^{31}Si	β^-	8.360	+0.0346
^{31}Si	^{31}P	β^-	2.002	-4.134
^{31}S	^{31}P	β^+	4.884	-0.574
^{31}Cl	^{31}S	β^+	11.463	(+0.405)
^{32}Na	^{32}Mg	β^-	19.811	+1.679
^{32}Mg	^{32}Al	β^-	8.911	(+0 EST)
^{32}Al	^{32}Si	β^-	13.311	(+1 EST)
^{32}Si	^{32}P	β^-	0.724	-9.694
^{32}P	^{32}S	β^-	2.221	-6.250
^{32}Cl	$^{32}S^{31}P^{28}Si$	$\beta^+ p \alpha$	12.176	+0.367
^{32}Ar	^{32}Cl	β^+	10.608	(+0.308)
^{33}Na	^{33}Mg	β^-	18.711	+1.540
^{33}Mg	^{33}Al	β^-	14.011	(+1 EST)
^{33}Al	^{33}Si	β^-	11.711	(+1 EST)
^{33}Si	^{33}P	β^-	6.278	-0.952
^{33}P	^{33}S	β^-	0.760	-6.499
^{33}Cl	^{33}S	β^+	5.072	-0.559
^{33}Ar	$^{33}Cl^{32}S$	$\beta^+ p$	11.107	+0.586
^{34}Si	^{34}P	β^-	4.811	-0.606
^{34}P	^{34}S	β^-	5.892	-1.253
^{34}Cl	^{34}S	β^+	4.982	-0.343
$^{34}Cl^m$	^{34}S	IT	0.146	-3.770
		β^+	5.128	-3.718
		SUM		-3.442

TABLE 1C
 TERRESTRIAL WEAK INTERACTION RATES (s^{-1})

Parent (1)	Daughter (2)	Decay (3)	Q_n (MeV) (4)	Log Rate (5)
^{34}Ar	^{34}Cl	β^+	+5.548	-0.0855
^{35}P	^{35}S	β^-	+4.417	-1.831
^{35}S	^{35}Cl	β^-	+0.678	-7.037
^{35}Ar	^{35}Cl	β^+	+5.454	-0.410
^{35}K	^{35}Ar	β^+	+11.369	(+0.592)
^{36}Cl	^{36}Ar	β^-	+1.221	-13.144
	^{36}S	ϵ^-	+0.633	-14.857
		β^+	+0.633	-17.905
		SUM		-13.135
^{36}K	^{36}Ar	β^+	+12.294	+0.309
^{36}Ca	^{36}K	β^+	+10.265	(+0.538)
^{37}S	^{37}Cl	β^-	+5.365	-2.636
^{37}Ar	^{37}Cl	ϵ^-	+0.303	-6.640
^{37}K	^{37}Ar	β^+	+5.638	-0.249
^{37}Ca	$^{37}\text{K}^{36}\text{Ar}$	β^+p	+11.125	+0.603
^{38}S	^{38}Cl	β^-	+3.447	-4.168
^{38}Cl	^{38}Ar	β^-	+5.428	-3.509
$^{38}\text{Cl}^m$...	^{38}Cl	IT	+0.671	-0.0135
^{38}K	^{38}Ar	β^+	+5.402	-2.819
$^{38}\text{K}^m$	^{38}Ar	β^+	+5.532	-0.128
^{38}Ca	^{38}K	β^+	+6.231	+0.197
^{39}Cl	^{39}Ar	β^-	+3.949	-3.686
^{39}Ar	^{39}K	β^-	+1.076	-10.088
^{39}Ca	^{39}Ar	β^+	+6.013	-0.0937
^{40}Cl	^{40}Ar	β^-	+8.011	-2.068
^{40}K	^{40}Ca	β^-	+1.823	-16.815
	^{40}Ar	ϵ^-	+0.994	-17.736
		β^+	+0.994	-21.765
		SUM		-16.765
^{40}Sc	$^{40}\text{Ca}^{39}\text{K}$	β^+p	+13.809	+0.581
^{40}Ti	^{40}Sc	β^+	+10.976	(+0.645)
^{41}Cl	^{41}Ar	β^-	+6.179	-1.691
^{41}Ar	^{41}K	β^-	+3.003	-3.978
^{41}Ca	^{41}K	ϵ^-	-0.0897	-12.658
^{41}Sc	^{41}Ca	β^+	+5.984	+0.0656
^{41}Ti	$^{41}\text{Sc}^{40}\text{Ca}$	β^+p	+12.351	+0.938
^{42}Ar	^{42}K	β^-	+1.114	-9.177
^{42}K	^{42}Ca	β^-	+4.032	-4.807
^{42}Sc	^{42}Ca	β^+	+5.912	+0.0070
$^{42}\text{Sc}^m$...	^{42}Ca	β^+	+6.529	-1.952

 TABLE 1D
 TERRESTRIAL WEAK INTERACTION RATES (s^{-1})

Parent (1)	Daughter (2)	Decay (3)	Q_n (MeV) (4)	Log Rate (5)
^{42}Ti	^{42}Sc	β^+	+6.488	+0.540
^{43}Cl	^{43}Ar	β^-	+9.351	(-2.341)
^{43}Ar	^{43}K	β^-	+5.119	-2.670
^{43}K	^{43}Ca	β^-	+2.328	-5.064
^{43}Sc	^{43}Ca	$\beta^+\epsilon^-$	+1.709	-4.305
^{43}Ti	^{43}Sc	β^+	+6.350	+0.151
^{44}Ar	^{44}K	β^-	+4.047	-3.013
^{44}K	^{44}Ca	β^-	+6.170	-3.282
^{44}Sc	^{44}Ca	β^+	+3.144	-4.332
		ϵ^-	+3.144	-5.611
		SUM		-4.310
$^{44}\text{Sc}^m$...	^{44}Sc	IT	+0.271	-5.489
	^{44}Ca	ϵ^-	+3.415	-7.340
		SUM		-5.483
^{44}Ti	^{44}Sc	ϵ^-	-0.246	-9.330
^{44}V	$^{44}\text{Ti}^{40}\text{Ca}$	$\beta^+\alpha$	+13.185	+0.887
^{45}K	^{45}Ca	β^-	+4.709	-3.238
^{45}Ca	^{45}Sc	β^-	+0.768	-7.313
$^{45}\text{Sc}^m$...	^{45}Sc	IT	+0.0124	+0.349
^{45}Ti	^{45}Sc	$\beta^+\epsilon^-$	+1.552	-4.205
^{45}V	^{45}Ti	β^+	+6.614	(-0.034)
^{45}Cr	$^{45}\text{V}^{44}\text{Ti}$	β^+p	+11.908	+1.142
^{46}K	^{46}Ca	β^-	+8.229	-2.220
^{46}Sc	^{46}Ca	$\beta^+\epsilon^-$	+0.872	(HI FRB)
^{46}Sc	^{46}Ti	β^-	+2.878	-7.019
$^{46}\text{Sc}^m$...	^{46}Sc	IT	+0.143	-1.431
^{46}V	^{46}Ti	β^+	+6.541	0.214
^{46}Cr	^{46}V	β^+	+7.099	0.426
^{47}K	^{47}Ca	β^-	+7.156	-1.402
^{47}Ca	^{47}Sc	β^-	+2.499	-5.752
^{47}Sc	^{47}Ti	β^-	+1.112	-5.630
^{47}V	^{47}Ti	$\beta^+\epsilon^-$	+2.419	-3.451
^{47}Cr	^{47}V	β^+	+6.872	(+0.052)
^{48}K	^{48}Ca	β^-	+12.507	-0.922
^{48}Ca	^{48}Sc	β^-	+0.792	(HI FRB)
^{48}Sc	^{48}Ti	β^-	+4.501	-5.356
^{48}V	^{48}Ti	ϵ^-	+3.504	-6.597
		β^+	+3.504	-6.604
		SUM		-6.299
^{48}Cr	^{48}V	ϵ^-	+1.144	(-5.049)
^{48}Mn	^{48}Cr	$\beta^+\epsilon^-$	+13.139	(+1 EST)
^{49}Cl	^{49}Ar	β^-	~ 18.480	(+1 EST)
^{49}Ar	^{49}K	β^-	~ 15.000	(+1 EST)

bound state electron capture. At low density intermediate mass nuclei are thermally ionized in the range $T_9 = 0.01$ to 0.5, at low temperature nuclei are completely pressure ionized due to the combined effects of nuclear charge screening and continuum lowering. At zero temperature, for example, ^{56}Fe will become completely pressure ionized for $\rho/\mu_e \gtrsim 10^4 \text{ g cm}^{-3}$. In general, whenever the density of continuum electrons is larger than the K-shell electron density at the nucleus, then continuum electron capture dominates over bound state capture. In the low temperature-low density corner of the temperature-density grid used here bound state capture is important; we do not calculate bound state electron capture, only continuum capture.

An estimate of the bound state electron capture rate for nuclear transitions where it is important can be

obtained from the terrestrial electron capture decay rate. Terrestrial electron capture decays generally proceed through the capture of electrons in low-lying atomic levels, usually K-shell electrons. Table 1 lists all of the nuclei considered in this survey, together with their terrestrial decay modes and rates, where these quantities are known. The logarithms of the electron capture rates for a full K-shell can be read from this table. We designate these rates by λ_K .

As the temperature rises at a given density in a stellar environment, the occupation of the K-shell is reduced from two electrons to one at a critical value of the temperature. Similarly, at a given temperature the oc-

TABLE 1E
 TERRESTRIAL WEAK INTERACTION RATES (s^{-1})

Parent (1)	Daughter (2)	Decay (3)	Q_n (MeV) (4)	Log Rate (5)
^{49}K	^{49}Ca	β^-	14.038	≤ -0.460
^{49}Ca	^{49}Sc	β^-	5.779	-2.878
^{49}Sc	^{49}Ti	β^-	2.515	-3.693
^{49}V	^{49}Ti	ϵ^-	0.0908	-7.614
^{49}Cr	^{49}V	$\beta^+ \epsilon^-$	2.117	-3.560
^{49}Mn	^{49}Cr	β^+	7.205	(+0.168)
^{49}Fe	$^{49}\text{Mn}^{48}\text{Cr}$	$\beta^+ p$	12.632	+0.996
^{50}K	^{50}Ca	β^-	16.511	$\approx +0.364$
^{50}Ca	^{50}Sc	β^-	5.478	-1.305
^{50}Sc	^{50}Ti	β^-	7.404	-2.170
$^{50}\text{Sc}^m$...	^{50}Sc	IT	0.257	+0.297
^{50}V	^{50}Ti	$\beta^+ \epsilon^-$	1.702	(HI FRB)
^{50}V	^{50}Cr	β^-	1.550	(HI FRB)
^{50}Mn	^{50}Cr	β^+	7.121	+0.389
$^{50}\text{Mn}^m$...	^{50}Cr	β^+	7.351	-2.178
^{51}Sc	^{51}Ti	β^-	7.024	-1.253
^{51}Ti	^{51}V	β^-	2.977	-2.701
^{51}Cr	^{51}V	ϵ^-	0.240	-6.538
^{51}Mn	^{51}Cr	$\beta^+ \epsilon^-$	2.697	-3.602
^{52}Ti	^{52}V	β^-	2.481	-2.168
^{52}V	^{52}Cr	β^-	4.488	-2.513
^{52}Mn	^{52}Cr	ϵ^-	4.200	-5.986
		β^+	4.200	-6.396
		SUM		-5.843
$^{52}\text{Mn}^m$..	^{52}Cr	$\beta^+ \epsilon^-$	4.578	-3.269
	^{52}Mn	IT	0.378	-5.019
		SUM		-3.262
^{52}Fe	^{52}Mn	β^+	1.861	-4.877
		ϵ^-	1.861	-5.000
		SUM		-4.633
^{53}Ti	^{53}V	β^-	5.484	-1.678
^{53}V	^{53}Cr	β^-	3.932	-2.141
^{53}Mn	^{53}Cr	ϵ^-	0.0853	-14.226
^{53}Fe	^{53}Mn	$\beta^+ \epsilon^-$	3.232	-2.867
$^{53}\text{Fe}^m$...	^{53}Fe	IT	3.041	-2.340
^{53}Co	^{53}Fe	β^+	7.793	+0.426
$^{53}\text{Co}^m$...	^{53}Fe	β^+	10.983	+0.436
	^{52}Fe	p	1.597	-1.381
		SUM		+0.443
^{53}Ni	^{53}Co	$\beta^+ p$	12.719	+1.142

 TABLE 1F
 TERRESTRIAL WEAK INTERACTION RATES (s^{-1})

Parent (1)	Daughter (2)	Decay (3)	Q_n (MeV) (4)	Log Rate (5)
^{54}V	^{54}Cr	β^-	+7.512	-1.793
^{54}Mn ...	^{54}Cr	ϵ^-	+0.866	-7.590
^{54}Mn ...	^{54}Fe	β^-	+1.208	(HI FRB)
^{54}Co	^{54}Fe	β^+	+7.731	+0.555
$^{54}\text{Co}^m$...	^{54}Fe	β^+	+7.930	-2.102
^{55}Ti	^{55}V	β^-	+9.151	(+0.130)
^{55}V	^{55}Cr	β^-	+6.607	(-0.486)
^{55}Cr	^{55}Mn	β^-	+3.115	-2.488
^{55}Fe	^{55}Mn	ϵ^-	-0.280	-8.090
^{55}Co	^{55}Fe	β^+	+2.944	+5.072
		ϵ^-	+2.944	-5.597
		SUM		-4.959
^{56}Sc	^{56}Ti	β^-	+16.251	(+0.957)
^{56}Ti	^{56}V	β^-	+6.801	(+0.528)
^{56}V	^{56}Cr	β^-	+9.566	(+0.505)
^{56}Cr	^{56}Mn	β^-	+2.154	-2.708
^{56}Mn	^{56}Fe	β^-	+4.206	-4.127
^{56}Co	^{56}Fe	ϵ^-	+4.057	-7.084
		β^+	+4.057	-7.713
		SUM		-6.992
^{56}Ni	^{56}Co	ϵ^-	+1.625	-5.881
^{57}Ti	^{57}V	β^-	+11.232	(+0.704)
^{57}V	^{57}Cr	β^-	+8.440	(-0.528)
^{57}Cr	^{57}Mn	β^-	+5.208	(-0.439)
^{57}Mn	^{57}Fe	β^-	+3.203	-2.141
^{57}Co	^{57}Fe	ϵ^-	+0.316	-7.529
^{57}Ni	^{57}Co	ϵ^-	+2.755	-5.494
		β^+	+2.755	-5.670
		SUM		-5.272
^{57}Cu	^{57}Ni	$\beta^+ \epsilon^-$	+7.968	+0.586
^{57}Zn	$^{57}\text{Cu}^{56}\text{Ni}$	$\beta^+ p$	+14.479	+1.239
^{58}Ti	^{58}V	β^-	+8.611	(+0.239)
^{58}V	^{58}Cr	β^-	+12.911	(+0.176)
^{58}Cr	^{58}Mn	β^-	+4.671	(-0.904)
^{58}Mn	^{58}Fe	β^-	+6.831	-0.636
$^{58}\text{Mn}^m$..	^{58}Fe	β^-	+6.861	-1.972
^{58}Co	^{58}Fe	ϵ^-	+1.797	-7.016
		β^+	+1.797	-7.770
		SUM		-6.946
^{58}Co	^{58}Ni	β^-	+0.891	(HI FRB)
$^{58}\text{Co}^m$...	^{58}Co	IT	+0.0249	-4.679
^{58}Cu	^{58}Ni	β^+	+8.052	(-0.664)

cupation of the K-shell increases from zero to one as the density rises to a critical value. Following Iben, Kalata, and Schwartz (1967), this critical density *neglecting screening* is given by

$$\left(\frac{\rho}{\mu_e}\right)_c = 2.536 \times 10^5 T_9^{3/2} \times \exp \left[-1.58 \times 10^{-4} (Z - 0.31)^2 / T_9 \right] \text{ g cm}^{-3}, \quad (3)$$

where $Z - 0.31$ is the effective charge of the capturing nucleus. For example, for $^{49}\text{V} + e^- \rightarrow ^{49}\text{Ti} + \nu_e$ one finds $(\rho/\mu_e)_c = 0.07 \text{ g cm}^{-3}$ for $T_9 = 0.01$, $3.55 \times 10^3 \text{ g cm}^{-3}$ for $T_9 = 0.1$, and $2.34 \times 10^5 \text{ g cm}^{-3}$ for $T_9 = 1$. Below

these critical densities the total capture rate is given by the continuum capture rate, λ_C , alone, while above these critical densities the total rate is $\lambda_C + \lambda_K$. The transition is not an abrupt one since $\lambda_C \sim \lambda_K$ near the critical transition density and $\lambda_C > \lambda_K$ above this density. For somewhat more accurate calculations a monotonically increasing function of $y = \log(\rho/\mu_e)/(\rho/\mu_e)_c$ can be used passing through $\lambda_C + \lambda_K/3$ at $y \approx -0.3$, $\lambda_C + \lambda_K/2$ at $y = 0$, and $\lambda_C + 2\lambda_K/3$ at $y \approx +0.3$.

The first column in Table 1 gives the parent nucleus, while the second column gives the daughter. In the stellar rate computations both forward and reverse rates are calculated, and the labels "parent" and "daughter" can alternately apply to both nuclei linked by weak transitions. For example, in the laboratory ^{56}Mn decays

TABLE 1G
TERRESTRIAL WEAK INTERACTION RATES (s^{-1})

Parent (1)	Daughter (2)	Decay (3)	Q_n (MeV) (4)	Log Rate (5)
^{59}V	^{59}Cr	β^-	10.161	(+0.005)
^{59}Cr	^{59}Mn	β^-	9.011	(-0.002)
^{59}Mn	^{59}Fe	β^-	5.692	(-1.012)
^{59}Fe	^{59}Co	β^-	2.076	-6.745
^{59}Ni	^{59}Co	ϵ^-	0.562	-12.533
		β^+	0.562	-19.357
		SUM		-12.533
^{59}Cu	^{59}Ni	β^+	4.290	-2.073
^{60}Ti	^{60}V	β^-	10.721	(+0.601)
^{60}V	^{60}Cr	β^-	14.911	(+1 EST)
^{60}Cr	^{60}Mn	β^-	5.771	(-0.802)
^{60}Mn	^{60}Fe	β^-	10.228	(+0 EST)
^{60}Fe	^{60}Co	β^-	0.720	-13.135
^{60}Co	^{60}Ni	β^-	3.335	-8.380
$^{60}\text{Co}^m$	^{60}Co	IT	0.0586	-2.960
	^{60}Ni	β^-	3.394	-5.561
		SUM		-2.959
^{60}Cu	^{60}Ni	β^+	5.616	-3.338
		ϵ^-	5.616	-4.461
		SUM		-3.307
^{60}Zn	^{60}Cu	β^+	3.648	-2.331
		ϵ^-	3.648	-3.840
		SUM		-2.318

by electron emission to ^{56}Fe , and this terrestrial decay rate is listed in Table 1, but at high density and temperature $^{56}\text{Fe} \rightarrow ^{56}\text{Mn}$ proceeds via continuum electron capture at high electron Fermi energy and/or via positron emission through thermally populated ^{56}Fe excited states. The stellar rates for both $^{56}\text{Fe} \rightarrow ^{56}\text{Mn}$ and $^{56}\text{Mn} \rightarrow ^{56}\text{Fe}$ are computed. The third column in Table 1 gives the terrestrial decay mode, either β^- for electron emission, β^+ for positron emission, ϵ^- for electron capture, or IT for γ -ray transition from a nuclear isomeric state (listed separately with an "m", e.g., $^{24}\text{Na}^m$) to the ground state. In addition, the sum of the rates for

TABLE 2
TEMPERATURE AND DENSITY POINTS AT WHICH
TABLE 3 RATES ARE EVALUATED (with total
electron Fermi energy W_F)

Point	T_9 (10^6 K)	$\log(\rho/\mu_e)$ (g cm^{-3})	W_F (MeV)
1	1	3	0.046
2	3	3	0.000
3	10	3	0.000
4	100	3	0.000
5	1	7	1.200
6	3	7	1.021
7	10	7	0.196
8	100	7	0.002
9	1	11	23.930
10	3	11	23.925
11	10	11	23.833
12	100	11	14.523

the various laboratory decay processes is denoted as "SUM." Where it is known that proton, neutron, or α -particle emission from the daughter follows a weak decay process, then that process is designated as, for example, β^+p , β^-n , $\beta^+\alpha$, respectively. In these cases the final nucleus resulting after particle emission from the daughter is listed after the daughter nucleus in column (2). For example, ^{21}Mg decays by positron emission to ^{21}Na which subsequently decays by proton emission to ^{20}Ne .

As indicated in equations (I-3a) and (I-3b), we have found it far simpler to use total particle energies, rest-mass plus kinetic rather than kinetic, and to use nuclear Q -values rather than atomic. Thus, column (4) in Table 1 lists the nuclear Q -value, Q_n , for each nuclear transition, where

$$Q_n = M_p c^2 - M_d c^2, \quad (4)$$

with M_p the nuclear mass of the parent ground state and M_d that of the daughter ground state. The dominant allowed transitions may involve excited states in the daughter nucleus. Differential atomic binding energies are negligible and have not been included. In the emission of both positrons and electrons the maximum kinetic energy is given by $Q_n - m_e c^2 = Q_n - 0.511$ MeV, and in the capture of positrons and electrons the minimum energy of the antineutrinos or neutrinos is $Q_n + m_e c^2 = Q_n + 0.511$ MeV. On the other hand, the tabulated Fermi energies, U_F , are kinetic energies but can easily be converted to total energies, $W_F = U_F + m_e c^2 = U_F + 0.511$ MeV. Finally, column (5) lists the logarithms of the indicated rates. Those entries in parentheses are cases where no terrestrial decay rate is known and the lowest temperature and density stellar rate from our calculations or an estimate (EST) is provided instead. Exoergic transitions, which are *highly forbidden* so that the "parent" nucleus is essentially stable, e.g., ^{50}V , are indicated by (HI FRB). At the lowest temperature, $T_9 = 0.01$, excited parent states are almost never appreciably populated, while at the lowest density, $\rho/\mu_e = 10$ g cm^{-3} , the continuum electron density is quite low, and, except for electron capture, the stellar rates should be quite close to the terrestrial values. The exception noted arises because only continuum electron capture and not bound state capture is calculated.

It transpires that the rates calculated for the lowest temperature-density points and the terrestrial rates often disagree. This is because what experimentalists actually measure are branching intensities, not matrix elements. To convert branching intensities for various transitions into $(\log ft)$ -values, equivalent to matrix elements, requires two input quantities: the overall lifetime of the decaying nucleus, and the f -factors (phase space factors) for each of the individual transitions. There is no difficulty with the lifetimes, which are commonly very accurately known, but the appropriate f -factors are usually complicated integrals involving electron and neutrino

TABLE 3
STELLAR WEAK RATES EVALUATED AT TABLE 2 TEMPERATURE AND DENSITY POINTS

${}^1\text{p} \rightarrow {}^1\text{n}$				${}^2\text{He} \rightarrow {}^2\text{He}$				${}^2\text{He} \rightarrow {}^2\text{He}$						
pt	$\log \beta^+$	$\log \epsilon^-$	$\log \nu$	$\log \beta^-$	$\log \epsilon^+$	$\log \nu$	$\log \bar{\nu}$	pt	$\log \beta^+$	$\log \epsilon^-$	$\log \nu$	$\log \beta^-$	$\log \epsilon^+$	$\log \bar{\nu}$
1	-99.999	-10.546	-11.083	-2.966	-5.767	-3.281	-0.295	1	-45.998	-35.139	-35.705	-0.759	-6.202	-0.295
2	-99.999	-4.722	-4.726	-2.987	-2.744	-2.297	-0.289	2	-16.335	-13.090	-13.142	-0.759	-3.211	-0.289
3	-99.999	-1.042	-0.457	-3.109	-0.422	0.297	0.033	3	-6.138	-3.968	-3.390	-0.759	-1.098	0.033
4	-99.999	4.286	5.920	-3.247	4.340	5.987	6.347	4	1.299	4.241	5.879	2.861	4.669	6.347
5	-99.999	-4.741	-3.271	-4.303	-11.586	-4.922	-0.332	5	-45.998	-29.322	-29.890	-0.783	-12.021	-0.332
6	-99.999	-3.017	-3.015	-3.457	-4.448	-3.632	-0.322	6	-16.330	-11.379	-11.430	-0.779	-4.915	-0.322
7	-99.999	-0.944	-0.359	-3.139	-0.517	0.201	0.016	7	-6.125	-3.870	-3.293	-0.795	-1.193	0.016
8	-99.999	4.286	5.920	-3.247	4.340	5.987	6.347	8	1.299	4.241	5.879	2.861	4.669	6.347
9	-99.999	4.409	5.682	-99.999	-99.999	-99.999	-92.055	9	-45.998	3.170	4.074	-91.464	-99.999	-92.055
10	-99.999	4.410	5.684	-41.704	-42.926	-41.985	-30.503	10	-16.330	3.179	4.088	-30.380	-43.393	-30.503
11	-99.999	4.419	5.701	-14.560	-12.416	-11.703	-7.594	11	-6.067	3.240	4.168	-7.960	-13.090	-7.594
12	-99.999	4.982	6.632	-3.737	3.618	5.261	5.625	12	1.429	4.943	6.589	2.544	3.948	5.625

${}^2\text{Mg} \rightarrow {}^2\text{Na}$				${}^2\text{O} \rightarrow {}^2\text{F}$				${}^2\text{Na} \rightarrow {}^2\text{Mg}$						
pt	$\log \beta^+$	$\log \epsilon^-$	$\log \nu$	$\log \beta^-$	$\log \epsilon^+$	$\log \nu$	$\log \bar{\nu}$	pt	$\log \beta^+$	$\log \epsilon^-$	$\log \nu$	$\log \beta^-$	$\log \epsilon^+$	$\log \bar{\nu}$
1	0.741	-4.186	1.462	-99.999	-66.837	-67.411	-1.546	1	-56.641	-49.924	-50.503	-2.181	-8.261	-1.546
2	0.721	-1.835	1.446	-33.550	-22.913	-22.985	-0.243	2	-20.040	-18.064	-18.139	-0.877	-3.954	-0.243
3	0.708	0.095	1.593	-8.811	-6.496	-5.986	0.285	3	-7.110	-5.449	-4.792	-0.461	-1.295	0.285
4	3.793	5.388	7.139	-0.181	3.713	5.290	6.477	4	0.333	3.929	5.557	2.963	4.790	6.477
5	0.741	-0.406	1.502	-99.999	-72.657	-73.230	-1.560	5	-56.641	-44.105	-44.684	-2.190	-14.081	-1.560
6	0.721	-0.398	1.488	-33.557	-24.629	-24.701	-0.256	6	-20.032	-16.350	-16.431	-0.885	-5.658	-0.256
7	0.710	0.188	1.624	-8.813	-6.595	-6.084	0.264	7	-7.100	-5.352	-4.697	-0.464	-1.391	0.264
8	3.793	5.389	7.139	-0.181	3.713	5.290	6.477	8	0.333	3.929	5.557	2.963	4.790	6.477
9	0.741	4.929	6.243	-99.999	-99.999	-99.999	-79.640	9	-56.641	2.710	3.493	-79.048	-99.999	-79.640
10	0.721	4.918	6.230	-62.197	-63.107	-62.278	-26.606	10	-20.032	2.725	3.521	-26.483	-44.135	-26.606
11	0.716	4.877	6.185	-17.987	-18.507	-17.517	-6.607	11	-7.055	2.779	3.598	-6.972	-13.289	-6.607
12	3.877	6.063	7.827	-0.602	2.985	4.561	5.755	12	0.462	4.632	6.269	2.645	4.071	5.755

${}^2\text{Ne} \rightarrow {}^2\text{Ne}$				${}^2\text{Mg} \rightarrow {}^2\text{Na}$				${}^2\text{Na} \rightarrow {}^2\text{Mg}$						
pt	$\log \beta^+$	$\log \epsilon^-$	$\log \nu$	$\log \beta^-$	$\log \epsilon^+$	$\log \nu$	$\log \bar{\nu}$	pt	$\log \beta^+$	$\log \epsilon^-$	$\log \nu$	$\log \beta^-$	$\log \epsilon^+$	$\log \bar{\nu}$
1	-1.479	-5.060	-1.321	-25.810	-19.741	-20.308	-26.848	1	-0.708	-4.470	-0.472	-50.789	-26.281	-26.848
2	-1.522	-2.691	-1.287	-11.492	-7.788	-7.842	-10.213	2	-0.717	-2.078	-0.435	-16.812	-10.156	-10.213
3	-1.342	-0.624	0.231	-3.510	-2.326	-1.751	-2.787	3	-0.673	-0.137	0.756	-4.907	-3.332	-2.787
4	1.621	4.869	6.549	0.580	4.505	6.136	5.834	4	2.623	5.181	6.874	0.199	4.230	5.834
5	-1.479	-1.245	-0.552	-27.896	-25.561	-26.125	-32.668	5	-0.708	-0.665	0.108	-50.812	-32.101	-32.668
6	-1.518	-1.239	-0.528	-11.769	-9.504	-9.555	-11.929	6	-0.715	-0.629	0.155	-16.832	-11.872	-11.929
7	-1.335	-0.530	0.319	-3.515	-2.425	-1.844	-2.884	7	-0.666	-0.044	0.842	-4.913	-3.430	-2.884
8	1.621	4.869	6.549	0.580	4.505	6.136	5.834	8	2.623	5.181	6.875	-0.199	4.229	5.834
9	-1.479	4.693	5.920	-99.999	-99.999	-99.999	-99.999	9	-0.708	4.970	6.256	-99.999	-99.999	-99.999
10	-1.518	4.682	5.906	-46.529	-47.981	-46.658	-49.656	10	-0.714	4.966	6.252	-49.587	-50.350	-49.656
11	-1.303	4.679	5.906	-13.472	-14.337	-13.109	-14.529	11	-0.636	4.893	6.170	-15.085	-15.343	-14.529
12	1.765	5.579	7.255	0.138	3.782	5.409	5.105	12	2.745	5.864	7.574	-0.648	3.503	5.105

TABLE 3—Continued

$^{22}\text{Ne} \rightarrow ^{22}\text{Ne}$				$^{22}\text{Ne} \rightarrow ^{22}\text{Ne}$				$^{22}\text{Ne} \rightarrow ^{22}\text{Ne}$						
pt	$\log \beta^+$	$\log \epsilon^-$	$\log \nu$	$\log \beta^-$	$\log \epsilon^+$	$\log \bar{\nu}$		pt	$\log \beta^+$	$\log \epsilon^-$	$\log \nu$	$\log \beta^-$	$\log \epsilon^+$	$\log \bar{\nu}$
1	-5.159	-8.653	-5.011	-21.452	-18.973	-19.532		1	-34.966	-29.299	-29.866	-1.729	-6.981	-1.364
2	-3.108	-4.254	-2.874	-9.738	-7.316	-7.362		2	-14.413	-11.629	-11.675	-1.708	-3.953	-1.331
3	-2.210	-1.410	-0.582	-3.000	-1.924	-1.317		3	-5.071	-3.611	-2.976	-1.014	-1.442	-0.207
4	1.311	4.700	6.343	1.578	4.632	6.284		4	1.398	4.706	6.360	2.269	4.687	6.333
5	-5.159	-4.751	-4.179	-23.730	-24.792	-24.370		5	-34.966	-23.490	-24.056	-1.771	-12.801	-1.432
6	-3.104	-2.797	-2.103	-10.008	-9.031	-9.032		6	-14.408	-9.922	-9.970	-1.742	-5.658	-1.388
7	-2.210	-1.316	-0.491	-3.004	-2.022	-1.406		7	-5.062	-3.514	-2.881	-1.018	-1.537	-0.246
8	1.311	4.700	6.343	1.578	4.632	6.283		8	1.398	4.706	6.361	2.269	4.687	6.333
9	-3.104	4.330	5.415	-99.999	-99.999	-99.999		9	-34.966	3.823	4.762	-98.160	-99.999	-98.753
10	-3.104	4.338	5.430	-44.134	-47.509	-44.269		10	-14.408	3.827	4.769	-32.665	-44.135	-32.791
11	-2.171	4.373	5.499	-11.845	-13.933	-11.524		11	-5.024	3.858	4.826	-8.717	-13.434	-8.367
12	1.455	5.396	7.053	1.169	3.910	5.558		12	1.544	5.399	7.068	1.909	3.964	5.607
$^{22}\text{Ne} \rightarrow ^{22}\text{F}$				$^{22}\text{F} \rightarrow ^{22}\text{Ne}$				$^{23}\text{Mg} \rightarrow ^{23}\text{Mg}$						
pt	$\log \beta^+$	$\log \epsilon^-$	$\log \nu$	$\log \beta^-$	$\log \epsilon^+$	$\log \bar{\nu}$		pt	$\log \beta^+$	$\log \epsilon^-$	$\log \nu$	$\log \beta^-$	$\log \epsilon^+$	$\log \bar{\nu}$
1	-99.999	-60.472	-61.046	-0.780	-6.320	-0.321		1	-1.181	-4.963	-0.953	-28.208	-22.255	-22.822
2	-8.707	-5.871	-5.372	-0.616	-3.305	-0.076		2	-1.204	-2.592	-0.930	-12.443	-8.583	-8.640
3	0.999	4.051	5.670	3.399	4.847	6.563		3	2.070	4.913	6.576	1.100	4.568	6.202
4	-99.999	-54.653	-55.226	-0.805	-12.140	-0.359		4	2.070	4.913	6.576	1.100	4.568	6.202
5	-37.209	-19.244	-19.318	-0.632	-5.009	-0.099		5	-1.181	-1.162	-0.374	-30.753	-28.074	-28.641
6	-8.707	-5.772	-5.274	-0.231	-1.220	0.484		6	-1.201	-1.144	-0.345	-12.725	-10.298	-10.355
7	0.999	4.051	5.670	3.399	4.847	6.563		7	-1.203	-0.467	0.400	-4.097	-2.641	-2.088
8	-99.999	2.168	2.549	-66.138	-99.999	-66.729		8	2.070	4.913	6.576	1.100	4.568	6.202
9	-37.209	2.203	2.633	-22.500	-43.486	-22.622		9	-1.181	4.677	5.886	-99.999	-99.999	-99.999
10	-8.703	2.524	3.248	-5.981	-13.111	-5.608		10	-1.201	4.670	5.877	-47.096	-48.776	-47.225
11	1.131	4.758	6.384	3.107	4.129	5.846		11	-1.164	4.666	5.876	-13.381	-14.553	-13.039
12								12	2.197	5.605	7.282	0.676	3.843	5.475
$^{23}\text{Al} \rightarrow ^{23}\text{Mg}$				$^{23}\text{Mg} \rightarrow ^{23}\text{Al}$				$^{23}\text{Ne} \rightarrow ^{23}\text{Ne}$						
pt	$\log \beta^+$	$\log \epsilon^-$	$\log \nu$	$\log \beta^-$	$\log \epsilon^+$	$\log \bar{\nu}$		pt	$\log \beta^+$	$\log \epsilon^-$	$\log \nu$	$\log \beta^-$	$\log \epsilon^+$	$\log \bar{\nu}$
1	0.204	-4.444	0.880	-85.080	-62.805	-63.377		1	-59.715	-49.286	-49.860	-0.468	-6.002	-0.013
2	0.209	-2.075	0.889	-27.595	-21.743	-21.811		2	-20.778	-17.673	-17.747	-0.407	-3.035	0.080
3	0.476	-0.138	1.385	-7.585	-6.300	-5.765		3	7.253	-5.263	-4.691	-0.205	-0.936	0.525
4	3.311	5.343	7.055	-0.458	4.039	5.637		4	1.024	4.109	5.741	3.559	4.910	6.503
5	0.204	-0.666	0.950	-85.109	-68.625	-69.197		5	-59.715	-43.466	-44.040	-0.493	-11.822	-0.053
6	0.209	-0.638	0.963	-27.619	-23.458	-23.527		6	-20.773	-15.958	-16.032	-0.426	-4.739	0.049
7	0.477	-0.045	1.413	-7.591	-6.399	-5.859		7	-7.240	-5.165	-4.594	-0.209	-1.030	0.496
8	3.311	5.343	7.055	-0.458	4.038	5.637		8	1.024	4.109	5.741	3.559	4.910	6.603
9	0.204	5.027	6.283	-99.999	-99.999	-99.999		9	-59.715	2.320	3.068	-77.064	-99.999	-77.655
10	0.209	5.027	6.284	-61.004	-61.936	-61.104		10	-20.773	2.340	3.090	-25.572	-43.216	-25.694
11	0.483	5.004	6.259	-17.910	-18.311	-17.440		11	-7.180	2.550	3.376	-6.432	-12.924	-6.059
12	3.411	6.023	7.751	-0.912	3.312	4.908		12	1.157	4.812	6.453	3.067	4.190	5.883

TABLE 3—Continued

$^{24}\text{Si} \rightarrow ^{24}\text{Al}$		$^{24}\text{Al} \rightarrow ^{24}\text{Si}$		$^{24}\text{Ne} \rightarrow ^{24}\text{Ne}$		$^{24}\text{Ne} \rightarrow ^{24}\text{Ne}$		$^{24}\text{Ne} \rightarrow ^{24}\text{Ne}$	
pt	$\log \beta^+$	$\log \epsilon^-$	$\log \nu$	$\log \beta^-$	$\log \epsilon^+$	$\log \nu$	$\log \beta^-$	$\log \epsilon^+$	$\log \nu$
1	0.560	-4.166	1.200	-76.477	-56.565	-21.123	-2.467	-6.689	-2.416
2	0.560	-1.811	1.203	-25.546	-20.220	-9.236	-2.460	-3.634	-2.323
3	0.706	0.049	1.583	-7.801	-6.465	-2.870	-1.087	-1.143	-0.126
4	3.348	5.347	7.056	-0.632	3.978	6.174	2.604	4.859	6.524
5	0.560	-0.403	1.270	-76.515	-62.384	-15.304	-2.707	-12.509	-2.756
6	0.560	-0.377	1.277	-25.579	-21.935	-7.501	-2.618	-5.339	-2.601
7	0.707	0.141	1.613	-7.809	-6.564	-3.384	-1.093	-1.238	-0.185
8	3.348	5.347	7.056	-0.632	3.978	6.174	2.604	4.859	6.523
9	0.560	5.164	6.441	-99.999	-99.999	4.573	-99.999	-99.999	-99.999
10	0.560	5.165	6.443	-59.753	-60.413	3.688	-34.802	-43.817	-34.929
11	0.714	5.122	6.392	-18.309	-18.476	3.759	-8.573	-13.135	-8.222
12	3.443	6.029	7.752	-1.090	3.252	5.230	2.248	4.138	5.799

$^{24}\text{Al} \rightarrow ^{24}\text{Mg}$		$^{24}\text{Mg} \rightarrow ^{24}\text{Al}$		$^{25}\text{Si} \rightarrow ^{25}\text{Si}$		$^{25}\text{Al} \rightarrow ^{25}\text{Si}$		$^{25}\text{Al} \rightarrow ^{25}\text{Si}$	
pt	$\log \beta^+$	$\log \epsilon^-$	$\log \nu$	$\log \beta^-$	$\log \epsilon^+$	$\log \nu$	$\log \beta^-$	$\log \epsilon^+$	$\log \nu$
1	-0.433	-4.558	-0.040	-99.999	-70.399	0.606	-96.216	-64.995	-65.568
2	-0.242	-2.186	0.345	-32.751	-23.680	-1.720	-30.849	-22.156	-22.228
3	0.247	-0.246	1.179	-7.857	-6.227	0.231	-8.141	-6.147	-5.636
4	3.020	5.043	6.732	0.713	4.244	3.350	6.904	4.030	5.632
5	-0.433	-0.775	0.257	-99.999	-76.218	-0.307	-96.230	-70.814	-71.398
6	-0.241	-0.747	0.507	-32.760	-25.396	0.286	-30.861	-23.871	-23.944
7	0.249	-0.153	1.214	-7.860	-6.326	0.740	-8.145	-6.246	-5.734
8	3.020	5.044	6.733	0.713	4.244	3.350	6.904	4.030	5.632
9	-0.433	4.864	6.104	-99.999	-99.999	0.606	-99.999	-99.999	-99.999
10	-0.241	4.861	6.100	-62.522	-63.873	0.629	-61.560	-62.349	-61.628
11	0.256	4.828	6.060	-17.312	-18.239	0.748	-17.826	-18.159	-17.300
12	3.112	5.731	7.433	0.284	3.519	5.869	-0.257	3.304	4.903

$^{24}\text{Mg} \rightarrow ^{24}\text{Na}$		$^{24}\text{Na} \rightarrow ^{24}\text{Mg}$		$^{25}\text{Mg} \rightarrow ^{25}\text{Mg}$		$^{25}\text{Al} \rightarrow ^{25}\text{Mg}$		$^{25}\text{Al} \rightarrow ^{25}\text{Mg}$	
pt	$\log \beta^+$	$\log \epsilon^-$	$\log \nu$	$\log \beta^-$	$\log \epsilon^+$	$\log \nu$	$\log \beta^-$	$\log \epsilon^+$	$\log \nu$
1	-42.297	-36.014	-36.567	-4.232	-8.731	-0.709	-30.102	-23.240	-23.809
2	-15.408	-13.466	-13.511	-2.474	-4.848	-0.688	-14.179	-8.812	-8.871
3	-4.977	-3.472	-2.844	-1.392	-1.689	0.475	-3.634	-2.526	-1.957
4	1.876	4.719	6.375	2.381	4.591	6.990	0.402	4.686	6.319
5	-42.297	-30.193	-30.753	-4.336	-14.550	-1.029	-33.453	-29.060	-29.628
6	-15.402	-11.754	-11.807	-2.499	-6.553	-0.165	-14.231	-10.528	-10.587
7	-4.967	-3.375	-2.748	-1.396	-1.785	0.559	-3.641	-2.625	-2.051
8	1.876	4.719	6.375	2.381	4.591	6.990	0.402	4.686	6.319
9	-42.297	3.795	4.652	-92.991	-99.999	6.110	-99.999	-99.999	-99.999
10	-15.402	3.802	4.666	-51.458	-45.030	6.102	-47.824	-49.006	-47.949
11	-4.924	3.897	4.839	-8.902	-13.683	6.102	-13.971	-14.537	-13.558
12	2.004	5.415	7.082	2.032	3.868	7.396	-0.051	3.963	5.592

TABLE 3—Continued

$^{25}\text{Mg} \rightarrow ^{25}\text{Na}$			$^{25}\text{Na} \rightarrow ^{25}\text{Mg}$			$^{26}\text{Al} \rightarrow ^{26}\text{Mg}$			$^{26}\text{Mg} \rightarrow ^{26}\text{Al}$		
pt	$\log \beta^+$	$\log \epsilon^-$	$\log \nu$	$\log \beta^-$	$\log \epsilon^+$	pt	$\log \beta^+$	$\log \epsilon^-$	$\log \nu$	$\log \beta^-$	$\log \epsilon^+$
1	-40.077	-26.377	-26.940	-1.785	-6.738	1	-3.073	-6.964	-2.806	-25.975	-22.996
2	-13.864	-10.336	-10.362	-1.723	-3.672	2	-2.324	-3.744	-2.018	-10.600	-8.597
3	4.924	-3.300	-2.696	-1.414	-1.389	3	-1.676	-0.959	-0.144	-2.879	-1.295
4	1.699	4.588	6.238	2.607	4.704	4	1.482	4.872	6.519	1.447	4.833
5	40.077	-20.561	-21.126	-1.856	-12.558	5	-3.073	-3.119	-2.325	-28.039	-28.815
6	-13.861	-8.625	-8.670	-1.777	-5.376	6	-2.323	-2.275	-1.501	-11.009	-10.312
7	-4.914	-3.203	-2.600	-1.421	-1.484	7	-1.669	-0.864	-0.055	-2.882	-2.026
8	1.699	4.588	6.238	2.607	4.704	8	1.482	4.872	6.519	1.447	4.833
9	40.077	3.686	4.577	-99.999	-99.999	9	-3.073	4.600	5.745	-99.999	-99.999
10	-13.861	3.692	4.587	-33.464	-43.854	10	-2.322	4.613	5.765	-45.902	-48.790
11	-4.871	3.737	4.666	-8.805	-13.382	11	-1.639	4.653	5.832	-12.336	-13.935
12	1.828	5.285	6.946	2.264	3.982	12	1.624	5.567	7.228	1.019	4.111

$^{25}\text{Ne} \rightarrow ^{25}\text{Na}$			$^{26}\text{Mg} \rightarrow ^{26}\text{Na}$			$^{27}\text{P} \rightarrow ^{27}\text{Si}$			$^{27}\text{Si} \rightarrow ^{27}\text{P}$		
pt	$\log \beta^+$	$\log \epsilon^-$	$\log \nu$	$\log \beta^-$	$\log \epsilon^+$	pt	$\log \beta^+$	$\log \epsilon^-$	$\log \nu$	$\log \beta^-$	$\log \epsilon^+$
1	-55.291	-43.072	-43.848	0.074	-5.801	1	-66.311	-52.346	-52.921	-0.099	-5.948
2	-19.621	-15.945	-16.023	0.075	-2.833	2	-21.908	-17.893	-17.959	-0.083	-2.959
3	-6.881	-4.603	-4.105	1.056	-0.444	3	-6.638	-4.679	-4.150	0.273	-0.921
4	0.880	4.461	6.093	2.348	5.009	4	-2.079	4.484	6.116	2.520	4.754
5	-55.291	-37.252	-37.828	0.061	-11.621	5	-66.311	-46.526	-47.101	-0.118	-11.767
6	-19.617	-14.229	-14.307	0.063	-4.536	6	-21.906	-16.178	-16.254	-0.096	-4.662
7	-6.872	-4.504	-4.007	1.054	-0.537	7	-6.627	-4.580	-4.052	0.271	-1.015
8	0.880	4.462	6.093	2.348	5.009	8	-2.079	4.484	6.116	2.520	4.754
9	-55.291	3.982	4.983	-83.429	-99.999	9	-66.311	3.901	4.825	-74.011	-99.999
10	-19.616	3.986	4.989	-27.482	-43.014	10	-21.906	3.904	4.831	-25.367	-43.140
11	-6.831	4.008	5.032	-7.063	-12.426	11	-6.580	3.946	4.905	-7.133	-12.906
12	1.027	5.161	6.805	1.957	4.288	12	2.172	5.187	6.828	2.151	4.035

$^{26}\text{Si} \rightarrow ^{26}\text{Al}$			$^{26}\text{Al} \rightarrow ^{26}\text{Si}$		
pt	$\log \beta^+$	$\log \epsilon^-$	$\log \nu$	$\log \beta^-$	$\log \epsilon^+$
1	-0.444	-4.379	-0.137	-35.360	-27.835
2	-0.445	-2.000	-0.111	-15.228	-10.826
3	-0.293	-0.049	0.923	-4.959	-3.575
4	2.579	5.255	6.942	-0.347	4.380
5	-0.444	-0.595	0.293	-36.483	-33.654
6	-0.444	-0.558	0.332	-15.504	-12.542
7	0.287	0.045	1.001	-4.967	-3.673
8	2.579	5.255	6.942	-0.347	4.380
9	-0.444	5.073	6.353	-99.999	-99.999
10	-0.443	5.074	6.354	-50.346	-51.020
11	-0.265	5.029	6.306	-15.509	-15.867
12	2.703	5.940	7.643	-0.807	3.655

TABLE 3—Continued

		$^{27}\text{Si} \rightarrow ^{27}\text{Al}$				$^{27}\text{Al} \rightarrow ^{27}\text{Si}$				$^{28}\text{S} \rightarrow ^{28}\text{P}$				$^{28}\text{P} \rightarrow ^{28}\text{S}$			
pt	$\log \beta^+$	$\log \epsilon^-$	$\log \nu$	$\log \beta^-$	$\log \epsilon^+$	$\log \bar{\nu}$	$\log \beta^-$	$\log \epsilon^+$	$\log \bar{\nu}$	$\log \beta^+$	$\log \epsilon^-$	$\log \nu$	$\log \beta^-$	$\log \epsilon^+$	$\log \bar{\nu}$		
1	-0.738	4.744	-0.415	-31.897	-25.882	-26.452				0.491	4.098	1.083	-99.999	-59.173	-59.749		
2	-0.744	-2.374	-0.397	-14.006	-9.676	-9.738				0.498	-1.757	1.100	-33.342	-21.075	-21.153		
3	-0.752	-0.370	0.561	-4.033	-2.767	-2.214				1.881	0.527	2.767	-8.717	-5.984	-5.510		
4	2.217	5.078	6.745	0.859	4.561	6.189				2.797	5.451	7.141	1.038	4.275	5.888		
5	-0.738	-0.964	-0.022	-34.040	-31.702	-32.270				0.491	-0.346	1.183	-99.999	-64.993	-65.568		
6	-0.742	-0.933	0.009	-14.556	-11.391	-11.453				0.499	-0.328	1.202	-33.347	-22.791	-22.868		
7	-0.745	-0.276	0.645	-4.037	-2.866	-2.307				1.381	0.619	2.777	-8.719	-6.083	-5.608		
8	2.217	5.078	6.745	0.859	4.561	6.189				2.797	5.451	7.141	1.038	4.275	5.888		
9	-0.738	4.837	6.063	-99.999	-99.999	-99.999				0.491	5.025	6.285	-99.999	-99.999	-99.999		
10	-0.742	4.837	6.063	-48.403	-49.869	-48.530				0.499	5.023	6.283	-59.834	-61.269	-59.951		
11	-0.716	4.831	6.059	-13.831	-14.778	-13.477				1.884	5.076	6.412	-17.350	-17.996	-16.911		
12	2.342	5.768	7.450	0.421	3.837	5.462				2.921	6.136	7.841	0.632	3.549	5.160		

		$^{27}\text{Mg} \rightarrow ^{27}\text{Al}$				$^{27}\text{Al} \rightarrow ^{27}\text{Mg}$				$^{28}\text{Si} \rightarrow ^{28}\text{P}$				$^{28}\text{P} \rightarrow ^{28}\text{Si}$			
pt	$\log \beta^+$	$\log \epsilon^-$	$\log \nu$	$\log \beta^-$	$\log \epsilon^+$	$\log \bar{\nu}$	$\log \beta^-$	$\log \epsilon^+$	$\log \bar{\nu}$	$\log \beta^+$	$\log \epsilon^-$	$\log \nu$	$\log \beta^-$	$\log \epsilon^+$	$\log \bar{\nu}$		
1	-26.749	-21.087	-21.642	-2.781	-7.045	-2.761				0.443	4.285	1.143	-99.999	-72.501	-73.075		
2	-12.636	-9.166	-9.192	-2.568	-3.948	-2.355				0.538	-1.936	1.291	-44.074	-24.235	-24.308		
3	-4.743	-2.444	-1.917	-0.119	-0.951	0.552				1.455	0.205	2.365	-10.185	-6.041	-5.558		
4	2.370	4.773	6.433	1.089	4.699	6.339				2.853	5.314	7.013	1.729	4.274	5.884		
5	-26.748	-15.270	-15.827	-3.047	-12.864	-3.155				0.443	-0.526	1.204	-99.999	-78.520	-78.894		
6	-12.628	-7.458	-7.485	-2.686	-5.654	-2.520				0.539	-0.505	1.338	-44.075	-25.950	-26.024		
7	-4.734	-2.345	-1.819	-0.123	-1.045	0.524				1.455	0.297	2.375	-10.185	-6.140	-5.657		
8	2.370	4.773	6.433	1.089	4.698	6.339				2.853	5.314	7.013	1.729	4.274	5.884		
9	-26.748	4.576	5.724	-99.999	-99.999	-99.999				0.443	4.693	6.013	-99.999	-99.999	-99.999		
10	-12.628	4.577	5.727	-35.612	-44.131	-35.756				0.539	4.686	6.006	-62.566	-64.428	-62.685		
11	-4.691	4.591	5.753	-10.032	-12.938	-9.757				1.458	4.733	6.092	-16.721	-18.053	-16.340		
12	2.472	5.467	7.139	0.649	3.976	5.612				2.971	5.997	7.711	1.377	3.548	5.156		

		$^{27}\text{Mg} \rightarrow ^{27}\text{Na}$				$^{27}\text{Na} \rightarrow ^{27}\text{Mg}$				$^{28}\text{Si} \rightarrow ^{28}\text{Al}$				$^{28}\text{Al} \rightarrow ^{28}\text{Si}$			
pt	$\log \beta^+$	$\log \epsilon^-$	$\log \nu$	$\log \beta^-$	$\log \epsilon^+$	$\log \bar{\nu}$	$\log \beta^-$	$\log \epsilon^+$	$\log \bar{\nu}$	$\log \beta^+$	$\log \epsilon^-$	$\log \nu$	$\log \beta^-$	$\log \epsilon^+$	$\log \bar{\nu}$		
1	-64.586	-50.586	-51.163	0.469	-5.577	1.067				-35.899	-29.983	-30.550	-2.341	-7.264	-2.130		
2	-21.790	-17.529	-17.611	0.469	-2.610	1.069				-14.153	-11.298	-11.351	-2.324	-4.238	-2.081		
3	-7.173	-4.936	-4.426	0.593	-0.601	1.341				-4.389	-2.850	-2.253	-0.775	-1.613	-0.055		
4	1.656	4.334	5.938	3.330	5.240	6.949				2.579	4.819	6.473	1.508	4.648	6.299		
5	-64.586	-44.766	-45.344	0.458	-11.396	1.049				-35.899	-24.165	-24.732	-2.441	-13.083	-2.288		
6	-21.786	-15.814	-15.896	0.460	-4.314	1.053				-14.143	-9.584	-9.638	-2.398	-5.942	-2.200		
7	-7.162	-4.837	-4.328	0.591	-0.695	1.328				-4.380	-2.753	-2.156	-0.778	-1.708	-0.077		
8	1.656	4.334	5.938	3.330	5.240	6.949				2.579	4.819	6.473	1.508	4.648	6.299		
9	-64.586	3.664	4.504	-75.274	-99.999	-75.866				-35.899	4.524	5.613	-97.858	-99.999	-98.454		
10	-21.786	3.673	4.520	-25.254	-42.791	-25.380				-14.143	4.526	5.617	-33.426	-44.420	-33.565		
11	-7.118	3.734	4.634	-6.430	-12.585	-6.076				1.434	4.566	5.665	-9.933	-13.605	-9.633		
12	1.750	5.045	6.656	2.981	4.522	6.228				2.670	5.514	7.180	1.089	3.927	5.573		

TABLE 3—Continued

$^{28}\text{Al} \rightarrow ^{28}\text{Mg}$				$^{28}\text{Mg} \rightarrow ^{28}\text{Al}$				$^{29}\text{P} \rightarrow ^{29}\text{Si}$				$^{29}\text{Si} \rightarrow ^{29}\text{P}$			
pt	$\log \beta^+$	$\log \epsilon^-$	$\log \nu$	$\log \beta^-$	$\log \epsilon^+$	$\log \bar{\nu}$		pt	$\log \beta^+$	$\log \epsilon^-$	$\log \nu$	$\log \beta^-$	$\log \epsilon^+$	$\log \bar{\nu}$	
1	-31.851	-18.186	-18.695	-4.967	-7.310	-5.462		1	-0.706	-4.791	-0.360	-34.243	-26.617	-27.188	
2	-11.756	-8.692	-8.663	-3.478	-4.101	-3.131		2	-0.707	-2.429	-0.541	-14.276	-9.969	-10.036	
3	-4.657	-2.895	-2.335	-0.082	-1.052	0.621		3	-0.676	-0.421	0.550	-4.112	-2.918	-2.367	
4	2.032	4.774	6.423	1.713	4.915	6.565		4	2.220	5.159	6.828	1.019	4.606	6.235	
5	-31.851	-12.697	-13.100	-7.371	-13.129	-7.919		5	-0.706	-1.023	-0.019	-35.160	-32.436	-33.007	
6	-11.754	-7.026	-6.977	-3.560	-5.808	-3.347		6	-0.706	-0.992	0.010	-14.654	-11.684	-11.752	
7	-4.647	-2.797	-2.238	-0.123	-1.147	0.563		7	-0.670	-0.328	0.630	-4.115	-3.017	-2.458	
8	2.032	4.774	6.423	1.713	4.914	6.565		8	2.220	5.159	6.828	1.019	4.606	6.234	
9	-31.851	4.473	5.577	-99.999	-99.999	-99.999		9	-0.706	4.838	6.035	-99.999	-99.999	-99.999	
10	-11.754	4.474	5.580	-36.143	-44.285	-36.282		10	-0.706	4.840	6.037	-48.487	-50.162	-48.618	
11	-4.608	4.491	5.611	-9.449	-13.040	-9.149		11	-0.645	4.850	6.055	-13.752	-14.929	-13.422	
12	2.145	5.470	7.132	1.288	4.193	5.839		12	2.350	5.848	7.532	0.586	3.883	5.507	

$^{28}\text{Mg} \rightarrow ^{28}\text{Na}$				$^{28}\text{Na} \rightarrow ^{28}\text{Mg}$				$^{29}\text{Si} \rightarrow ^{29}\text{Al}$				$^{29}\text{Al} \rightarrow ^{29}\text{Si}$			
pt	$\log \beta^+$	$\log \epsilon^-$	$\log \nu$	$\log \beta^-$	$\log \epsilon^+$	$\log \bar{\nu}$		pt	$\log \beta^+$	$\log \epsilon^-$	$\log \nu$	$\log \beta^-$	$\log \epsilon^+$	$\log \bar{\nu}$	
1	-89.238	-75.102	-75.683	1.235	-5.459	2.048		1	-30.847	-25.705	-26.263	-2.719	-7.250	-2.590	
2	-29.708	-25.492	-25.584	1.173	-2.572	1.987		2	-13.236	-10.217	-10.232	-2.691	-4.148	-2.503	
3	-9.236	-6.631	-6.165	2.012	-0.119	2.919		3	-4.536	-2.950	-2.346	-0.798	-1.455	-0.016	
4	1.424	4.420	6.003	3.937	5.668	7.397		4	2.437	4.800	6.460	1.853	4.724	6.372	
5	-89.238	-69.282	-69.864	1.233	-11.279	2.043		5	-30.847	-19.888	-20.448	-2.883	-13.070	-2.825	
6	-29.706	-23.776	-23.869	1.171	-4.275	1.983		6	-13.222	-8.513	-8.532	-2.801	-5.854	-2.678	
7	-9.225	-6.532	-6.067	2.011	-0.212	2.917		7	-4.528	-2.852	-2.249	-0.801	-1.551	-0.040	
8	1.424	4.421	6.003	3.937	5.668	7.397		8	2.437	4.800	6.460	1.853	4.723	6.372	
9	-89.238	3.690	4.469	-50.373	-99.999	-50.965		9	-30.847	4.410	5.460	-99.999	-99.999	-99.999	
10	-29.706	3.696	4.478	-16.992	-42.753	-17.117		10	-13.221	4.413	5.465	-34.324	-44.331	-34.458	
11	-9.177	3.737	4.565	-3.994	-12.098	-3.634		11	-4.495	4.444	5.519	-9.525	-13.448	-9.205	
12	1.513	5.136	6.725	3.600	4.952	6.677		12	2.539	5.495	7.166	1.447	4.001	5.646	

$^{29}\text{S} \rightarrow ^{29}\text{P}$				$^{29}\text{P} \rightarrow ^{29}\text{S}$				$^{29}\text{Mg} \rightarrow ^{29}\text{Al}$				$^{29}\text{Al} \rightarrow ^{29}\text{Mg}$			
pt	$\log \beta^+$	$\log \epsilon^-$	$\log \nu$	$\log \beta^-$	$\log \epsilon^+$	$\log \bar{\nu}$		pt	$\log \beta^+$	$\log \epsilon^-$	$\log \nu$	$\log \beta^-$	$\log \epsilon^+$	$\log \bar{\nu}$	
1	0.674	-3.976	1.319	-99.999	-69.884	-70.460		1	-59.256	-44.083	-44.657	-0.172	-5.975	0.374	
2	0.675	-1.631	1.323	-39.297	-23.545	-23.623		2	-20.282	-15.998	-16.073	-0.099	-2.970	0.476	
3	1.276	0.309	2.212	-9.542	-6.362	-5.871		3	-6.714	-3.918	-3.439	1.471	-0.015	2.199	
4	3.311	5.595	7.311	1.108	4.188	5.781		4	1.916	4.609	6.231	2.470	5.214	6.893	
5	0.674	-0.224	1.400	-99.999	-75.704	-76.280		5	-59.256	-38.268	-38.842	-0.190	-11.794	0.349	
6	0.675	-0.201	1.407	-39.300	-25.261	-25.339		6	-20.280	-14.283	-14.358	-0.112	-4.674	0.457	
7	1.276	0.401	2.226	-9.543	-6.461	-5.970		7	-6.704	-3.819	-3.341	1.469	-0.108	2.190	
8	3.311	5.595	7.311	1.108	4.188	5.781		8	1.916	4.609	6.231	2.470	5.214	6.893	
9	0.674	4.995	6.310	-99.999	-99.999	-99.999		9	-59.256	4.333	5.382	-82.412	-99.999	-83.007	
10	0.675	4.996	6.311	-62.319	-63.738	-62.431		10	-20.280	4.336	5.385	-27.402	-43.151	-27.537	
11	1.280	4.954	6.272	-17.279	-18.375	-16.894		11	-6.660	4.355	5.422	-7.177	-11.996	-6.859	
12	3.422	6.274	8.006	0.725	3.461	5.052		12	2.013	5.312	6.945	2.064	4.495	6.169	

TABLE 3—Continued

		^{29}Ne			^{29}Mg			^{30}Al			^{30}Si		
pt		$\log \beta^+$	$\log \epsilon^-$	$\log \nu$	$\log \beta^-$	$\log \epsilon^+$	$\log \bar{\nu}$	$\log \beta^+$	$\log \epsilon^-$	$\log \nu$	$\log \beta^-$	$\log \epsilon^+$	$\log \bar{\nu}$
1	-86.944	-73.559	-74.140	1.127	-5.655	1.950		-65.168	-48.698	-49.268	-0.689	-6.171	-0.258
2	-29.490	-25.542	-25.636	1.140	-2.700	1.965		-21.353	-16.945	-17.011	-0.783	-3.289	-0.307
3	-9.472	-6.791	-6.327	2.096	-0.044	2.996		-6.142	-4.164	-3.652	0.596	-0.903	1.358
4	1.733	4.272	5.896	3.142	5.048	6.743		1.849	4.622	6.229	2.532	5.331	7.024
5	-86.944	-67.739	-68.321	1.125	-11.475	1.961		-65.168	-42.879	-43.450	-0.722	-11.991	-0.306
6	-29.487	-23.826	-23.920	1.138	-4.403	1.961		-21.351	-15.228	-15.295	-0.808	-4.993	-0.343
7	-9.480	-6.693	-6.229	2.096	-0.137	2.994		-6.133	-4.065	-3.555	0.594	-0.996	1.350
8	1.733	4.272	5.896	3.142	5.048	6.743		1.849	4.622	6.229	2.532	5.331	7.024
9	-86.944	3.447	4.248	-52.436	-99.999	-53.029		-65.168	4.332	5.345	-77.806	-99.999	-78.401
10	-29.487	3.452	4.257	-17.396	-42.881	-17.522		-21.351	4.334	5.349	-26.583	-43.470	-26.715
11	-9.408	3.499	4.346	-4.093	-12.024	-3.735		-6.096	4.357	5.392	-7.610	-12.886	-7.282
12	1.832	4.978	6.610	2.799	4.329	6.021		1.937	5.330	6.946	2.438	4.613	6.301

		^{30}P			^{30}S			^{31}Cl			^{31}S		
pt		$\log \beta^+$	$\log \epsilon^-$	$\log \nu$	$\log \beta^-$	$\log \epsilon^+$	$\log \bar{\nu}$	$\log \beta^+$	$\log \epsilon^-$	$\log \nu$	$\log \beta^-$	$\log \epsilon^+$	$\log \bar{\nu}$
1	-0.202	-4.343	0.195	-51.088	-32.712	-33.283		0.405	-4.118	0.977	-84.741	-60.861	-61.436
2	-0.203	-1.982	0.209	-16.830	-12.070	-12.136		0.408	-1.789	0.991	-27.106	-20.778	-20.854
3	-0.134	0.027	1.023	-5.063	-3.805	-3.238		0.507	0.062	1.418	-7.073	-5.662	-5.144
4	3.277	5.629	7.340	-0.688	4.286	5.876		3.449	5.451	7.165	-0.096	4.181	5.781
5	-0.202	-0.577	0.480	-51.133	-38.531	-39.102		0.405	-0.374	1.096	-84.766	-66.681	-67.256
6	-0.202	-0.545	0.506	-16.868	-13.785	-13.851		0.409	-0.361	1.110	-27.127	-22.493	-22.569
7	-0.129	0.120	1.100	-5.072	-3.903	-3.353		0.510	0.155	1.462	-7.079	-5.761	-5.240
8	3.277	5.629	7.340	-0.688	4.286	5.876		3.449	5.451	7.165	-0.096	4.181	5.781
9	-0.202	5.157	6.422	-99.999	-99.999	-99.999		0.405	5.162	6.424	-99.999	-99.999	-99.999
10	-0.202	5.158	6.423	-51.442	-52.263	-51.535		0.409	5.160	6.422	-60.032	-60.971	-60.131
11	-0.107	5.152	6.422	-15.663	-15.816	-15.073		0.519	5.131	6.386	-17.287	-17.674	-16.810
12	3.390	6.308	8.036	-1.149	3.558	5.147		3.543	6.131	7.860	-0.546	3.455	5.052

		^{30}Si			^{31}P			^{31}S					
pt		$\log \beta^+$	$\log \epsilon^-$	$\log \nu$	$\log \beta^-$	$\log \epsilon^+$	$\log \bar{\nu}$	$\log \beta^+$	$\log \epsilon^-$	$\log \nu$	$\log \beta^-$	$\log \epsilon^+$	$\log \bar{\nu}$
1	-2.317	-6.000	-2.067	-29.240	-23.865	-24.423		-0.498	-4.674	-0.107	-34.907	-29.054	-29.625
2	-1.984	-3.405	-1.650	-11.883	-9.278	-9.308		-0.500	-2.309	-0.094	-15.089	-10.714	-10.777
3	-1.236	-0.856	0.048	-3.899	-2.508	-1.733		-0.442	-0.272	0.716	-4.312	-3.037	-2.485
4	1.762	5.040	6.704	1.587	4.680	6.311		2.288	5.231	6.904	0.629	4.544	6.164
5	-2.317	-2.163	-1.463	-30.684	-29.684	-30.189		-0.498	-0.905	0.168	-37.761	-34.874	-35.444
6	-1.982	-1.939	-1.146	-12.168	-10.993	-10.999		-0.499	-0.870	0.193	-15.379	-12.430	-12.492
7	-1.231	-0.762	0.129	-3.903	-2.406	-1.828		-0.437	-0.179	0.794	-4.317	-3.136	-2.579
8	1.762	5.040	6.704	1.587	4.680	6.310		2.288	5.231	6.904	0.629	4.544	6.164
9	-2.317	4.520	5.645	-99.999	-99.999	-99.999		-0.498	4.936	6.168	-99.999	-99.999	-99.999
10	-1.982	4.525	5.656	-46.637	-49.471	-46.770		-0.499	4.936	6.169	-49.491	-50.907	-49.619
11	-1.210	4.563	5.726	-12.501	-14.316	-12.171		-0.416	4.919	6.155	-14.203	-15.047	-13.841
12	1.906	5.731	7.410	1.183	3.956	5.584		2.417	5.918	7.607	0.189	3.820	5.436

TABLE 3—Continued

$^{31}\text{P} \rightarrow ^{31}\text{Si}$				$^{31}\text{Si} \rightarrow ^{31}\text{P}$				$^{32}\text{Cl} \rightarrow ^{32}\text{S}$				$^{32}\text{S} \rightarrow ^{32}\text{Cl}$			
pt	$\log \beta^+$	$\log \epsilon^-$	$\log \nu$	$\log \beta^-$	$\log \epsilon^+$	$\log \bar{\nu}$		pt	$\log \beta^+$	$\log \epsilon^-$	$\log \nu$	$\log \beta^-$	$\log \epsilon^+$	$\log \bar{\nu}$	
1	-20.936	-15.731	-16.277	-4.064	-8.091	-4.097		1	0.322	-4.273	0.832	-97.594	-64.458	-65.033	
2	-9.517	-7.427	-7.396	-3.902	-4.846	-3.777		2	0.287	-1.947	0.894	-30.626	-21.691	-21.767	
3	-3.373	-2.293	-1.578	-2.359	-1.823	-1.036		3	0.291	-0.070	1.233	-7.251	-5.664	-5.152	
4	1.884	4.810	6.458	2.349	4.800	6.458		4	3.431	5.499	7.221	0.301	4.131	5.722	
5	-20.936	-9.959	-10.501	-4.414	-13.910	-4.605		5	0.322	-0.529	1.028	-97.605	-70.277	-70.853	
6	-9.506	-5.746	-5.720	-4.090	-6.553	-4.114		6	0.287	-0.519	1.000	-30.635	-23.406	-23.483	
7	-3.365	-2.197	-1.484	-2.363	-1.920	-1.108		7	0.293	0.023	1.281	-7.254	-5.763	-5.247	
8	1.884	4.810	6.458	2.349	4.800	6.458		8	3.431	5.499	7.221	0.301	4.131	5.722	
9	-20.936	4.257	5.249	-99.999	-99.999	-99.999		9	0.322	4.955	6.203	-99.999	-99.999	-99.999	
10	-9.505	4.260	5.254	-37.640	-45.031	-37.769		10	0.287	4.953	6.200	-60.592	-61.884	-60.710	
11	-3.333	4.296	5.321	-10.284	-13.823	-9.944		11	0.304	4.934	6.175	-16.755	-17.676	-16.394	
12	2.008	5.508	7.167	1.966	4.078	5.733		12	3.531	6.178	7.915	-0.129	3.404	4.993	

$^{31}\text{Si} \rightarrow ^{31}\text{Al}$				$^{31}\text{Al} \rightarrow ^{31}\text{Si}$				$^{32}\text{P} \rightarrow ^{32}\text{Si}$				$^{32}\text{Si} \rightarrow ^{32}\text{P}$			
pt	$\log \beta^+$	$\log \epsilon^-$	$\log \nu$	$\log \beta^-$	$\log \epsilon^+$	$\log \bar{\nu}$		pt	$\log \beta^+$	$\log \epsilon^-$	$\log \nu$	$\log \beta^-$	$\log \epsilon^+$	$\log \bar{\nu}$	
1	-62.311	-45.794	-46.371	-0.112	-6.137	0.471		1	-23.666	-18.087	-18.267	-6.435	-8.653	-6.411	
2	-20.960	-16.444	-16.525	-0.083	-3.146	0.511		2	-10.054	-7.787	-7.684	-4.061	-5.296	-3.802	
3	-6.628	-4.111	-3.633	1.235	-0.305	1.971		3	-3.141	-1.974	-1.301	-2.201	-2.138	-1.220	
4	1.815	4.556	6.176	2.501	5.171	6.851		4	2.636	5.014	6.708	1.303	4.411	6.025	
5	-62.311	-39.975	-40.552	-0.124	-11.957	0.451		5	-23.666	-13.137	-13.559	-6.730	-14.472	-6.838	
6	-20.958	-14.728	-14.810	-0.094	-4.849	0.494		6	-10.047	-6.183	-6.058	-4.127	-7.005	-3.928	
7	-6.619	-4.012	-3.535	1.233	-0.398	1.963		7	-3.135	-1.881	-1.209	-2.206	-2.234	-1.281	
8	1.815	4.556	6.176	2.501	5.171	6.851		8	2.636	5.014	6.708	1.303	4.411	6.025	
9	-62.311	4.271	5.310	-80.827	-99.999	-81.422		9	-23.666	4.528	5.629	-99.999	-99.999	-99.999	
10	-20.958	4.273	5.313	-27.107	-43.327	-27.240		10	-10.047	4.530	5.632	-38.037	-45.482	-38.172	
11	-6.580	4.292	5.348	-7.256	-12.287	-6.935		11	-3.107	4.510	5.624	-11.203	-14.136	-10.885	
12	1.912	5.260	6.890	2.099	4.452	6.127		12	2.747	5.699	7.407	0.897	3.685	5.297	

$^{32}\text{Ar} \rightarrow ^{32}\text{Cl}$				$^{32}\text{Cl} \rightarrow ^{32}\text{Ar}$			
pt	$\log \beta^+$	$\log \epsilon^-$	$\log \nu$	$\log \beta^-$	$\log \epsilon^+$	$\log \bar{\nu}$	
1	0.308	-4.058	0.801	-69.276	-57.766	-58.341	
2	0.309	-1.725	0.812	-23.703	-20.533	-20.609	
3	0.549	0.150	1.515	-7.765	-6.202	-5.666	
4	3.190	5.397	7.093	-1.196	4.319	5.927	
5	0.308	-0.319	0.982	-69.416	-63.586	-64.161	
6	0.310	-0.298	0.998	-23.807	-22.249	-22.307	
7	0.551	0.243	1.555	-7.781	-6.300	-5.763	
8	3.190	5.397	7.093	-1.196	4.319	5.927	
9	0.308	5.305	6.593	-99.999	-99.999	-99.999	
10	0.310	5.306	6.595	-60.478	-60.727	-60.439	
11	0.559	5.276	6.561	-18.833	-18.212	-17.647	
12	3.287	6.083	7.793	-1.672	3.594	5.199	

TABLE 3—Continued

$^{33}\text{Ar} \rightarrow ^{33}\text{Cl}$		$^{33}\text{Cl} \rightarrow ^{33}\text{Ar}$		$^{33}\text{P} \rightarrow ^{33}\text{Si}$		$^{33}\text{Si} \rightarrow ^{33}\text{P}$	
pt	$\log \beta^+$	$\log \epsilon^-$	$\log \nu$	$\log \beta^-$	$\log \epsilon^+$	$\log \nu$	$\log \bar{\nu}$
1	0.652	-3.973	1.297	-80.962	-59.808	-60.383	-0.586
2	0.653	-1.642	1.302	-26.498	-20.761	-20.836	-0.580
3	0.761	0.135	1.666	-7.379	-6.004	-5.487	-0.045
4	3.083	5.352	7.059	-0.375	4.088	5.687	6.746
5	0.652	-0.233	1.381	-80.986	-65.628	-66.203	-0.683
6	0.653	-0.215	1.388	-26.519	-22.476	-22.552	-0.652
7	0.762	0.227	1.697	-7.396	-6.103	-5.583	-0.012
8	3.083	5.352	7.059	-0.375	4.088	5.687	6.746
9	0.652	5.173	6.478	-99.999	-99.999	-99.999	-91.809
10	0.653	5.172	6.477	-60.378	-60.954	-60.415	-43.307
11	0.769	5.087	6.377	-17.819	-18.015	-17.256	-7.687
12	3.188	6.032	7.755	-0.832	3.362	4.959	6.024

$^{33}\text{Cl} \rightarrow ^{33}\text{S}$		$^{33}\text{S} \rightarrow ^{33}\text{Cl}$		$^{34}\text{Ar} \rightarrow ^{34}\text{Cl}$		$^{34}\text{Cl} \rightarrow ^{34}\text{Ar}$	
pt	$\log \beta^+$	$\log \epsilon^-$	$\log \nu$	$\log \beta^-$	$\log \epsilon^+$	$\log \nu$	$\log \bar{\nu}$
1	-0.538	-4.659	-0.144	-35.045	-29.772	-30.343	-32.700
2	-0.539	-2.305	-0.129	-14.945	-10.967	-11.033	-12.192
3	-0.521	-0.272	0.694	-4.229	-3.141	-2.572	-3.336
4	2.317	5.050	6.718	-0.226	4.570	6.193	5.850
5	-0.538	-0.960	0.154	-38.155	-35.591	-36.162	-38.431
6	-0.538	-0.869	0.179	-15.014	-12.683	-12.744	-13.888
7	-0.516	-0.179	0.775	-4.239	-3.240	-2.666	-3.434
8	2.317	5.050	6.718	-0.226	4.569	6.193	5.850
9	-0.538	4.967	6.223	-99.999	-99.999	-99.999	-99.999
10	-0.538	4.967	6.224	-50.257	-51.161	-50.369	-52.351
11	-0.492	4.964	6.226	-14.980	-15.151	-14.401	-15.344
12	2.433	5.739	7.423	-0.692	3.846	5.466	5.121

$^{33}\text{S} \rightarrow ^{33}\text{P}$		$^{33}\text{P} \rightarrow ^{33}\text{S}$		$^{34}\text{Cl} \rightarrow ^{34}\text{S}$		$^{34}\text{S} \rightarrow ^{34}\text{Cl}$	
pt	$\log \beta^+$	$\log \epsilon^-$	$\log \nu$	$\log \beta^-$	$\log \epsilon^+$	$\log \nu$	$\log \bar{\nu}$
1	-16.890	-10.328	-10.818	-6.500	-8.055	-7.189	-29.687
2	-8.947	-5.890	-5.804	-5.104	-4.745	-4.401	-10.662
3	-3.255	-2.075	-1.409	-1.721	-1.850	-0.822	-2.055
4	-2.343	5.075	6.759	1.093	4.497	6.112	6.174
5	-16.890	-5.118	-5.428	-9.459	-13.874	-10.177	-35.506
6	-8.937	-4.277	-4.160	-5.277	-6.453	-5.218	-12.364
7	-3.249	-1.978	-1.315	-1.725	-1.946	-0.871	-2.142
8	-2.343	5.075	6.760	1.093	4.497	6.112	6.174
9	-16.890	4.469	5.587	-99.999	-99.999	-99.999	-99.999
10	-8.937	4.470	5.588	-39.578	-44.931	-39.717	-50.790
11	-3.221	4.465	5.595	-11.029	-13.846	-10.726	-14.704
12	2.466	5.760	7.461	0.672	3.772	5.384	5.446

TABLE 3—Continued

$^{34}\text{S} \rightarrow$		$^{34}\text{P} \rightarrow$		$^{34}\text{Si} \rightarrow$		$^{34}\text{S} \rightarrow$		$^{35}\text{Ar} \rightarrow$		$^{35}\text{Cl} \rightarrow$		$^{35}\text{Cl} \rightarrow$		$^{35}\text{Ar} \rightarrow$					
pt	$\log \beta^+$	$\log \epsilon^-$	$\log \nu$	$\log \beta^-$	$\log \epsilon^+$	$\log \bar{\nu}$	$\log \beta^+$	$\log \epsilon^-$	$\log \nu$	$\log \beta^-$	$\log \epsilon^+$	$\log \bar{\nu}$	pt	$\log \beta^+$	$\log \epsilon^-$	$\log \nu$	$\log \beta^-$	$\log \epsilon^+$	$\log \bar{\nu}$
1	-52.827	-33.574	-34.139	-1.221	-6.620	-0.791	-0.367	4.635	0.067	-37.059	-31.703	-32.276	1	-0.367	4.635	0.067	-37.059	-31.703	-32.276
2	-17.299	-12.340	-12.386	-1.302	-3.597	-0.877	-0.368	-2.291	0.078	-13.611	-11.594	-11.661	2	-0.368	-2.291	0.078	-13.611	-11.594	-11.661
3	-4.936	-3.383	-2.799	-1.144	-1.368	-0.260	-0.337	0.116	6.918	-2.696	4.347	5.956	3	-0.337	0.116	6.918	-2.696	4.347	5.956
4	1.645	4.437	6.076	2.592	4.775	6.447	2.298	5.237	0.294	-37.967	-37.523	-37.933	4	2.298	5.237	0.294	-37.967	-37.523	-37.933
5	-52.827	-27.764	-28.328	-1.257	-12.440	-0.841	-0.367	0.889	0.313	-13.976	-13.309	-13.323	5	-0.367	0.889	0.313	-13.976	-13.309	-13.323
6	-17.298	-10.617	-10.666	-1.333	-5.302	-0.923	-0.333	0.021	0.899	-5.572	-3.351	-2.758	6	-0.333	0.021	0.899	-5.572	-3.351	-2.758
7	-4.929	-3.285	-2.702	-1.149	-1.463	-0.210	-0.333	0.021	6.918	-2.696	4.347	5.956	7	-0.333	0.021	6.918	-2.696	4.347	5.956
8	1.645	4.437	6.076	2.592	4.775	6.447	2.298	5.237	0.294	-37.967	-37.523	-37.933	8	2.298	5.237	0.294	-37.967	-37.523	-37.933
9	-52.827	-27.764	-28.328	-1.257	-12.440	-0.841	-0.367	0.889	0.313	-13.976	-13.309	-13.323	9	-0.367	0.889	0.313	-13.976	-13.309	-13.323
10	-17.298	-10.617	-10.666	-1.333	-5.302	-0.923	-0.333	0.021	6.918	-2.696	4.347	5.956	10	-0.367	0.889	0.313	-13.976	-13.309	-13.323
11	-4.899	3.856	4.835	-8.890	-13.358	-8.544	-0.314	5.006	6.307	-16.955	-15.259	-14.666	11	-0.314	5.006	6.307	-16.955	-15.259	-14.666
12	1.758	5.137	6.786	2.225	4.054	5.724	2.425	5.922	7.620	-3.185	3.622	5.227	12	2.425	5.922	7.620	-3.185	3.622	5.227

$^{34}\text{P} \rightarrow$		$^{34}\text{Si} \rightarrow$		$^{34}\text{S} \rightarrow$		$^{34}\text{P} \rightarrow$		$^{35}\text{S} \rightarrow$		$^{35}\text{Cl} \rightarrow$		$^{35}\text{S} \rightarrow$		$^{35}\text{Cl} \rightarrow$					
pt	$\log \beta^+$	$\log \epsilon^-$	$\log \nu$	$\log \beta^-$	$\log \epsilon^+$	$\log \bar{\nu}$	$\log \beta^+$	$\log \epsilon^-$	$\log \nu$	$\log \beta^-$	$\log \epsilon^+$	$\log \bar{\nu}$	pt	$\log \beta^+$	$\log \epsilon^-$	$\log \nu$	$\log \beta^-$	$\log \epsilon^+$	$\log \bar{\nu}$
1	-48.202	-30.113	-30.681	-0.583	-5.664	-0.335	-14.327	-9.676	-10.183	-7.000	-8.334	-7.729	1	-14.327	-9.676	-10.183	-7.000	-8.334	-7.729
2	-16.648	-11.415	-11.475	-0.585	-2.634	-0.328	-7.802	-5.755	-5.701	-5.925	-5.110	-4.787	2	-7.802	-5.755	-5.701	-5.925	-5.110	-4.787
3	-5.786	-3.601	-3.067	-0.518	-0.655	0.397	-3.112	-2.126	-1.396	-2.457	-2.110	-1.301	3	-3.112	-2.126	-1.396	-2.457	-2.110	-1.301
4	1.297	4.360	6.026	2.353	4.694	6.331	2.079	4.752	6.426	1.386	4.452	6.079	4	2.079	4.752	6.426	1.386	4.452	6.079
5	-48.202	-24.294	-24.862	-0.661	-11.483	-0.462	-14.327	-4.618	-4.882	-10.184	-14.154	-11.085	5	-14.327	-4.618	-4.882	-10.184	-14.154	-11.085
6	-16.646	-9.689	-9.759	-0.648	-4.338	-0.432	-7.791	-4.109	-4.031	-6.108	-6.818	-5.934	6	-7.791	-4.109	-4.031	-6.108	-6.818	-5.934
7	-5.779	-3.502	-2.969	-0.526	-0.749	0.335	-3.106	-2.030	-1.304	-2.460	-2.208	-1.367	7	-3.106	-2.030	-1.304	-2.460	-2.208	-1.367
8	1.297	4.360	6.026	2.353	4.694	6.331	2.079	4.752	6.426	1.386	4.452	6.079	8	2.079	4.752	6.426	1.386	4.452	6.079
9	-48.202	-24.294	-24.862	-0.661	-11.483	-0.462	-14.327	-4.618	-4.882	-10.184	-14.154	-11.085	9	-14.327	-4.618	-4.882	-10.184	-14.154	-11.085
10	-16.646	-9.689	-9.759	-0.648	-4.338	-0.432	-7.791	-4.109	-4.031	-6.108	-6.818	-5.934	10	-7.791	-4.109	-4.031	-6.108	-6.818	-5.934
11	-5.749	3.456	4.428	-8.188	-12.643	-7.835	-3.078	4.244	5.343	-40.044	-45.296	-40.179	11	-3.078	4.244	5.343	-40.044	-45.296	-40.179
12	1.434	5.051	6.731	2.001	3.970	5.605	2.198	5.441	7.129	0.976	3.728	5.352	12	2.198	5.441	7.129	0.976	3.728	5.352

$^{35}\text{K} \rightarrow$		$^{35}\text{Ar} \rightarrow$		$^{35}\text{S} \rightarrow$		$^{35}\text{P} \rightarrow$		$^{35}\text{S} \rightarrow$		$^{35}\text{P} \rightarrow$		$^{35}\text{S} \rightarrow$							
pt	$\log \beta^+$	$\log \epsilon^-$	$\log \nu$	$\log \beta^-$	$\log \epsilon^+$	$\log \bar{\nu}$	$\log \beta^+$	$\log \epsilon^-$	$\log \nu$	$\log \beta^-$	$\log \epsilon^+$	$\log \bar{\nu}$	pt	$\log \beta^+$	$\log \epsilon^-$	$\log \nu$	$\log \beta^-$	$\log \epsilon^+$	$\log \bar{\nu}$
1	0.592	-4.029	1.217	-99.999	-60.912	-61.488	-45.792	-26.859	-27.419	-1.809	-6.554	-1.667	1	-45.792	-26.859	-27.419	-1.809	-6.554	-1.667
2	0.591	-1.702	1.221	-99.999	-20.980	-21.057	-15.550	-10.652	-10.698	-1.795	-3.500	-1.611	2	-15.550	-10.652	-10.698	-1.795	-3.500	-1.611
3	0.500	0.239	1.455	-99.999	-5.768	-5.219	-4.952	-3.470	-2.886	-1.070	-1.349	-0.186	3	-4.952	-3.470	-2.886	-1.070	-1.349	-0.186
4	3.124	5.238	6.934	-99.999	4.037	5.643	1.209	4.228	5.872	2.337	4.794	6.456	4	1.209	4.228	5.872	2.337	4.794	6.456
5	0.592	-0.299	1.308	-99.999	-66.732	-67.308	-45.792	-21.039	-21.600	-2.029	-12.373	-1.983	5	-45.792	-21.039	-21.600	-2.029	-12.373	-1.983
6	0.592	-0.275	1.315	-99.999	-22.696	-22.773	-15.549	-8.937	-8.982	-1.933	-5.205	-1.812	6	-15.549	-8.937	-8.982	-1.933	-5.205	-1.812
7	0.503	0.333	1.506	-99.999	-5.866	-5.317	-4.945	-3.372	-2.790	-1.075	-1.444	-0.230	7	-4.945	-3.372	-2.790	-1.075	-1.444	-0.230
8	3.124	5.238	6.934	-99.999	4.037	5.643	1.209	4.228	5.872	2.337	4.794	6.456	8	1.209	4.228	5.872	2.337	4.794	6.456
9	0.592	5.248	6.569	-99.999	-99.999	-99.999	-45.792	3.704	4.704	-99.999	-99.999	-99.999	9	-45.792	3.704	4.704	-99.999	-99.999	-99.999
10	0.592	5.249	6.571	-99.999	-61.174	-61.250	-15.549	3.707	4.709	-33.572	-43.683	-33.703	10	-15.549	3.707	4.709	-33.572	-43.683	-33.703
11	0.513	5.220	6.538	-99.999	-17.776	-17.227	-4.915	3.729	4.756	-9.202	-13.339	-8.865	11	-4.915	3.729	4.756	-9.202	-13.339	-8.865
12	3.214	5.921	7.633	-99.999	3.311	4.915	1.333	4.925	6.581	1.953	4.073	5.732	12	1.333	4.925	6.581	1.953	4.073	5.732

TABLE 3—Continued

		$^{36}\text{Ca} \rightarrow ^{36}\text{K}$			$^{36}\text{K} \rightarrow ^{36}\text{Ca}$			$^{36}\text{Cl} \rightarrow ^{36}\text{S}$			$^{36}\text{S} \rightarrow ^{36}\text{Cl}$		
pt	$\log \beta^+$	$\log \epsilon^-$	$\log \nu$	$\log \beta^-$	$\log \epsilon^+$	$\log \bar{\nu}$	pt	$\log \beta^+$	$\log \epsilon^-$	$\log \nu$	$\log \beta^-$	$\log \epsilon^+$	$\log \bar{\nu}$
1	0.539	-3.910	1.065	-99.999	-57.024	-57.600	1	-10.261	-12.820	-10.366	-18.656	-14.910	-15.464
2	0.537	-1.981	1.072	-99.999	-20.128	-20.201	2	-6.155	-6.407	-5.742	-7.545	-6.911	-6.812
3	0.618	0.431	1.609	-99.999	-6.157	-5.608	3	-2.789	-2.336	-1.509	-2.066	-1.995	-1.995
4	2.832	5.234	6.909	-99.999	3.945	5.562	4	0.615	4.666	6.326	1.084	4.624	6.252
5	0.538	-0.181	1.218	-99.999	-62.843	-63.420	5	-10.261	-9.001	-8.541	-18.932	-20.730	-18.949
6	0.538	-0.152	1.229	-99.999	-21.843	-21.916	6	-6.147	-4.934	-4.431	-7.729	-8.627	-7.626
7	0.620	0.525	1.663	-99.999	-6.255	-5.706	7	-2.785	-2.240	-1.427	-2.070	-2.091	-1.153
8	2.832	5.234	6.909	-99.999	3.945	5.562	8	0.615	4.667	6.326	1.084	4.624	6.252
9	0.538	5.356	6.681	-99.999	-99.999	-99.999	9	-10.261	4.043	5.166	-99.999	-99.999	-99.999
10	0.538	5.357	6.682	-99.999	-60.321	-60.394	10	-6.146	4.045	5.170	-41.983	-47.105	-42.124
11	0.631	5.344	6.672	-99.999	-18.165	-17.617	11	-2.767	4.052	5.193	-11.428	-13.996	-11.132
12	2.925	5.921	7.612	-99.999	3.221	4.834	12	0.782	5.353	7.029	0.660	3.900	5.525

		$^{36}\text{Ar} \rightarrow ^{36}\text{K}$			$^{36}\text{K} \rightarrow ^{36}\text{Ar}$			$^{37}\text{Ca} \rightarrow ^{37}\text{K}$			$^{37}\text{K} \rightarrow ^{37}\text{Ca}$		
pt	$\log \beta^+$	$\log \epsilon^-$	$\log \nu$	$\log \beta^-$	$\log \epsilon^+$	$\log \bar{\nu}$	pt	$\log \beta^+$	$\log \epsilon^-$	$\log \nu$	$\log \beta^-$	$\log \epsilon^+$	$\log \bar{\nu}$
1	0.357	-4.182	0.949	-77.783	-65.016	-65.591	1	0.648	-3.878	1.219	-99.999	-59.563	-60.139
2	0.368	-1.851	0.969	-25.509	-21.943	-22.021	2	0.648	-1.555	1.224	-99.999	-20.454	-20.531
3	0.432	0.085	1.370	-7.188	-5.626	-5.102	3	0.649	0.408	1.613	-99.999	-5.781	-5.249
4	3.055	5.179	6.884	-1.397	3.951	5.553	4	2.810	5.132	6.823	-99.999	3.758	5.364
5	0.357	-0.450	1.059	-77.893	-70.835	-71.411	5	0.648	-0.153	1.340	-99.999	-65.383	-65.959
6	0.368	-0.426	1.080	-25.593	-23.658	-23.728	6	0.648	-0.130	1.348	-99.999	-22.170	-22.247
7	0.434	0.177	1.419	-7.203	-5.724	-5.199	7	0.651	0.501	1.668	-99.999	-5.879	-5.347
8	3.055	5.179	6.884	-1.397	3.951	5.553	8	2.810	5.132	6.823	-99.999	3.758	5.364
9	0.357	5.034	6.335	-99.999	-99.999	-99.999	9	0.648	5.212	6.554	-99.999	-99.999	-99.999
10	0.368	5.035	6.337	-61.953	-62.136	-61.880	10	0.648	5.213	6.556	-99.999	-60.648	-60.724
11	0.445	5.025	6.330	-18.189	-17.636	-17.075	11	0.663	5.198	6.542	-99.999	-17.790	-17.259
12	3.150	5.860	7.581	-1.871	3.226	4.825	12	2.908	5.815	7.523	-99.999	3.033	4.636

		$^{36}\text{Ar} \rightarrow ^{36}\text{Cl}$			$^{37}\text{Ar} \rightarrow ^{37}\text{K}$								
pt	$\log \beta^+$	$\log \epsilon^-$	$\log \nu$	$\log \beta^-$	$\log \epsilon^+$	$\log \bar{\nu}$	pt	$\log \beta^+$	$\log \epsilon^-$	$\log \nu$	$\log \beta^-$	$\log \epsilon^+$	$\log \bar{\nu}$
1	-16.473	-16.274	-16.169	-9.664	-10.778	-9.599	1	-0.219	-4.435	0.223	-38.848	-32.449	-33.022
2	-8.929	-7.008	-6.795	-5.631	-6.037	-5.386	2	-0.221	-2.098	0.233	-15.224	-11.756	-11.825
3	-2.660	-1.837	-1.070	-2.648	-2.422	-1.601	3	-0.269	-0.174	0.850	-4.884	-3.361	-2.819
4	1.949	4.712	6.373	1.159	4.441	6.078	4	0.219	4.864	6.540	-1.092	4.184	5.802
5	-16.473	-11.456	-11.811	-9.955	-16.598	-10.030	5	-0.220	-0.692	0.463	-41.085	-38.269	-38.841
6	-8.921	-5.446	-5.220	-5.777	-7.749	-5.739	6	-0.220	-0.664	0.484	-15.329	-13.470	-13.530
7	-2.654	-1.742	-0.979	-2.651	-2.520	-1.663	7	-0.264	-0.081	0.926	-4.899	-3.459	-2.917
8	1.949	4.712	6.373	1.159	4.441	6.078	8	2.121	4.865	6.540	-1.092	4.184	5.802
9	-16.473	4.357	5.467	-99.999	-99.999	-99.999	9	-0.219	4.870	6.171	-99.999	-99.999	-99.999
10	-8.921	4.359	5.470	-39.976	-46.227	-40.116	10	-0.220	4.832	6.132	-15.891	-15.948	-14.667
11	-2.629	4.395	5.531	-12.004	-14.426	-11.709	11	-0.245	4.832	6.132	-15.891	-15.371	-14.792
12	2.066	5.404	7.079	0.733	3.718	5.352	12	2.237	5.551	7.243	-1.567	3.460	5.074

TABLE 3—Continued

$^{37}\text{Ar} \rightarrow ^{37}\text{Cl}$		$^{37}\text{Cl} \rightarrow ^{37}\text{Ar}$		$^{37}\text{Cl} \rightarrow ^{37}\text{S}$		$^{37}\text{S} \rightarrow ^{37}\text{Cl}$		$^{38}\text{Ar} \rightarrow ^{38}\text{Ar}$		$^{38}\text{Ar} \rightarrow ^{38}\text{K}$		$^{38}\text{K} \rightarrow ^{38}\text{Ar}$		$^{38}\text{Ar} \rightarrow ^{38}\text{Cl}$			
pt	$\log \beta^+$	$\log \epsilon^-$	$\log \nu$	$\log \beta^-$	$\log \epsilon^+$	$\log \bar{\nu}$	$\log \beta^-$	$\log \epsilon^+$	$\log \beta^-$	$\log \nu$	$\log \beta^-$	$\log \epsilon^+$	$\log \beta^-$	$\log \nu$	$\log \beta^-$	$\log \epsilon^+$	$\log \bar{\nu}$
1	-11.795	-7.629	-7.640	-13.095	-9.500	-9.818											
2	-6.820	-4.992	-7.175	-5.841	-3.729	-1.382											
3	-2.767	-1.950	-1.201	-2.298	-2.281	-1.382											
4	-1.750	4.625	6.304	0.484	4.325	5.941											
5	-11.795	-3.648	-3.507	-14.131	-15.319	-14.618											
6	-6.812	-3.467	-3.211	-7.485	-7.552	-7.198											
7	-2.761	-1.854	-1.110	-2.302	-2.377	-1.440											
8	-1.750	4.625	6.304	0.484	4.325	5.941											
9	-11.795	4.206	5.371	-99.999	-99.999	-99.999											
10	-6.812	4.207	5.373	-42.280	-46.030	-42.427											
11	-2.736	4.213	5.392	-12.263	-14.281	-11.987											
12	1.879	5.311	7.006	0.042	3.601	5.213											
$^{37}\text{Cl} \rightarrow ^{37}\text{S}$		$^{37}\text{S} \rightarrow ^{37}\text{Cl}$		$^{38}\text{Ar} \rightarrow ^{38}\text{Cl}$		$^{38}\text{Cl} \rightarrow ^{38}\text{Ar}$		$^{38}\text{Cl} \rightarrow ^{38}\text{S}$		$^{38}\text{S} \rightarrow ^{38}\text{Cl}$		$^{38}\text{Cl} \rightarrow ^{38}\text{S}$		$^{38}\text{S} \rightarrow ^{38}\text{Cl}$			
pt	$\log \beta^+$	$\log \epsilon^-$	$\log \nu$	$\log \beta^-$	$\log \epsilon^+$	$\log \bar{\nu}$	$\log \beta^+$	$\log \epsilon^-$	$\log \nu$	$\log \beta^-$	$\log \epsilon^+$	$\log \beta^+$	$\log \epsilon^-$	$\log \nu$	$\log \beta^-$	$\log \epsilon^+$	$\log \bar{\nu}$
1	-51.224	-31.546	-32.101	-2.577	-6.974	-2.523											
2	-16.837	-12.067	-12.102	-2.621	-3.935	-2.509											
3	-4.735	-3.752	-3.081	-2.942	-1.881	-1.125											
4	-1.990	4.237	5.955	-3.603	4.226	5.796											
5	-51.224	-25.704	-26.261	-2.845	-12.794	-2.874											
6	-16.836	-10.360	-10.393	-2.818	-5.640	-2.805											
7	-4.729	-3.655	-2.988	-2.962	-1.977	-1.220											
8	-1.990	4.237	5.955	-3.603	4.226	5.796											
9	-51.224	0.168	1.348	-99.999	-99.999	-99.999											
10	-16.836	0.175	1.356	-37.356	-44.118	-37.515											
11	-4.702	1.871	3.134	-14.044	-13.875	-13.074											
12	2.093	4.914	6.649	-4.084	3.497	5.066											
$^{38}\text{Ca} \rightarrow ^{38}\text{K}$		$^{38}\text{K} \rightarrow ^{38}\text{Ca}$		$^{38}\text{K} \rightarrow ^{38}\text{S}$		$^{38}\text{S} \rightarrow ^{38}\text{K}$		$^{38}\text{S} \rightarrow ^{38}\text{Cl}$		$^{38}\text{Cl} \rightarrow ^{38}\text{S}$		$^{38}\text{Cl} \rightarrow ^{38}\text{S}$		$^{38}\text{S} \rightarrow ^{38}\text{Cl}$			
pt	$\log \beta^+$	$\log \epsilon^-$	$\log \nu$	$\log \beta^-$	$\log \epsilon^+$	$\log \bar{\nu}$	$\log \beta^+$	$\log \epsilon^-$	$\log \nu$	$\log \beta^-$	$\log \epsilon^+$	$\log \beta^+$	$\log \epsilon^-$	$\log \nu$	$\log \beta^-$	$\log \epsilon^+$	$\log \bar{\nu}$
1	0.211	-3.973	0.656	-40.480	-35.851	-36.424											
2	0.210	-1.640	0.669	-17.123	-13.220	-13.291											
3	0.130	0.234	1.258	-8.998	-4.126	-3.598											
4	2.206	4.835	6.523	-5.418	3.804	5.410											
5	0.211	-0.237	0.911	-43.531	-41.670	-42.241											
6	0.211	-0.210	0.931	-17.886	-14.936	-15.006											
7	0.135	0.327	1.333	-9.034	-4.224	-3.696											
8	2.206	4.835	6.523	-5.418	3.804	5.410											
9	0.211	5.069	6.423	-99.999	-99.999	-99.999											
10	0.211	5.070	6.425	-56.289	-53.413	-53.484											
11	0.153	4.976	6.329	-20.538	-16.136	-15.608											
12	2.320	5.518	7.223	-5.913	3.079	4.681											

TABLE 3—Continued

$^{39}\text{Ca} \rightarrow ^{39}\text{K}$			$^{39}\text{K} \rightarrow ^{39}\text{Ca}$			$^{40}\text{Ti} \rightarrow ^{40}\text{Sc}$			$^{40}\text{Sc} \rightarrow ^{40}\text{Ti}$			
pt	$\log \beta^+$	$\log \epsilon^-$	$\log \nu$	$\log \beta^-$	$\log \epsilon^+$	$\log \nu$	$\log \beta^+$	$\log \epsilon^-$	$\log \nu$	$\log \beta^-$	$\log \epsilon^+$	$\log \nu$
1	-0.069	-4.386	0.400	-38.915	-34.287	-34.862	0.645	-3.853	1.181	-73.276	-59.386	-59.964
2	-0.070	-2.057	0.409	-16.087	-12.351	-12.427	0.638	-1.551	1.180	-25.296	-21.210	-21.293
3	-0.108	-0.045	0.990	-8.222	-3.486	-2.966	0.228	-0.060	1.170	-7.928	-6.352	-5.846
4	1.852	4.794	6.475	-5.377	4.076	5.667	-0.547	4.941	6.557	-0.151	3.960	5.607
5	-0.069	-0.656	0.606	-41.845	-40.106	-40.678	0.645	-0.140	1.318	-73.375	-65.206	-65.784
6	-0.069	-0.629	0.621	-16.828	-14.066	-14.142	0.639	-0.133	1.320	-25.372	-22.925	-23.005
7	-0.103	0.048	1.064	-8.258	-3.584	-3.064	0.230	0.033	1.228	-7.937	-6.451	-5.943
8	1.852	4.794	6.476	-5.377	4.076	5.667	-0.547	4.941	6.557	-0.151	3.960	5.607
9	-0.069	4.770	6.106	-99.999	-99.999	-99.999	0.645	5.200	6.503	-99.999	-99.999	-99.999
10	-0.069	4.771	6.107	-55.224	-52.544	-52.620	0.639	5.198	6.501	-60.875	-61.403	-60.906
11	-0.085	4.766	6.106	-19.756	-15.496	-14.976	0.242	5.079	6.340	-18.387	-18.363	-17.693
12	1.977	5.478	7.177	-5.871	3.349	4.938	-0.398	5.641	7.272	-0.604	3.239	4.881

$^{39}\text{K} \rightarrow ^{39}\text{Ar}$			$^{39}\text{Ar} \rightarrow ^{39}\text{K}$			$^{40}\text{Co} \rightarrow ^{40}\text{Ca}$			$^{40}\text{Ca} \rightarrow ^{40}\text{Co}$			
pt	$\log \beta^+$	$\log \epsilon^-$	$\log \nu$	$\log \beta^-$	$\log \epsilon^+$	$\log \nu$	$\log \beta^+$	$\log \epsilon^-$	$\log \nu$	$\log \beta^-$	$\log \epsilon^+$	$\log \nu$
1	-18.174	-15.946	-16.471	-9.964	-13.057	-10.252	0.536	-3.979	1.114	-97.772	-72.067	-72.644
2	-8.497	-8.018	-7.775	-5.588	-6.992	-5.414	0.517	-1.682	1.099	-31.170	-23.903	-23.983
3	-2.794	-2.133	-1.343	-3.341	-2.432	-1.764	0.459	0.186	1.419	-7.750	-5.910	-5.411
4	2.331	4.594	6.312	-1.126	4.035	5.605	1.030	4.695	6.332	-0.356	3.356	5.007
5	-18.174	-10.238	-10.718	-10.946	-18.876	-10.952	0.536	-0.261	1.226	-31.189	-25.618	-25.699
6	-8.489	-6.363	-6.250	-5.694	-8.702	-5.588	0.517	-0.261	1.237	-97.795	-77.887	-78.464
7	-2.789	-2.038	-1.255	-3.353	-2.529	-1.857	0.462	0.278	1.477	-7.756	-6.009	-5.508
8	2.331	4.594	6.312	-1.126	4.035	5.605	1.030	4.695	6.332	-0.356	3.356	5.007
9	-18.174	3.286	4.484	-99.999	-99.999	-99.999	0.536	4.907	6.243	-99.999	-99.999	-99.999
10	-8.489	3.287	4.486	-41.090	-47.180	-41.227	0.517	4.898	6.232	-63.571	-64.096	-63.592
11	-2.768	3.337	4.580	-13.013	-14.434	-12.660	0.474	4.872	6.205	-17.829	-17.922	-17.200
12	2.434	5.271	7.006	-1.525	3.306	4.874	1.149	5.390	7.042	-0.802	2.635	4.281

$^{39}\text{Ar} \rightarrow ^{39}\text{Cl}$			$^{39}\text{Cl} \rightarrow ^{39}\text{Ar}$			$^{40}\text{K} \rightarrow ^{40}\text{Ca}$			$^{40}\text{Ca} \rightarrow ^{40}\text{K}$			
pt	$\log \beta^+$	$\log \epsilon^-$	$\log \nu$	$\log \beta^-$	$\log \epsilon^+$	$\log \nu$	$\log \beta^+$	$\log \epsilon^-$	$\log \nu$	$\log \beta^-$	$\log \epsilon^+$	$\log \nu$
1	-45.928	-25.645	-26.188	-3.618	-7.697	-3.556	-21.597	-24.046	-21.684	-14.542	-15.743	-14.227
2	-15.385	-10.761	-10.781	-3.203	-4.462	-3.040	-8.907	-8.984	-8.404	-6.906	-7.382	-6.527
3	-4.869	-3.901	-3.233	-2.591	-2.088	-1.281	-2.481	-1.919	-1.065	-4.506	-2.705	-2.134
4	1.867	4.101	5.834	-2.142	4.590	6.161	2.039	4.307	6.032	-4.245	3.860	5.438
5	-45.928	-19.909	-20.420	-3.865	-13.516	-3.878	-21.597	-19.621	-19.680	-14.648	-21.562	-14.383
6	-15.384	-9.056	-9.070	-3.337	-6.188	-3.263	-8.899	-7.493	-7.047	-6.952	-9.097	-6.664
7	-4.863	-3.804	-3.140	-2.602	-2.164	-1.369	-2.477	-1.825	-0.979	-4.516	-2.803	-2.232
8	1.867	4.101	5.834	-2.142	4.590	6.161	2.039	4.307	6.032	-4.245	3.860	5.438
9	-45.928	-0.622	0.598	-99.999	-99.999	-99.999	-21.597	2.495	3.705	-99.999	-99.999	-99.999
10	-15.384	0.228	1.449	-39.441	-44.645	-39.609	-8.899	2.496	3.708	-42.197	-47.575	-42.370
11	-4.839	1.915	3.155	-13.125	-14.063	-12.779	-2.489	3.054	4.368	-15.264	-14.713	-14.102
12	1.977	4.774	6.526	-2.596	3.861	5.430	2.145	4.982	6.725	-4.711	3.132	4.708

TABLE 3—Continued

pt	$^{40}\text{Ar} \rightarrow ^{40}\text{K}$				$^{41}\text{Sc} \rightarrow ^{41}\text{Ca}$			
	$\log \beta^+$	$\log \epsilon^-$	$\log \beta^-$	$\log \epsilon^+$	$\log \nu$	$\log \beta^-$	$\log \epsilon^+$	$\log \bar{\nu}$
1	-14.718	-16.884	-14.688	-20.201	-20.591	-20.067	0.074	4.233
2	-7.280	-7.461	-6.818	-8.271	-7.455	-7.555	0.073	-1.913
3	-3.008	-2.343	-3.564	-2.413	-1.722	-2.920	0.006	-0.019
4	2.054	4.534	6.245	4.130	5.702	4.609	1.070	1.280
5	-14.718	-12.508	-12.555	-20.404	-26.411	-20.408	0.074	-0.509
6	-7.276	-5.910	-5.579	-7.804	-9.984	-7.716	0.074	-0.490
7	-3.003	-2.248	-1.476	-3.492	-2.509	-1.817	0.010	0.073
8	2.054	4.534	6.245	4.130	5.702	4.609	1.489	4.609
9	-14.718	3.014	4.247	-99.999	-99.999	-99.999	0.074	4.729
10	-7.275	3.009	4.244	-44.373	-48.462	-44.570	0.074	4.730
11	-2.980	3.065	4.337	-14.487	-14.412	-13.652	0.027	4.699
12	2.167	5.211	6.941	-3.474	3.401	4.972	1.618	5.296

pt	$^{40}\text{Ar} \rightarrow ^{40}\text{Cl}$				$^{41}\text{Ca} \rightarrow ^{41}\text{K}$			
	$\log \beta^+$	$\log \epsilon^-$	$\log \beta^-$	$\log \epsilon^+$	$\log \nu$	$\log \beta^-$	$\log \epsilon^+$	$\log \bar{\nu}$
1	-67.467	-44.544	-45.112	-2.008	-7.225	-1.700	-14.341	-12.627
2	-21.683	-16.202	-16.265	-1.898	-4.165	-1.559	-2.746	-6.490
3	-5.871	-4.913	-4.285	-1.584	-1.933	-0.819	-2.727	-1.964
4	1.797	4.052	5.773	1.637	4.351	5.921	2.108	4.512
5	-67.467	-38.725	-39.293	-2.080	-13.044	-1.802	-14.341	-6.865
6	-21.682	-14.487	-14.550	-1.946	-5.870	-1.630	-7.338	-4.817
7	-5.866	-4.815	-4.194	-1.592	-2.027	-0.877	-2.722	-1.869
8	1.797	4.052	5.773	1.637	4.351	5.921	2.108	4.512
9	-67.467	0.322	1.430	-87.457	-99.999	-88.055	-14.341	3.055
10	-21.682	0.317	1.426	-32.685	-44.347	-32.827	-7.338	3.057
11	-5.845	1.517	2.719	-12.001	-13.920	-11.765	-2.215	3.224
12	1.901	4.728	6.467	-2.094	3.622	5.191	2.215	5.189

pt	$^{41}\text{Ti} \rightarrow ^{41}\text{Sc}$				$^{41}\text{Ar} \rightarrow ^{41}\text{K}$			
	$\log \beta^+$	$\log \epsilon^-$	$\log \beta^-$	$\log \epsilon^+$	$\log \nu$	$\log \beta^-$	$\log \epsilon^+$	$\log \bar{\nu}$
1	0.932	-3.663	1.527	-81.646	-66.270	-66.848	-41.538	-20.267
2	0.923	-1.370	1.526	-27.571	-22.771	-22.855	-13.378	-8.461
3	0.758	0.222	1.652	-8.056	-6.233	-5.738	-3.973	-2.846
4	0.503	4.779	6.404	-0.552	3.479	5.121	2.030	4.386
5	0.932	0.047	1.634	-81.731	-72.090	-72.668	-41.538	-14.508
6	0.923	0.047	1.632	-27.637	-24.487	-24.570	-13.378	-6.769
7	0.759	0.314	1.694	-8.064	-6.332	-5.836	-3.968	-2.748
8	0.503	4.779	6.405	-0.552	3.478	5.121	2.030	4.386
9	0.932	5.161	6.513	-99.999	-99.999	-99.999	-41.538	2.917
10	0.923	5.153	6.504	-62.746	-62.965	-62.670	-13.377	2.952
11	0.768	4.981	6.298	-18.413	-18.244	-17.619	-3.945	2.920
12	0.651	5.476	7.117	-1.002	2.757	4.395	2.143	5.061

TABLE 3—Continued

$^{41}\text{Ar} \rightarrow ^{41}\text{Cl}$		$^{41}\text{Cl} \rightarrow ^{41}\text{Ar}$		$^{42}\text{Ca} \rightarrow ^{42}\text{K}$		$^{42}\text{K} \rightarrow ^{42}\text{Ca}$	
pt	$\log \beta^+$	$\log \epsilon^-$	$\log \nu$	$\log \beta^-$	$\log \epsilon^+$	$\log \nu$	$\log \bar{\nu}$
1	-56.936	-36.193	-36.765	-1.687	-7.095	-1.361	1.361
2	-19.160	-14.261	-14.330	-1.683	-4.062	-1.351	4.704
3	-6.082	-5.068	-4.446	-0.832	-1.721	-0.131	-3.944
4	1.785	4.064	5.781	-0.204	4.437	6.010	-1.416
5	-56.936	-30.373	-30.945	-1.740	-12.914	-1.449	5.692
6	-19.159	-12.546	-12.614	-1.726	-5.766	-1.422	4.263
7	-6.076	-4.970	-4.353	-0.836	-1.816	-0.153	-1.511
8	1.785	4.064	5.782	-0.204	4.437	6.010	5.692
9	-56.936	2.169	3.239	-93.575	-99.999	-94.171	-99.999
10	-19.159	2.236	3.307	-32.352	-44.244	-32.488	-40.428
11	-6.052	2.291	3.396	-9.933	-13.710	-9.627	-13.367
12	1.890	4.740	6.476	-0.623	3.708	5.279	4.961

$^{42}\text{Ti} \rightarrow ^{42}\text{Sc}$		$^{42}\text{Sc} \rightarrow ^{42}\text{Ti}$		$^{42}\text{Ar} \rightarrow ^{42}\text{K}$		$^{42}\text{K} \rightarrow ^{42}\text{Ar}$	
pt	$\log \beta^+$	$\log \epsilon^-$	$\log \nu$	$\log \beta^-$	$\log \epsilon^+$	$\log \nu$	$\log \bar{\nu}$
1	0.556	-3.757	1.041	-46.845	-36.126	-36.702	-9.543
2	0.552	-1.444	1.047	-16.681	-13.026	-13.104	-5.319
3	0.173	0.055	1.194	-6.254	-4.256	-3.743	-1.434
4	1.972	4.735	6.414	-1.776	3.880	5.493	5.937
5	0.556	-0.037	1.244	-47.067	-41.946	-42.521	-11.756
6	0.553	-0.022	1.253	-16.820	-14.741	-14.814	-5.675
7	0.176	0.148	1.260	-6.272	-4.355	-3.841	-1.524
8	1.972	4.735	6.414	-1.776	3.880	5.493	5.937
9	0.556	5.098	6.469	-99.999	-99.999	-99.999	-99.999
10	0.553	5.096	6.467	-53.957	-53.219	-53.243	-42.749
11	0.191	4.816	6.155	-17.427	-16.267	-15.746	-13.240
12	2.088	5.420	7.116	-2.256	3.155	4.765	5.206

$^{42}\text{Sc} \rightarrow ^{42}\text{Ca}$		$^{42}\text{Ca} \rightarrow ^{42}\text{Sc}$		$^{43}\text{Ti} \rightarrow ^{43}\text{Sc}$		$^{43}\text{Sc} \rightarrow ^{43}\text{Ti}$	
pt	$\log \beta^+$	$\log \epsilon^-$	$\log \nu$	$\log \beta^-$	$\log \epsilon^+$	$\log \nu$	$\log \bar{\nu}$
1	0.045	-4.281	0.518	-54.795	-33.714	-34.290	-36.482
2	-0.270	-2.259	0.218	-17.556	-11.988	-12.063	-12.972
3	-0.668	-0.631	0.427	-4.449	-3.305	-2.766	-3.299
4	2.098	4.546	6.220	-0.292	3.924	5.548	5.703
5	0.045	-0.559	0.718	-54.830	-39.534	-40.109	-42.301
6	-0.269	-0.835	0.424	-17.586	-13.703	-13.779	-14.671
7	-0.663	-0.538	0.501	-4.456	-3.404	-2.860	-3.396
8	2.098	4.546	6.220	-0.292	3.924	5.548	5.703
9	0.045	4.695	6.024	-99.999	-99.999	-99.999	-99.999
10	-0.269	4.563	5.857	-51.502	-52.181	-51.565	-52.961
11	-0.646	4.465	5.729	-14.900	-15.317	-14.446	-15.838
12	2.198	5.234	6.923	-0.749	3.200	4.821	4.975

TABLE 3—Continued

$^{43}\text{Sc} \rightarrow ^{43}\text{Ca}$			$^{43}\text{Co} \rightarrow ^{43}\text{Sc}$			$^{43}\text{Ar} \rightarrow ^{43}\text{Cl}$			$^{43}\text{Ar} \rightarrow ^{43}\text{Ar}$										
pt	$\log \beta^+$	$\log \epsilon^-$	$\log \nu$	$\log \beta^-$	$\log \bar{\nu}$	pt	$\log \beta^+$	$\log \epsilon^-$	$\log \nu$	$\log \beta^-$	$\log \bar{\nu}$	pt	$\log \beta^+$	$\log \epsilon^-$	$\log \nu$	$\log \beta^-$	$\log \bar{\nu}$		
1	-4.374	-6.459	-4.551	-20.658	-14.845	15.385	1	-72.022	-53.344	-53.923	-2.341	1	-23.756	-19.788	-19.873	-1.547	1	-8.626	-1.722
2	-4.208	-3.975	-3.499	-13.169	-7.099	-7.083	2	-23.756	-19.788	-19.873	-1.547	2	-6.753	-5.862	-5.207	-0.641	2	-4.802	-0.943
3	-1.995	-1.373	-0.538	-3.306	-2.621	-1.954	3	-6.753	-5.862	-5.207	-0.641	3	1.862	4.358	6.070	-0.648	3	1.812	0.023
4	1.861	4.853	6.537	0.513	4.274	5.883	4	1.862	4.358	6.070	-0.648	4	-72.022	-53.344	-53.923	-2.341	4	1.812	0.023
5	-4.374	-2.605	-2.231	-24.093	-20.664	-21.205	5	-72.022	-53.344	-53.923	-2.341	5	-23.756	-19.788	-19.873	-1.547	5	-14.445	-1.739
6	-4.198	-2.487	-2.068	-13.727	-8.814	-8.798	6	-23.756	-19.788	-19.873	-1.547	6	-6.747	-5.764	-5.116	-0.644	6	-6.506	-0.959
7	-1.990	-1.279	-0.451	-3.310	-2.719	-2.036	7	-6.747	-5.764	-5.116	-0.644	7	1.862	4.358	6.070	-0.648	7	-1.906	0.007
8	1.861	4.853	6.537	0.513	4.274	5.883	8	1.862	4.358	6.070	-0.648	8	-72.022	-53.344	-53.923	-2.341	8	4.605	6.181
9	-4.374	4.205	5.375	-99.999	-99.999	-99.999	9	-72.022	-53.344	-53.923	-2.341	9	-23.756	-19.788	-19.873	-1.547	9	-80.466	-99.999
10	-4.198	4.202	5.371	-44.497	-47.291	-44.640	10	-23.756	-19.788	-19.873	-1.547	10	-6.721	1.637	2.756	-9.957	10	-44.984	-30.100
11	-1.970	4.218	5.404	-12.951	-14.627	-12.658	11	-6.721	1.637	2.756	-9.957	11	1.978	5.035	6.766	-1.075	11	-13.798	-9.662
12	1.991	5.537	7.238	0.079	3.549	5.155	12	1.978	5.035	6.766	-1.075	12	-72.022	-53.344	-53.923	-2.341	12	3.876	5.451

$^{43}\text{Ca} \rightarrow ^{43}\text{K}$			$^{43}\text{K} \rightarrow ^{43}\text{Ca}$			$^{44}\text{V} \rightarrow ^{44}\text{Ti}$			$^{44}\text{Ti} \rightarrow ^{44}\text{V}$									
pt	$\log \beta^+$	$\log \epsilon^-$	$\log \nu$	$\log \beta^-$	$\log \bar{\nu}$	pt	$\log \beta^+$	$\log \epsilon^-$	$\log \nu$	$\log \beta^-$	$\log \bar{\nu}$	pt	$\log \beta^+$	$\log \epsilon^-$	$\log \nu$	$\log \beta^-$	$\log \bar{\nu}$	
1	-40.223	-18.152	-18.649	-4.961	-8.196	5.115	1	0.695	-4.059	1.386	-86.328	1	0.695	-4.059	1.386	-86.328	-69.306	-69.885
2	-13.377	-8.164	-8.165	-3.144	-4.551	-2.953	2	0.391	-2.070	1.082	-27.479	2	0.391	-2.070	1.082	-27.479	-23.234	-23.318
3	-3.902	-2.730	-2.104	-2.308	-1.796	-0.990	3	0.228	-0.331	1.130	-7.405	3	0.228	-0.331	1.130	-7.405	-6.504	-5.949
4	1.965	4.329	6.040	-2.191	4.071	5.641	4	3.026	5.187	6.894	-0.814	4	3.026	5.187	6.894	-0.814	3.884	5.485
5	-40.223	-12.465	-12.981	-5.680	-14.016	-3.125	5	0.695	-4.059	1.386	-86.328	5	0.391	-2.070	1.082	-27.479	-75.704	-75.704
6	-13.377	-6.470	-6.464	-3.250	-6.257	-3.722	6	0.391	-2.070	1.082	-27.479	6	0.230	-0.238	1.168	-7.415	-24.949	-25.031
7	-3.897	-2.632	-2.010	-2.321	-1.891	-1.079	7	0.230	-0.238	1.168	-7.415	7	3.026	5.187	6.894	-0.814	-6.602	-6.041
8	1.965	4.329	6.040	-2.191	4.071	5.641	8	3.026	5.187	6.894	-0.814	8	0.695	-4.059	1.386	-86.328	3.884	5.485
9	-40.223	2.997	4.218	-99.999	-99.999	-99.999	9	-72.022	-53.344	-53.923	-2.341	9	0.695	-4.059	1.386	-86.328	-99.999	-99.999
10	-13.377	3.032	4.257	-39.454	-44.735	-39.635	10	0.391	-2.070	1.082	-27.479	10	0.391	-2.070	1.082	-27.479	-62.600	-62.701
11	-3.878	3.052	4.300	-13.168	-13.788	-12.729	11	0.237	4.917	6.172	-18.120	11	0.237	4.917	6.172	-18.120	-18.514	-17.676
12	2.069	5.007	6.735	-2.660	3.342	4.911	12	3.120	5.868	7.590	-1.279	12	3.120	5.868	7.590	-1.279	3.158	4.757

$^{43}\text{K} \rightarrow ^{43}\text{Ar}$			$^{44}\text{Ti} \rightarrow ^{44}\text{Sc}$			$^{44}\text{Sc} \rightarrow ^{44}\text{Ti}$												
pt	$\log \beta^+$	$\log \epsilon^-$	$\log \nu$	$\log \beta^-$	$\log \bar{\nu}$	pt	$\log \beta^+$	$\log \epsilon^-$	$\log \nu$	$\log \beta^-$	$\log \bar{\nu}$	pt	$\log \beta^+$	$\log \epsilon^-$	$\log \nu$	$\log \beta^-$	$\log \bar{\nu}$	
1	-52.618	-31.143	-31.708	-2.745	-7.721	-2.525	1	-11.534	-9.839	-10.265	-9.869	1	-11.534	-9.839	-10.265	-9.869	-11.154	-10.377
2	-17.396	-12.684	-12.738	-2.638	-4.646	-2.339	2	-6.514	-5.297	-5.069	-8.118	2	-6.514	-5.297	-5.069	-8.118	-6.631	-6.504
3	-5.443	-4.499	-3.860	-1.160	-1.874	-0.492	3	-2.768	-1.618	-0.846	-3.682	3	-2.768	-1.618	-0.846	-3.682	-3.071	-2.380
4	1.961	4.327	6.044	-0.983	4.719	6.287	4	2.188	4.870	6.551	1.139	4	2.188	4.870	6.551	1.139	4.227	5.848
5	-52.618	-25.324	-25.889	-2.855	-13.541	-2.681	5	-11.534	-9.839	-10.265	-9.869	5	-11.534	-9.839	-10.265	-9.869	-16.973	-13.210
6	-17.395	-10.968	-11.022	-2.706	-6.351	-2.430	6	-6.506	-3.736	-3.499	-8.801	6	-6.506	-3.736	-3.499	-8.801	-8.343	-8.192
7	-5.438	-4.401	-3.768	-1.165	-1.968	-0.526	7	-2.762	-1.523	-0.754	-3.685	7	-2.762	-1.523	-0.754	-3.685	-3.169	-2.454
8	1.962	4.327	6.044	-0.983	4.719	6.287	8	2.188	4.870	6.551	1.139	8	2.188	4.870	6.551	1.139	4.227	5.848
9	-52.618	-0.625	0.516	-99.999	-99.999	-99.999	9	-11.534	-9.839	-10.265	-9.869	9	-11.534	-9.839	-10.265	-9.869	-99.999	-99.999
10	-17.395	1.831	2.977	-35.361	-44.829	-35.506	10	-6.506	4.321	5.393	-99.999	10	-6.506	4.321	5.393	-99.999	-42.021	-42.158
11	-5.415	2.342	3.508	-11.068	-13.863	-10.798	11	-2.734	4.364	5.478	-12.606	11	-2.734	4.364	5.478	-12.606	-15.078	-12.295
12	2.070	5.003	6.739	-1.420	3.990	5.556	12	2.306	5.557	7.253	0.724	12	2.306	5.557	7.253	0.724	3.502	5.120

TABLE 3—Continued

		$^{44}\text{Ca} \rightarrow ^{44}\text{Ca}$			$^{44}\text{Ca} \rightarrow ^{44}\text{Sc}$			$^{45}\text{V} \rightarrow ^{45}\text{Cr}$					
pt		$\log \beta^+$	$\log \epsilon^-$	$\log \nu$	$\log \beta^-$	$\log \epsilon^+$	$\log \bar{\nu}$	$\log \beta^+$	$\log \epsilon^-$	$\log \nu$	$\log \beta^-$	$\log \epsilon^+$	$\log \bar{\nu}$
1		-4.490	-6.946	-4.544	-26.137	-21.701	-22.239	0.945	-3.875	1.656	-77.339	-63.580	-64.158
2		-4.117	-4.476	-3.683	-10.617	-8.763	-8.742	0.879	-1.662	1.596	-25.708	-21.877	-21.962
3		-2.190	-1.696	-0.845	-3.109	-2.689	-1.937	0.703	0.035	1.597	-7.615	-6.049	-5.549
4		-1.969	-4.923	6.612	0.574	4.364	5.965	2.839	5.175	6.856	-0.901	4.081	5.698
5		-4.490	-3.104	-2.681	-27.974	-27.521	-27.905	0.945	-0.178	1.714	-77.438	-69.399	-69.978
6		-4.113	-2.990	-2.538	-10.984	-10.477	-10.385	0.879	-0.249	1.653	-25.785	-23.592	-23.672
7		-2.186	-1.601	-0.762	-3.112	-2.786	-2.009	0.705	0.127	1.629	-7.629	-6.148	-5.646
8		-1.969	-4.923	6.612	0.574	4.363	5.965	2.839	5.176	6.857	-0.901	4.081	5.698
9		-4.490	-3.104	-2.681	-27.974	-27.521	-27.905	0.945	-0.178	1.714	-77.438	-69.399	-69.978
10		-4.113	-2.990	-2.538	-10.984	-10.477	-10.385	0.879	-0.249	1.653	-25.785	-23.592	-23.672
11		-2.168	-1.601	-0.762	-3.112	-2.786	-2.009	0.711	0.127	1.629	-7.629	-6.148	-5.646
12		-2.099	-5.605	7.312	0.143	3.637	5.237	2.932	5.863	7.558	-1.373	3.357	4.970

		$^{44}\text{K} \rightarrow ^{44}\text{Ca}$			$^{44}\text{K} \rightarrow ^{44}\text{Ca}$			$^{45}\text{Ti} \rightarrow ^{45}\text{V}$					
pt		$\log \beta^+$	$\log \epsilon^-$	$\log \nu$	$\log \beta^-$	$\log \epsilon^+$	$\log \bar{\nu}$	$\log \beta^+$	$\log \epsilon^-$	$\log \nu$	$\log \beta^-$	$\log \epsilon^+$	$\log \bar{\nu}$
1		-58.832	-35.315	-35.857	-2.917	-7.286	-2.721	-0.029	-4.406	0.484	-45.890	-37.427	-38.004
2		-18.510	-12.716	-12.739	-2.554	-4.066	-2.341	0.029	-2.099	0.492	-15.847	-13.480	-13.558
3		-4.772	-3.698	-3.061	-1.762	-1.885	-0.862	0.000	-0.087	1.029	-5.518	-3.960	-3.398
4		-1.991	-4.431	6.147	-1.307	4.363	5.933	2.431	5.388	7.075	-1.842	4.264	5.866
5		-58.832	-29.634	-30.160	-3.078	-13.106	-2.892	-0.029	-0.697	0.660	-46.150	-43.247	-43.822
6		-18.509	-11.012	-11.031	-2.661	-5.772	-2.494	0.028	-0.681	0.671	-16.023	-15.196	-15.208
7		-4.767	-3.600	-2.969	-1.768	-1.980	-0.919	0.003	0.006	1.094	-5.538	-4.058	-3.495
8		-1.991	-4.431	6.147	-1.307	4.363	5.933	2.431	5.388	7.075	-1.842	4.264	5.866
9		-58.832	-29.634	-30.160	-3.078	-13.106	-2.892	-0.029	-0.697	0.660	-46.150	-43.247	-43.822
10		-18.509	-11.012	-11.031	-2.661	-5.772	-2.494	0.028	-0.681	0.671	-16.023	-15.196	-15.208
11		-4.747	-2.626	-3.796	-11.441	-13.876	-11.150	0.017	5.014	6.306	-16.763	-15.968	-15.391
12		-2.103	-5.108	6.842	-1.745	3.634	5.203	2.558	6.070	7.775	-2.324	3.538	5.138

		$^{44}\text{K} \rightarrow ^{44}\text{Ar}$			$^{44}\text{K} \rightarrow ^{44}\text{Ar}$			$^{45}\text{Sc} \rightarrow ^{45}\text{Ti}$					
pt		$\log \beta^+$	$\log \epsilon^-$	$\log \nu$	$\log \beta^-$	$\log \epsilon^+$	$\log \bar{\nu}$	$\log \beta^+$	$\log \epsilon^-$	$\log \nu$	$\log \beta^-$	$\log \epsilon^+$	$\log \bar{\nu}$
1		-47.675	-26.183	-26.740	-2.986	-7.353	-2.990	-4.363	-6.336	-4.579	-19.831	-13.893	-14.429
2		-16.429	-11.527	-11.564	-2.985	-4.284	-2.901	-4.327	-3.874	-3.442	-12.950	-6.703	-6.696
3		-5.493	-4.752	-4.042	-2.105	-2.013	-1.102	-2.029	-1.472	0.626	-3.463	-2.759	-2.082
4		-1.650	-4.190	5.844	-1.498	4.504	6.077	2.158	4.918	6.599	-1.255	4.368	5.988
5		-47.675	-20.363	-20.920	-3.293	-13.173	-3.442	-4.383	-2.499	-2.130	-23.265	-19.712	-20.249
6		-16.428	-9.811	-9.848	-3.181	-5.989	-3.212	-4.315	-2.395	-1.972	-13.796	-8.418	-8.411
7		-5.488	-4.655	-3.953	-2.114	-2.108	-1.176	-2.025	-1.378	0.541	-3.465	-2.857	-2.160
8		-1.650	-4.190	5.844	-1.498	4.504	6.077	2.158	4.918	6.599	-1.254	4.368	5.988
9		-47.675	-20.363	-20.920	-3.293	-13.173	-3.442	-4.383	-2.499	-2.130	-23.265	-19.712	-20.249
10		-16.428	-9.811	-9.848	-3.181	-5.989	-3.212	-4.315	-2.395	-1.972	-13.796	-8.418	-8.411
11		-5.466	-1.301	-2.516	-12.437	-14.005	-12.170	-4.315	-4.325	5.436	-99.999	-99.999	-99.999
12		-1.765	-4.807	6.539	-1.946	3.775	5.346	-2.276	5.604	7.300	0.840	3.643	5.260

TABLE 3—Continued

$^{45}\text{Sc} \rightarrow ^{45}\text{Co}$				$^{45}\text{Ca} \rightarrow ^{45}\text{Sc}$				$^{46}\text{V} \rightarrow ^{46}\text{Ti}$				$^{46}\text{Ti} \rightarrow ^{46}\text{V}$			
pt	$\log \beta^+$	$\log \epsilon^-$	$\log \nu$	$\log \beta^-$	$\log \epsilon^+$	$\log \nu$	$\log \beta^-$	$\log \epsilon^-$	$\log \nu$	$\log \beta^-$	$\log \epsilon^+$	$\log \nu$	$\log \beta^-$	$\log \epsilon^+$	$\log \nu$
1	-14.782	-10.587	-11.064	-6.397	-8.609	-6.935									
2	-8.772	-5.869	-5.787	-5.449	-5.012	-4.688									
3	-3.253	-2.358	-2.146	-2.413	-2.146	-1.277									
4	1.848	4.799	6.485	1.277	4.485	6.094									
5	-14.782	-5.207	-5.588	-8.954	-14.429	-9.688									
6	-8.750	-4.243	-4.139	-5.714	-6.721	-5.657									
7	-3.249	-2.261	-1.562	-2.417	-2.243	-1.340									
8	-1.848	4.799	6.485	1.277	4.485	6.093									
9	-14.782	3.953	5.036	-99.999	-99.999	-99.999									
10	-8.750	3.960	5.047	-40.039	-45.198	-40.173									
11	-3.232	3.978	5.081	-11.202	-14.144	-10.885									
12	1.978	5.483	7.186	0.868	3.759	5.365									
$^{45}\text{Ca} \rightarrow ^{45}\text{K}$				$^{45}\text{K} \rightarrow ^{45}\text{Ca}$				$^{46}\text{Ti} \rightarrow ^{46}\text{Sc}$				$^{46}\text{Sc} \rightarrow ^{46}\text{Ti}$			
pt	$\log \beta^+$	$\log \epsilon^-$	$\log \nu$	$\log \beta^-$	$\log \epsilon^+$	$\log \nu$	$\log \beta^-$	$\log \epsilon^-$	$\log \nu$	$\log \beta^-$	$\log \epsilon^+$	$\log \nu$	$\log \beta^-$	$\log \epsilon^+$	$\log \nu$
1	-52.282	-29.694	-30.255	-3.200	-7.993	-3.055									
2	-17.395	-12.234	-12.290	-2.328	-4.600	-1.941									
3	-5.116	-4.189	-3.549	-1.487	-1.962	-0.770									
4	1.820	4.230	5.947	-1.439	4.427	5.999									
5	-52.282	-23.875	-24.436	-3.364	-13.812	-3.287									
6	-17.394	-10.518	-10.574	-2.372	-6.305	-1.999									
7	-5.111	-4.092	-3.458	-1.494	-2.057	-0.819									
8	1.820	4.230	5.947	-1.439	4.427	5.999									
9	-52.282	2.397	3.566	-99.999	-99.999	-99.999									
10	-17.394	2.398	3.570	-35.441	-44.782	-35.596									
11	-5.090	2.341	3.531	-11.743	-13.951	-11.505									
12	1.930	4.906	6.642	-1.888	3.698	5.268									
$^{46}\text{Cr} \rightarrow ^{46}\text{V}$				$^{46}\text{V} \rightarrow ^{46}\text{Cr}$				$^{46}\text{Ca} \rightarrow ^{46}\text{Sc}$				$^{46}\text{Sc} \rightarrow ^{46}\text{Ca}$			
pt	$\log \beta^+$	$\log \epsilon^-$	$\log \nu$	$\log \beta^-$	$\log \epsilon^+$	$\log \nu$	$\log \beta^-$	$\log \epsilon^-$	$\log \nu$	$\log \beta^-$	$\log \epsilon^+$	$\log \nu$	$\log \beta^-$	$\log \epsilon^+$	$\log \nu$
1	0.488	-3.988	1.038	-46.123	-39.466	-40.044									
2	0.475	-1.699	1.030	-16.463	-14.124	-14.204									
3	0.327	0.166	1.318	-6.590	-4.554	-3.998									
4	2.736	5.381	7.075	-2.419	4.166	5.767									
5	0.488	-0.287	1.179	-46.685	-45.285	-45.833									
6	0.476	-0.284	1.173	-16.767	-15.839	-15.882									
7	0.330	0.259	1.379	-6.615	-4.652	-4.095									
8	2.736	5.381	7.075	-2.419	4.166	5.767									
9	0.488	5.223	6.533	-99.999	-99.999	-99.999									
10	0.476	5.222	6.532	-54.708	-54.317	-54.303									
11	0.342	5.197	6.502	-17.953	-16.561	-16.003									
12	2.850	6.063	7.773	-2.906	3.440	5.039									

TABLE 3—Continued

		$^{46}\text{Ca} \rightarrow$		$^{46}\text{K} \rightarrow$		$^{46}\text{Ca} \rightarrow$		$^{47}\text{Ti} \rightarrow$		$^{47}\text{Sc} \rightarrow$		$^{47}\text{Ti} \rightarrow$	
pt		$\log \beta^+$	$\log \epsilon^-$	$\log \nu$	$\log \beta^-$	$\log \epsilon^-$	$\log \nu$	$\log \beta^+$	$\log \epsilon^-$	$\log \nu$	$\log \beta^-$	$\log \epsilon^+$	$\log \nu$
1	68.652	45.902	46.469	-2.109	-7.522	-1.704		-16.890	-11.743	-12.260	-5.592	-8.375	-6.057
2	-21.933	-16.326	-16.394	-1.480	-4.009	-1.089		-8.889	-6.401	-6.341	-4.725	-5.038	-4.444
3	-5.758	-4.573	-3.995	-0.885	-1.589	-0.186		-3.098	-2.326	-1.598	-2.960	-2.338	-1.555
4	2.160	4.459	6.179	-0.386	4.437	6.005		2.251	4.956	6.647	1.662	4.464	6.072
5	68.652	40.062	40.649	-2.183	-13.341	-1.778		-16.889	-6.129	-6.555	-7.655	-14.194	-8.190
6	-21.932	-14.610	-14.678	-1.525	-5.714	-1.153		-8.872	-4.752	-4.679	-4.967	-6.746	-5.017
7	-5.753	-4.474	-3.901	-0.890	-1.683	-0.220		-3.095	-2.230	-1.510	-2.963	-2.434	-1.631
8	2.160	4.459	6.179	-0.386	4.437	6.005		2.251	4.956	6.647	1.662	4.464	6.072
9	68.652	2.074	3.114	-84.220	-99.999	-84.815		-16.889	4.000	5.020	-99.999	-99.999	-99.999
10	-21.932	2.102	3.145	-30.166	-44.191	-30.300		-8.872	4.004	5.027	-39.100	-45.224	-39.231
11	-5.734	2.453	3.568	-10.015	-13.575	-9.700		-3.079	4.030	5.076	-10.966	-14.336	-10.631
12	2.265	5.135	6.873	-0.796	3.708	5.274		2.370	5.639	7.346	1.274	3.738	5.344

		$^{47}\text{Cr} \rightarrow$		$^{47}\text{V} \rightarrow$		$^{47}\text{Cr} \rightarrow$		$^{47}\text{Sc} \rightarrow$		$^{47}\text{Ca} \rightarrow$		$^{47}\text{Sc} \rightarrow$	
pt		$\log \beta^+$	$\log \epsilon^-$	$\log \nu$	$\log \beta^-$	$\log \epsilon^+$	$\log \nu$	$\log \beta^+$	$\log \epsilon^-$	$\log \nu$	$\log \beta^-$	$\log \epsilon^+$	$\log \nu$
1	0.063	4.301	0.587	-53.072	-38.674	-39.250		42.111	-19.379	-19.912	-5.721	-9.069	-5.951
2	0.062	-2.005	0.595	-17.476	-13.845	-13.925		-13.692	-9.505	-9.506	-5.110	-5.895	-4.788
3	0.042	-0.083	1.063	-5.118	-4.047	-3.499		-4.133	-3.516	-2.786	-1.644	-2.275	-0.890
4	2.671	5.336	7.028	-0.721	4.271	5.875		1.827	4.780	6.470	1.608	4.606	6.209
5	0.063	-0.596	0.762	-53.154	-44.494	-45.070		-42.111	-13.602	-14.117	-6.601	-14.888	-6.673
6	0.063	-0.587	0.771	-17.541	-15.561	-15.632		-13.692	-7.796	-7.790	-5.226	-7.602	-4.973
7	0.045	0.010	1.129	-5.130	-4.145	-3.594		-4.128	-3.418	-2.701	-1.648	-2.370	-0.918
8	2.671	5.336	7.028	-0.721	4.271	5.875		1.827	4.780	6.470	1.608	4.605	6.209
9	0.063	5.053	6.321	-99.999	-99.999	-99.999		42.111	3.744	4.777	-99.999	-99.999	-99.999
10	0.063	5.052	6.320	-53.284	-54.039	-53.380		-13.691	3.745	4.781	-37.142	-46.080	-37.273
11	0.059	5.054	6.325	-15.977	-16.057	-15.360		-4.111	3.743	4.792	-10.079	-14.267	-9.745
12	2.787	6.019	7.727	-1.191	3.545	5.146		1.957	5.463	7.170	1.216	3.879	5.481

		$^{47}\text{V} \rightarrow$		$^{47}\text{Ti} \rightarrow$		$^{47}\text{V} \rightarrow$		$^{47}\text{K} \rightarrow$		$^{47}\text{Ca} \rightarrow$		$^{47}\text{Ca} \rightarrow$	
pt		$\log \beta^+$	$\log \epsilon^-$	$\log \nu$	$\log \beta^-$	$\log \epsilon^+$	$\log \nu$	$\log \beta^+$	$\log \epsilon^-$	$\log \nu$	$\log \beta^-$	$\log \epsilon^+$	$\log \nu$
1	-3.302	-6.107	-3.254	-43.131	-18.068	-18.620		-64.186	-41.140	-41.712	-1.347	-6.910	-0.987
2	-3.290	-3.682	-2.913	-13.325	-7.909	-7.922		-21.219	-15.587	-15.656	-1.300	-3.825	-0.930
3	-1.833	-1.289	-0.431	-2.928	-2.825	-2.006		-6.159	-5.164	-4.549	-1.310	-1.687	-0.568
4	2.080	5.077	6.750	-0.759	4.507	6.129		1.802	4.112	5.832	-2.009	4.494	6.062
5	-3.302	-2.303	-1.816	-43.182	-23.888	-24.440		-64.186	-35.320	-35.892	-1.391	-12.729	-1.060
6	-3.284	-2.215	-1.698	-13.340	-9.624	-9.637		-21.218	-13.871	-13.940	-1.335	-5.530	-0.988
7	-1.829	-1.195	-0.347	-2.932	-2.923	-2.067		-6.155	-5.066	-4.457	-1.318	-1.781	-0.626
8	2.080	5.077	6.750	-0.759	4.507	6.129		1.802	4.112	5.832	-2.009	4.494	6.062
9	-3.302	4.665	5.832	-99.999	-99.999	-99.999		-64.186	-9.289	-8.104	-99.999	-99.999	-99.999
10	-3.284	4.667	5.835	-45.285	-48.102	-45.398		-21.218	-1.732	-0.536	-35.636	-44.007	-35.798
11	-1.811	4.677	5.857	-12.911	-14.832	-12.646		-6.136	1.226	2.437	-11.868	-13.674	-11.643
12	2.206	5.764	7.453	0.315	3.783	5.401		1.908	4.788	6.526	-2.470	3.765	5.331

TABLE 3—Continued

$^{48}\text{Cr} \rightarrow ^{48}\text{V}$			$^{48}\text{V} \rightarrow ^{48}\text{Cr}$			$^{48}\text{Cr} \rightarrow ^{48}\text{Cr}$			$^{48}\text{Cr} \rightarrow ^{48}\text{Cr}$				
pt	$\log \beta^+$	$\log \epsilon^-$	$\log \nu$	$\log \beta^-$	$\log \epsilon^+$	$\log \bar{\nu}$	pt	$\log \beta^+$	$\log \epsilon^-$	$\log \nu$	$\log \beta^-$	$\log \epsilon^+$	$\log \bar{\nu}$
1	-6.780	-6.389	-6.219	-43.419	-13.128	-15.632	1	-17.810	-20.086	-17.860	-20.188	-14.616	-15.166
2	-4.714	-3.869	-3.515	-14.033	-7.306	-7.284	2	-9.584	-9.437	-8.912	-7.001	-6.944	-6.489
3	-1.440	-1.199	-0.235	-3.644	-3.448	-2.654	3	-4.374	-3.658	-2.940	-1.492	-2.103	-0.707
4	2.517	5.226	6.912	0.935	4.369	5.983	4	1.816	4.781	6.470	1.645	4.658	6.261
5	-6.779	-2.518	-2.264	-43.431	-18.947	-19.451	5	-17.810	-16.284	-15.839	-20.266	-20.436	-19.982
6	-4.705	-2.385	-2.015	-14.043	-9.020	-8.999	6	-9.470	-7.973	-7.487	-8.660	-8.660	-7.727
7	-1.437	-1.105	-0.158	-3.648	-3.546	-2.714	7	-4.370	-3.561	-2.852	-1.496	-2.198	-0.733
8	2.517	5.226	6.912	0.935	4.369	5.983	8	1.816	4.781	6.470	1.645	4.658	6.261
9	-6.779	4.706	5.839	-99.999	-99.999	-99.999	9	-17.810	3.663	4.665	-99.999	-99.999	-99.999
10	-4.705	4.707	5.840	-44.104	-47.498	-44.246	10	-9.573	3.675	4.685	-38.644	-47.138	-38.775
11	-1.422	4.725	5.875	-13.177	-15.456	-12.890	11	-4.352	3.712	4.749	-9.787	-14.096	-9.455
12	2.633	5.911	7.612	0.504	3.644	5.255	12	1.947	5.463	7.170	1.253	3.932	5.532

$^{48}\text{V} \rightarrow ^{48}\text{Ti}$			$^{48}\text{Ti} \rightarrow ^{48}\text{V}$			$^{48}\text{V} \rightarrow ^{48}\text{V}$			$^{48}\text{V} \rightarrow ^{48}\text{V}$				
pt	$\log \beta^+$	$\log \epsilon^-$	$\log \nu$	$\log \beta^-$	$\log \epsilon^+$	$\log \bar{\nu}$	pt	$\log \beta^+$	$\log \epsilon^-$	$\log \nu$	$\log \beta^-$	$\log \epsilon^+$	$\log \bar{\nu}$
1	-4.657	-7.478	-4.472	-50.546	-24.019	-24.562	1	-89.496	-66.421	-66.997	-0.628	-6.653	-0.097
2	-3.584	-4.105	-3.192	-14.937	-9.134	-9.137	2	-28.639	-22.756	-22.836	-0.386	-3.489	0.170
3	-2.062	-1.516	-0.675	-2.692	-2.726	-1.821	3	-7.413	-6.184	-5.626	-0.341	-1.412	0.304
4	2.202	5.037	6.713	1.015	4.558	6.179	4	1.839	3.804	5.534	-0.524	4.466	6.032
5	-4.657	-3.644	-3.214	-50.585	-29.839	-30.381	5	-89.496	-60.601	-61.177	-0.646	-12.472	-0.126
6	-3.581	-2.634	-2.127	-14.950	-10.849	-10.852	6	-28.639	-21.040	-21.121	-0.399	-5.193	0.149
7	-2.059	-1.421	-0.591	-2.696	-2.823	-1.873	7	-7.409	-6.085	-5.532	-0.344	-1.505	0.284
8	2.202	5.037	6.713	1.015	4.558	6.179	8	1.839	3.804	5.534	-0.524	4.466	6.032
9	-4.657	4.570	5.706	-99.999	-99.999	-99.999	9	-89.496	-18.203	-17.114	-83.322	-99.999	-83.918
10	-3.581	4.585	5.730	-45.967	-49.327	-46.112	10	-28.639	-4.372	-3.264	-30.050	-43.671	-30.191
11	-2.043	4.606	5.767	-12.463	-14.730	-12.187	11	-7.389	1.109	2.247	-9.902	-13.396	-9.617
12	2.321	5.724	7.415	0.577	3.834	5.452	12	1.927	4.479	6.226	-0.958	3.737	5.301

$^{48}\text{Ti} \rightarrow ^{48}\text{Sc}$			$^{48}\text{Sc} \rightarrow ^{48}\text{Ti}$			$^{49}\text{Fe} \rightarrow ^{49}\text{Mn}$			$^{49}\text{Mn} \rightarrow ^{49}\text{Fe}$				
pt	$\log \beta^+$	$\log \epsilon^-$	$\log \nu$	$\log \beta^-$	$\log \epsilon^+$	$\log \bar{\nu}$	pt	$\log \beta^+$	$\log \epsilon^-$	$\log \nu$	$\log \beta^-$	$\log \epsilon^+$	$\log \bar{\nu}$
1	-52.753	-27.105	-27.652	-3.796	-8.010	-3.760	1	0.986	-3.699	1.651	-77.061	-66.850	-67.430
2	-16.261	-10.056	-10.082	-3.077	-4.554	-2.855	2	0.992	-1.419	1.667	-25.682	-22.745	-22.830
3	-3.929	-2.799	-2.179	-2.115	-2.020	-1.078	3	0.855	0.328	1.769	-7.827	-6.340	-5.813
4	2.305	4.993	6.688	1.885	4.517	6.122	4	3.191	5.418	7.115	-1.400	4.127	5.733
5	-52.753	-21.315	-21.851	-4.070	-13.829	-4.112	5	0.986	-0.011	1.731	-77.258	-72.670	-73.250
6	-16.260	-8.344	-8.368	-3.186	-6.260	-3.001	6	0.993	0.008	1.745	-25.822	-24.460	-24.521
7	-3.925	-2.701	-2.086	-2.123	-2.115	-1.146	7	0.857	0.421	1.809	-7.845	-6.439	-5.911
8	2.306	4.993	6.688	1.885	4.517	6.122	8	3.191	5.418	7.116	-1.400	4.127	5.733
9	-52.753	3.816	4.748	-99.999	-99.999	-99.999	9	0.986	5.364	6.674	-99.999	-99.999	-99.999
10	-16.260	3.828	4.768	-34.728	-44.738	-34.856	10	0.993	5.363	6.673	-62.898	-62.938	-62.768
11	-3.908	3.916	4.928	-10.029	-14.011	-9.684	11	0.864	5.325	6.625	-18.987	-18.350	-17.798
12	2.425	5.675	7.366	1.514	3.790	5.394	12	3.281	6.101	7.813	-1.879	3.401	5.005

TABLE 3—Continued

$^{49}\text{Mn} \rightarrow ^{49}\text{Cr}$		$^{49}\text{Cr} \rightarrow ^{49}\text{Mn}$		$^{49}\text{Ti} \rightarrow ^{49}\text{Sc}$		$^{49}\text{Sc} \rightarrow ^{49}\text{Ti}$	
pt	$\log \beta^+$	$\log \epsilon^-$	$\log \nu$	$\log \beta^-$	$\log \epsilon^+$	$\log \bar{\nu}$	$\log \bar{\nu}$
1	0.169	-4.259	0.719	-45.704	-40.314	-40.891	-3.548
2	0.171	-1.964	0.730	-16.323	-14.386	-14.461	-3.501
3	0.219	0.122	1.235	-6.147	-3.995	-3.411	-0.950
4	2.353	5.329	7.005	-2.304	4.502	6.114	6.222
5	0.169	-0.559	0.870	-46.536	-46.134	-46.530	-3.858
6	0.172	-0.546	0.881	-16.707	-16.102	-16.115	-3.753
7	0.222	0.216	1.296	-6.176	-4.093	-3.509	-0.994
8	2.353	5.329	7.005	-2.304	4.502	6.114	6.221
9	0.169	5.216	6.509	-99.999	-99.999	-99.999	-99.999
10	0.172	5.216	6.509	-54.835	-54.579	-54.543	-36.893
11	0.233	5.221	6.521	-17.562	-16.001	-15.416	-9.534
12	2.476	6.014	7.707	-2.793	3.777	5.386	5.494

$^{49}\text{Cr} \rightarrow ^{49}\text{V}$		$^{49}\text{V} \rightarrow ^{49}\text{Cr}$		$^{49}\text{Sc} \rightarrow ^{49}\text{Ca}$		$^{49}\text{Ca} \rightarrow ^{49}\text{Sc}$	
pt	$\log \beta^+$	$\log \epsilon^-$	$\log \nu$	$\log \beta^-$	$\log \epsilon^+$	$\log \bar{\nu}$	$\log \bar{\nu}$
1	-3.484	-6.040	-3.526	-50.925	-16.755	-17.307	-2.767
2	-3.410	-3.622	-2.950	-15.765	-7.749	-7.773	-2.689
3	-2.089	-1.341	-0.505	-3.499	-3.117	-2.385	0.664
4	2.405	5.104	6.785	1.171	4.398	6.017	6.145
5	-3.484	-2.255	-1.776	-50.934	-22.574	-23.127	-3.055
6	-3.403	-2.165	-1.642	-15.773	-9.465	-9.489	-2.895
7	-2.084	-1.247	-0.417	-3.502	-3.215	-2.451	-2.895
8	2.406	5.104	6.785	1.171	4.398	6.017	6.145
9	-3.484	4.632	5.749	-99.999	-99.999	-99.999	-99.999
10	-3.403	4.636	5.754	-44.776	-47.942	-44.915	-31.707
11	-2.064	4.651	5.783	-12.771	-15.125	-12.472	-8.527
12	2.522	5.791	7.486	0.748	3.673	5.290	5.415

$^{49}\text{V} \rightarrow ^{49}\text{Ti}$		$^{49}\text{Ti} \rightarrow ^{49}\text{V}$		$^{49}\text{K} \rightarrow ^{49}\text{Ca}$		$^{49}\text{Ca} \rightarrow ^{49}\text{K}$	
pt	$\log \beta^+$	$\log \epsilon^-$	$\log \nu$	$\log \beta^-$	$\log \epsilon^+$	$\log \bar{\nu}$	$\log \bar{\nu}$
1	-11.128	-8.177	-8.249	-11.519	-9.326	-9.547	0.159
2	-7.045	-5.326	-5.143	-6.069	-5.693	-5.453	0.549
3	-3.043	-2.138	-1.433	-2.080	-2.270	-1.205	1.340
4	2.079	5.030	6.709	1.498	4.739	6.357	6.458
5	-11.128	-4.180	-4.081	-12.826	-15.145	-13.331	0.148
6	-7.031	-3.763	-3.543	-6.362	-7.404	-6.418	0.541
7	-3.040	-2.041	-1.343	-2.083	-2.247	-1.247	0.541
8	2.079	5.030	6.709	1.498	4.739	6.357	6.458
9	-11.128	4.439	5.543	-99.999	-99.999	-99.999	-99.999
10	-7.031	4.443	5.550	-41.013	-45.881	-41.152	-19.400
11	-3.025	4.447	5.564	-11.238	-14.267	-10.937	-6.085
12	2.206	5.717	7.411	1.077	4.015	5.630	5.729

TABLE 3—Continued

pt	$^{50}\text{Mn} \rightarrow ^{50}\text{Cr}$				$^{50}\text{Ti} \rightarrow ^{50}\text{Sc}$				$^{50}\text{Ti} \rightarrow ^{50}\text{Sc}$							
	log β^+	log ϵ^-	log ν	log $\bar{\nu}$	log β^+	log ϵ^-	log ν	log $\bar{\nu}$	log β^+	log ϵ^-	log ν	log $\bar{\nu}$	log β^+	log ϵ^+	log $\bar{\nu}$	
1	0.151	4.280	0.676	52.019	-39.660	-40.238	-1.835	-7.271	-1.835	-7.271	-1.835	-7.271	-1.835	-7.271	-1.835	
2	-0.306	-2.355	-0.240	-16.610	-13.923	-14.001	-3.981	-3.981	-3.981	-3.981	-3.981	-3.981	-3.981	-3.981	-3.981	
3	-0.349	-0.368	0.712	-4.492	-3.788	-3.157	-3.157	-3.157	-3.157	-3.157	-3.157	-3.157	-3.157	-3.157	-3.157	
4	2.356	5.303	6.982	-0.566	4.520	6.133	6.425	6.425	6.425	6.425	6.425	6.425	6.425	6.425	6.425	
5	0.131	-0.578	0.836	-52.174	-45.480	-46.057	-35.801	-35.801	-35.801	-35.801	-35.801	-35.801	-35.801	-35.801	-35.801	
6	-0.306	-0.938	0.417	-16.739	-15.639	-15.662	-12.798	-12.798	-12.798	-12.798	-12.798	-12.798	-12.798	-12.798	-12.798	
7	-0.346	-0.275	0.779	-4.506	-3.886	-3.249	-3.872	-3.872	-3.872	-3.872	-3.872	-3.872	-3.872	-3.872	-3.872	
8	2.356	5.304	6.982	-0.566	4.520	6.133	6.425	6.425	6.425	6.425	6.425	6.425	6.425	6.425	6.425	
9	0.131	5.115	6.383	-99.999	-99.999	-99.999	3.941	3.941	3.941	3.941	3.941	3.941	3.941	3.941	3.941	
10	-0.306	5.077	6.327	-53.045	-54.116	-53.192	3.944	3.944	3.944	3.944	3.944	3.944	3.944	3.944	3.944	
11	-0.333	5.080	6.335	-15.498	-15.795	-14.987	3.981	3.981	3.981	3.981	3.981	3.981	3.981	3.981	3.981	
12	2.481	5.989	7.683	-1.040	3.795	5.405	5.429	5.429	5.429	5.429	5.429	5.429	5.429	5.429	5.429	
pt	$^{50}\text{Cr} \rightarrow ^{50}\text{V}$				$^{50}\text{Cr} \rightarrow ^{50}\text{Cr}$				$^{50}\text{Ca} \rightarrow ^{50}\text{Sc}$				$^{50}\text{Ca} \rightarrow ^{50}\text{Sc}$			
	log β^+	log ϵ^-	log ν	log $\bar{\nu}$	log β^+	log ϵ^-	log ν	log $\bar{\nu}$	log β^+	log ϵ^-	log ν	log $\bar{\nu}$	log β^+	log ϵ^+	log $\bar{\nu}$	
1	-19.060	-14.444	-14.948	-6.932	-9.917	-7.314	-6.932	-6.932	-6.932	-6.932	-6.932	-6.932	-6.932	-6.932	-6.932	
2	-8.119	-6.323	-6.239	-5.244	-5.624	-4.985	-5.244	-5.244	-5.244	-5.244	-5.244	-5.244	-5.244	-5.244	-5.244	
3	-2.632	-1.691	-0.959	-2.904	-2.403	-1.630	-2.403	-2.403	-2.403	-2.403	-2.403	-2.403	-2.403	-2.403	-2.403	
4	2.372	5.110	6.792	1.683	4.526	6.147	4.526	4.526	4.526	4.526	4.526	4.526	4.526	4.526	4.526	
5	-19.060	-8.720	-9.220	-8.784	-15.737	-9.400	-8.784	-8.784	-8.784	-8.784	-8.784	-8.784	-8.784	-8.784	-8.784	
6	-8.108	-4.685	-4.594	-5.465	-7.333	-5.462	-5.465	-5.465	-5.465	-5.465	-5.465	-5.465	-5.465	-5.465	-5.465	
7	-2.629	-1.596	-0.868	-2.907	-2.500	-1.702	-2.907	-2.907	-2.907	-2.907	-2.907	-2.907	-2.907	-2.907	-2.907	
8	2.372	5.111	6.792	1.683	4.526	6.147	1.683	1.683	1.683	1.683	1.683	1.683	1.683	1.683	1.683	
9	-19.060	4.439	5.487	-99.999	-99.999	-99.999	3.694	3.694	3.694	3.694	3.694	3.694	3.694	3.694	3.694	
10	-8.108	4.451	5.507	-39.521	-45.810	-39.655	3.704	3.704	3.704	3.704	3.704	3.704	3.704	3.704	3.704	
11	-2.614	4.493	5.583	-11.466	-14.404	-11.144	3.730	3.730	3.730	3.730	3.730	3.730	3.730	3.730	3.730	
12	2.488	5.797	7.493	1.279	3.801	5.420	5.138	5.138	5.138	5.138	5.138	5.138	5.138	5.138	5.138	
pt	$^{50}\text{V} \rightarrow ^{50}\text{Ti}$				$^{51}\text{Mn} \rightarrow ^{51}\text{Cr}$				$^{51}\text{Cr} \rightarrow ^{51}\text{Mn}$				$^{51}\text{Cr} \rightarrow ^{51}\text{Mn}$			
	log β^+	log ϵ^-	log ν	log $\bar{\nu}$	log β^+	log ϵ^-	log ν	log $\bar{\nu}$	log β^+	log ϵ^-	log ν	log $\bar{\nu}$	log β^+	log ϵ^+	log $\bar{\nu}$	
1	-10.217	-9.165	-9.055	-18.588	-16.758	-17.197	-9.055	-9.055	-9.055	-9.055	-9.055	-9.055	-9.055	-9.055	-9.055	
2	-5.780	-5.402	-5.034	-8.141	-7.335	-7.184	-5.034	-5.034	-5.034	-5.034	-5.034	-5.034	-5.034	-5.034	-5.034	
3	-3.034	-2.151	-1.425	-2.038	-2.208	-1.160	-2.038	-2.038	-2.038	-2.038	-2.038	-2.038	-2.038	-2.038	-2.038	
4	2.065	5.037	6.717	1.415	4.657	6.274	1.415	1.415	1.415	1.415	1.415	1.415	1.415	1.415	1.415	
5	-10.217	-5.118	-5.011	-20.093	-22.578	-20.596	-5.011	-5.011	-5.011	-5.011	-5.011	-5.011	-5.011	-5.011	-5.011	
6	-5.777	-3.853	-3.595	-8.483	-9.047	-8.474	-3.595	-3.595	-3.595	-3.595	-3.595	-3.595	-3.595	-3.595	-3.595	
7	-3.030	-2.055	-1.335	-2.041	-2.304	-1.202	-2.041	-2.041	-2.041	-2.041	-2.041	-2.041	-2.041	-2.041	-2.041	
8	2.065	5.037	6.717	1.415	4.657	6.274	1.415	1.415	1.415	1.415	1.415	1.415	1.415	1.415	1.415	
9	-10.217	4.402	5.500	-99.999	-99.999	-99.999	6.027	6.027	6.027	6.027	6.027	6.027	6.027	6.027	6.027	
10	-5.776	4.410	5.512	-42.634	-47.524	-42.773	4.868	4.868	4.868	4.868	4.868	4.868	4.868	4.868	4.868	
11	-3.014	4.430	5.548	-11.175	-14.214	-10.874	4.884	4.884	4.884	4.884	4.884	4.884	4.884	4.884	4.884	
12	2.192	5.723	7.418	0.995	3.932	5.546	6.020	6.020	6.020	6.020	6.020	6.020	6.020	6.020	6.020	

TABLE 3—Continued

$^{51}\text{Cr} \rightarrow ^{51}\text{V}$			$^{51}\text{Ti} \rightarrow ^{51}\text{Cr}$			$^{52}\text{Fe} \rightarrow ^{52}\text{Mn}$			$^{52}\text{Mn} \rightarrow ^{52}\text{Fe}$		
pt	$\log \beta^+$	$\log \epsilon^-$	$\log \nu$	$\log \beta^-$	$\log \epsilon^+$	pt	$\log \beta^+$	$\log \epsilon^-$	$\log \nu$	$\log \beta^-$	$\log \epsilon^+$
1	-10.642	-7.821	-7.880	-13.151	-9.742	1	-4.815	-6.444	-5.086	-42.794	-16.886
2	-6.166	-5.042	-4.796	-7.059	-5.973	2	-4.062	-3.922	-3.386	-13.867	-8.589
3	-2.676	-1.832	-1.064	-2.732	-2.360	3	-1.227	-1.107	-0.081	-3.683	-2.863
4	-2.192	5.010	6.682	1.846	4.645	4	2.744	5.416	7.107	0.731	4.411
5	-10.642	-3.831	-3.725	-13.872	-15.561	5	-4.814	-2.266	-2.266	-42.810	-22.706
6	-6.156	-3.522	-3.249	-7.373	-7.684	6	-4.054	-2.462	-1.986	-13.881	-10.304
7	-2.673	-1.737	-0.975	-2.734	-2.457	7	-1.224	-1.014	-0.008	-3.687	-2.913
8	-2.192	5.010	6.682	1.846	4.644	8	2.744	5.416	7.107	0.731	4.411
9	-10.642	4.422	5.478	-99.999	-99.999	9	-4.814	4.891	6.037	-99.999	-99.999
10	-6.156	4.422	5.483	-41.344	-46.162	10	-4.054	4.893	6.041	-45.293	-48.782
11	-2.657	4.453	5.534	-11.328	-14.364	11	-1.210	4.919	6.086	-13.546	-15.771
12	2.310	5.699	7.385	1.441	3.921	12	2.858	6.099	7.806	0.291	3.685

$^{51}\text{V} \rightarrow ^{51}\text{Ti}$			$^{51}\text{Ti} \rightarrow ^{51}\text{V}$			$^{52}\text{Cr} \rightarrow ^{52}\text{Mn}$			$^{52}\text{Mn} \rightarrow ^{52}\text{Cr}$		
pt	$\log \beta^+$	$\log \epsilon^-$	$\log \nu$	$\log \beta^-$	$\log \epsilon^+$	pt	$\log \beta^+$	$\log \epsilon^-$	$\log \nu$	$\log \beta^-$	$\log \epsilon^+$
1	-46.911	-20.318	-20.877	-2.671	-7.446	1	-5.069	-7.362	-4.803	-30.520	-27.352
2	-15.440	-8.986	-9.013	-2.578	-4.300	2	-3.406	-4.213	-3.014	-12.493	-10.424
3	-4.254	-2.843	-2.283	-0.612	-1.617	3	-1.792	-1.145	-0.368	-2.586	-2.781
4	-2.596	5.037	6.732	1.332	4.574	4	2.262	5.254	6.931	0.211	4.641
5	-46.911	-14.502	-15.062	-2.868	-13.265	5	-5.069	-3.478	-3.169	-33.850	-33.171
6	-15.440	-7.280	-7.309	-2.695	-6.006	6	-3.404	-2.752	-2.138	-12.535	-12.139
7	-4.256	-2.744	-2.187	-0.615	-1.711	7	-1.789	-1.049	-0.283	-2.595	-2.877
8	-2.596	5.037	6.732	1.332	4.574	8	2.262	5.254	6.931	0.211	4.641
9	-46.911	4.393	5.495	-99.999	-99.999	9	-5.069	4.901	6.104	-99.999	-99.999
10	-15.440	4.396	5.500	-35.799	-44.483	10	-3.404	4.904	6.109	-47.382	-50.617
11	-4.234	4.407	5.525	-9.914	-13.604	11	-1.774	4.921	6.138	-13.261	-14.778
12	2.700	5.721	7.431	0.909	3.849	12	2.387	5.940	7.633	-0.253	3.916

$^{51}\text{Ti} \rightarrow ^{51}\text{Sc}$			$^{51}\text{Sc} \rightarrow ^{51}\text{Ti}$			$^{52}\text{V} \rightarrow ^{52}\text{Cr}$			$^{52}\text{Cr} \rightarrow ^{52}\text{V}$		
pt	$\log \beta^+$	$\log \epsilon^-$	$\log \nu$	$\log \beta^-$	$\log \epsilon^+$	pt	$\log \beta^+$	$\log \epsilon^-$	$\log \nu$	$\log \beta^-$	$\log \epsilon^+$
1	-64.928	-39.329	-39.898	-1.261	-6.706	1	-54.330	-26.180	-26.731	-2.592	-7.350
2	-20.949	-14.399	-14.463	-1.173	-3.634	2	-16.541	-9.487	-9.507	-2.505	-4.146
3	-5.761	-4.374	-3.826	-0.254	-1.449	3	-3.786	-2.385	-1.796	-1.059	-1.699
4	2.102	4.565	6.240	2.352	4.744	4	2.515	4.972	6.651	1.506	4.639
5	-64.928	-33.509	-34.079	-1.321	-12.525	5	-54.330	-20.395	-20.942	-2.739	-13.169
6	-20.948	-12.683	-12.748	-1.213	-5.339	6	-16.540	-7.795	-7.809	-2.604	-5.852
7	-5.757	-4.276	-3.731	-0.256	-1.543	7	-3.783	-2.288	-1.701	-1.062	-1.794
8	2.102	4.565	6.240	2.352	4.744	8	2.515	4.973	6.651	1.506	4.639
9	-64.928	3.837	4.805	-87.763	-99.999	9	-54.330	4.505	5.605	-99.999	-99.999
10	-20.948	3.839	4.809	-29.567	-43.817	10	-16.540	4.507	5.609	-35.035	-44.330
11	-5.740	3.858	4.851	-8.034	-13.434	11	-3.769	4.538	5.659	-10.364	-13.690
12	2.204	5.254	6.943	1.973	4.020	12	2.615	5.660	7.353	1.082	3.915

TABLE 3—Continued

$^{52}\text{V} \rightarrow ^{52}\text{Ti}$			$^{52}\text{Ti} \rightarrow ^{52}\text{V}$			$^{53}\text{Mn} \rightarrow ^{53}\text{Cr}$			$^{53}\text{Cr} \rightarrow ^{53}\text{Mn}$			
pt	$\log \beta^+$	$\log \epsilon^-$	$\log \nu$	$\log \beta^-$	$\log \epsilon^+$	$\log \bar{\nu}$	$\log \beta^+$	$\log \epsilon^-$	$\log \nu$	$\log \beta^-$	$\log \epsilon^+$	$\log \bar{\nu}$
1	45.186	-18.162	-18.721	-2.110	-6.779	-2.060	-11.864	-9.255	-9.222	-10.170	-9.681	-9.991
2	15.557	-8.560	-8.601	-2.029	-3.666	-1.896	-7.101	-5.221	-5.058	-5.500	-5.599	-5.087
3	4.795	-2.439	-1.935	0.318	-0.611	0.934	-2.919	-1.130	-0.562	-1.487	-1.528	-0.593
4	2.184	4.855	6.527	1.106	4.808	6.436	2.595	5.111	6.789	-0.025	4.670	6.290
5	45.186	-12.342	-12.901	-2.417	-12.599	-2.505	11.864	4.830	4.960	-12.200	-15.501	-12.795
6	15.556	-6.845	-6.886	-2.171	-5.371	-2.102	-7.091	-3.631	-3.460	-5.657	-7.310	-5.490
7	4.792	-2.340	-1.837	0.312	-0.705	0.906	-2.916	-1.032	-0.465	-1.499	-1.623	-0.668
8	2.184	4.855	6.527	1.106	4.808	6.435	2.595	5.111	6.789	-0.025	4.670	6.290
9	45.186	4.525	5.685	-99.999	-99.999	-99.999	-11.864	4.913	6.135	-99.999	-99.999	-99.999
10	15.556	4.526	5.687	-35.886	-43.849	-36.036	-7.091	4.915	6.138	-41.587	-45.788	-41.768
11	4.775	4.538	5.710	-9.708	-12.596	-9.459	-2.901	4.923	6.156	-12.367	-13.518	-12.110
12	2.293	5.544	7.230	0.661	4.084	5.709	2.694	5.797	7.490	-0.495	3.946	5.563

$^{53}\text{Co} \rightarrow ^{53}\text{Fe}$			$^{53}\text{Fe} \rightarrow ^{53}\text{Co}$			$^{53}\text{Cr} \rightarrow ^{53}\text{V}$			$^{53}\text{V} \rightarrow ^{53}\text{Cr}$			
pt	$\log \beta^+$	$\log \epsilon^-$	$\log \nu$	$\log \beta^-$	$\log \epsilon^+$	$\log \bar{\nu}$	$\log \beta^+$	$\log \epsilon^-$	$\log \nu$	$\log \beta^-$	$\log \epsilon^+$	$\log \bar{\nu}$
1	0.484	-4.035	1.077	-46.710	-43.104	-43.683	-52.268	-23.853	-24.411	-2.018	-6.900	-1.845
2	0.479	-1.738	1.077	-17.936	-15.203	-15.278	-16.521	-9.129	-9.169	-1.890	-3.749	-1.664
3	0.453	0.331	1.460	-7.987	-4.124	-3.543	-4.267	-2.675	-2.114	-0.713	-1.484	0.034
4	2.504	5.454	7.135	4.228	4.516	6.124	2.564	5.001	6.684	1.773	4.651	6.276
5	0.484	-0.342	1.200	-49.702	-48.924	-49.461	-52.268	-18.046	-18.601	-2.166	-12.720	-2.047
6	0.479	-0.315	1.202	-18.687	-16.919	-16.992	-16.521	-7.412	-7.452	-1.981	-5.455	-1.794
7	0.455	0.425	1.519	-8.023	-4.222	-3.641	-4.264	-2.577	-2.018	-0.716	-1.578	0.012
8	2.504	5.454	7.136	4.228	4.516	6.124	2.564	5.002	6.684	1.773	4.651	6.276
9	0.484	5.349	6.658	-99.999	-99.999	-99.999	-52.268	4.458	5.534	-99.999	-99.999	-99.999
10	0.479	5.349	6.659	-57.089	-55.396	-55.469	-16.521	4.461	5.538	-34.834	-43.933	-34.969
11	0.464	5.349	6.662	-19.524	-16.129	-15.550	-4.249	4.479	5.575	-9.682	-13.473	-9.366
12	2.626	6.138	7.836	-4.722	3.791	5.396	2.664	5.688	7.385	1.360	3.927	5.549

$^{53}\text{Fe} \rightarrow ^{53}\text{Mn}$			$^{53}\text{Mn} \rightarrow ^{53}\text{Fe}$			$^{53}\text{Ti} \rightarrow ^{53}\text{V}$			$^{53}\text{V} \rightarrow ^{53}\text{Ti}$			
pt	$\log \beta^+$	$\log \epsilon^-$	$\log \nu$	$\log \beta^-$	$\log \epsilon^+$	$\log \bar{\nu}$	$\log \beta^+$	$\log \epsilon^-$	$\log \nu$	$\log \beta^-$	$\log \epsilon^+$	$\log \bar{\nu}$
1	-2.878	-5.842	-2.722	-49.725	-22.039	-22.589	-44.651	-32.557	-33.123	-1.544	-6.794	-1.257
2	-2.818	-3.416	-2.454	-15.426	-9.309	-9.315	-15.555	-12.377	-12.440	-0.936	-3.486	-0.523
3	-1.340	-0.978	-0.054	-3.423	-3.219	-2.442	-5.388	-3.451	-2.893	0.444	-0.906	1.136
4	2.457	5.238	6.913	1.104	4.558	6.180	1.599	4.731	6.381	2.157	5.011	6.659
5	-2.878	-2.040	-1.533	-49.767	-27.859	-28.409	-44.651	-26.738	-27.304	-1.640	-12.613	-1.382
6	-2.815	-1.950	-1.410	-15.438	-11.023	-11.030	-15.552	-10.662	-10.725	-0.970	-5.191	-0.572
7	-1.336	-0.884	0.026	-3.427	-3.317	-2.504	-5.377	-3.353	-2.795	0.441	-1.000	1.125
8	2.457	5.238	6.913	1.104	4.558	6.180	1.599	4.731	6.381	2.157	5.011	6.658
9	-2.878	4.862	6.019	-99.999	-99.999	-99.999	-44.651	4.306	5.378	-94.664	-99.999	-95.260
10	-2.815	4.863	6.021	-46.512	-49.501	-46.656	-15.552	4.309	5.383	-31.491	-43.668	-31.628
11	-1.321	4.873	6.042	-13.209	-15.226	-12.930	-5.330	4.326	5.414	-8.472	-12.892	-8.163
12	2.572	5.925	7.615	0.666	3.834	5.453	1.725	5.425	7.088	1.743	4.289	5.933

TABLE 3—Continued

		$^{54}\text{Co} \rightarrow ^{54}\text{Fe}$			$^{54}\text{Fe} \rightarrow ^{54}\text{Mn}$			$^{54}\text{Mn} \rightarrow ^{54}\text{Cr}$			$^{54}\text{Cr} \rightarrow ^{54}\text{V}$			$^{54}\text{V} \rightarrow ^{54}\text{Cr}$					
pt		$\log \beta^+$	$\log \epsilon^-$	$\log \nu$	$\log \beta^-$	$\log \epsilon^+$	$\log \bar{\nu}$	$\log \beta^+$	$\log \epsilon^-$	$\log \nu$	$\log \beta^-$	$\log \epsilon^+$	$\log \bar{\nu}$	$\log \beta^+$	$\log \epsilon^-$	$\log \nu$	$\log \beta^-$	$\log \epsilon^+$	$\log \bar{\nu}$
1		0.173	-4.341	0.763	-51.249	-42.707	-43.285	-16.769	-13.539	-13.635	-10.578	-9.445	-9.614	-69.513	-41.036	-41.600	-1.047	-6.626	-0.593
2		-0.319	-2.531	0.274	-16.590	-14.998	-15.066	-7.419	-6.022	-5.823	-6.039	-5.861	-5.490	-21.734	-14.106	-14.168	-0.747	-3.435	-0.287
3		-0.042	-0.320	0.927	-4.958	-4.175	-3.457	-2.451	-1.247	-0.570	-2.008	-2.262	-1.256	5	-3.452	-3.160	-0.077	-1.272	0.671
4		2.680	5.602	7.286	-1.315	4.475	6.077	2.841	5.228	6.912	0.411	4.543	6.161	3	2.374	4.846	2.312	4.784	6.428
5		0.173	-0.655	0.888	-51.535	-48.526	-49.103	-16.769	-9.508	-9.439	-10.889	-15.264	-10.893	4	-69.513	-35.216	-1.086	-12.445	-0.641
6		-0.319	-1.120	0.403	-16.746	-16.714	-16.465	-7.408	-4.476	-4.252	-6.173	-7.572	-5.995	6	-21.734	-12.391	-0.774	-5.140	-0.326
7		-0.040	-0.227	0.983	-4.978	-4.271	-3.551	-2.448	-1.151	-0.477	-2.015	-2.358	-1.313	8	-2.374	4.846	2.312	4.784	6.428
8		2.680	5.602	7.286	-1.315	4.475	6.077	2.841	5.228	6.912	0.411	4.543	6.161	9	-69.513	4.270	5.276	85.697	99.999
9		0.173	-0.655	0.888	-51.535	-48.526	-49.103	-7.419	-6.022	-5.823	-6.039	-5.861	-5.490	10	-21.734	4.275	5.283	-29.380	-43.618
10		-0.319	-1.120	0.403	-16.746	-16.714	-16.465	5.692	54.111	-55.192	-54.293			11	-5.433	4.306	5.337	-8.277	-13.258
11		-0.030	-0.448	5.952	-16.184	-16.173	-15.398	5.952	-16.184	-16.173	-15.398			12	2.424	5.538	7.217	1.920	4.061
12		2.802	6.286	7.986	-1.796	3.749	5.349	2.802	6.286	7.986	-1.796	3.749	5.349						

		$^{55}\text{Co} \rightarrow ^{55}\text{Fe}$			$^{55}\text{Fe} \rightarrow ^{55}\text{Mn}$			$^{55}\text{Mn} \rightarrow ^{55}\text{Cr}$			$^{55}\text{Cr} \rightarrow ^{55}\text{V}$								
pt		$\log \beta^+$	$\log \epsilon^-$	$\log \nu$	$\log \beta^-$	$\log \epsilon^+$	$\log \bar{\nu}$	$\log \beta^+$	$\log \epsilon^-$	$\log \nu$	$\log \beta^-$	$\log \epsilon^+$	$\log \bar{\nu}$	$\log \beta^+$	$\log \epsilon^-$	$\log \nu$	$\log \beta^-$	$\log \epsilon^+$	$\log \bar{\nu}$
1		-5.078	-6.985	-5.187	-22.069	-21.584	-22.014	-16.769	-13.539	-13.635	-10.578	-9.445	-9.614	-11.887	-9.185	-9.537	-10.726	-9.887	-9.934
2		-4.842	-3.275	-3.229	-9.445	-8.751	-8.431	-7.419	-6.022	-5.823	-6.039	-5.861	-5.490	2	-6.714	-5.286	-4.869	-5.728	-4.675
3		-1.722	-0.061	0.560	-5.513	-2.265	-1.580	-2.451	-1.247	-0.570	-2.008	-2.262	-1.256	3	-2.856	-0.203	-1.783	-1.396	-0.563
4		2.854	5.329	7.018	-3.856	4.558	6.165	2.841	5.228	6.912	0.411	4.543	6.161	4	2.807	5.253	6.937	0.621	4.647
5		-3.078	-2.273	-2.466	-24.763	-27.404	-25.541	-16.769	-9.508	-9.439	-10.889	-15.264	-10.893	5	-11.886	-4.917	-4.988	-11.530	-11.939
6		-4.836	-1.616	-1.563	-10.069	-10.041		-7.408	-4.476	-4.252	-6.173	-7.572	-5.995	6	-6.703	-3.723	-3.494	-7.440	-4.895
7		-1.718	0.035	0.656	-5.548	-2.361	-1.677	-2.448	-1.151	-0.477	-2.015	-2.358	-1.313	7	-2.853	-0.106	-1.800	-1.491	-0.652
8		2.854	5.329	7.019	-3.856	4.558	6.165	2.841	5.228	6.913	0.411	4.543	6.161	8	2.517	6.846	0.447	4.741	6.356
9		-5.078	-6.985	-5.187	-22.069	-21.584	-22.014	-7.419	-6.022	-5.823	-6.039	-5.861	-5.490	9	-11.886	6.197	-99.999	-99.999	-99.999
10		-4.836	-1.616	-1.563	-10.069	-10.041		6.125	40.673	46.050	-40.835			10	-6.703	6.198	-42.203	-46.141	-42.403
11		-1.703	5.228	6.518	-17.041	-14.262	-13.582	6.125	40.673	46.050	-40.835			11	-2.840	6.214	-12.285	-12.907	-11.856
12		2.953	6.012	7.718	-4.350	3.833	5.437	2.953	6.012	7.718	-4.350	3.833	5.437	12	2.903	7.637	-1.089	3.923	5.534

		$^{55}\text{Fe} \rightarrow ^{55}\text{Mn}$			$^{55}\text{Mn} \rightarrow ^{55}\text{Cr}$		
pt		$\log \beta^+$	$\log \epsilon^-$	$\log \nu$	$\log \beta^-$	$\log \epsilon^+$	$\log \bar{\nu}$
1		-11.887	-9.185	-9.537	-10.726	-9.887	-9.934
2		-6.714	-5.286	-5.055	-4.869	-5.728	-4.675
3		-2.856	-0.203	-1.783	-1.396	-0.563	
4		2.807	5.253	6.937	0.621	4.647	6.261
5		-11.886	-4.917	-4.988	-11.530	-11.939	
6		-6.703	-3.723	-3.494	-7.440	-4.895	
7		-2.853	-0.106	-1.800	-1.491	-0.652	
8		2.517	6.846	0.447	4.741	6.356	
9		-11.886	5.045	6.283	-99.999	-99.999	
10		-6.703	5.046	6.285	-41.870	-45.918	
11		-2.840	5.061	6.309	-13.900	-13.387	
12		2.903	5.938	7.637	-1.089	3.923	

TABLE 3—Continued

		$^{55}\text{Mn} \rightarrow ^{55}\text{Cr}$			$^{55}\text{Cr} \rightarrow ^{55}\text{Mn}$			$^{56}\text{Ni} \rightarrow ^{56}\text{Co}$			$^{56}\text{Co} \rightarrow ^{56}\text{Ni}$		
pt		$\log \beta^+$	$\log \epsilon^-$	$\log \nu$	$\log \beta^-$	$\log \epsilon^+$	$\log \bar{\nu}$	$\log \beta^+$	$\log \epsilon^-$	$\log \nu$	$\log \beta^-$	$\log \epsilon^+$	$\log \bar{\nu}$
1		-52.522	-20.911	-21.474	-2.440	-7.460	-2.270	-14.981	-7.199	-7.425	-19.208	-18.034	-18.097
2		-16.973	-8.824	-8.866	-2.188	-4.111	-1.956	-5.846	-4.308	-4.203	-8.150	-8.909	-8.020
3		-4.426	-2.364	-1.847	-0.172	-1.208	0.454	-1.111	-0.309	0.382	-4.049	-3.183	-2.430
4		-2.423	-4.997	-6.666	1.403	4.799	6.433	3.202	5.500	7.203	-1.543	4.378	5.977
5		-52.522	-15.095	-15.657	-2.582	-13.279	-2.481	-14.981	-3.079	-3.074	-21.007	-23.854	-21.185
6		-16.973	-7.107	-7.149	-2.273	-5.816	-2.080	-5.843	-2.711	-2.590	-8.343	-10.618	-8.391
7		-4.423	-2.265	-1.750	-0.177	-1.302	0.432	-1.109	-0.212	0.469	-4.071	-3.278	-2.524
8		-2.423	-4.997	-6.666	1.403	4.799	6.432	3.202	5.501	7.203	-1.543	4.378	5.977
9		-52.522	-4.703	5.846	-99.999	-99.999	-99.999	-14.981	5.234	6.492	-99.999	-99.999	-99.999
10		-16.973	-4.703	5.847	-35.703	-44.294	-35.848	-5.843	5.235	6.494	-46.025	-49.096	-46.270
11		-4.411	-4.715	5.870	-9.998	-13.193	-9.728	-1.096	5.248	6.517	-15.346	-15.177	-14.394
12		-2.524	-5.686	7.369	0.964	4.076	5.706	3.295	6.181	7.899	-2.027	3.652	5.249

		$^{55}\text{Cr} \rightarrow ^{55}\text{V}$			$^{55}\text{V} \rightarrow ^{55}\text{Cr}$			$^{56}\text{Fe} \rightarrow ^{56}\text{Co}$			$^{56}\text{Co} \rightarrow ^{56}\text{Fe}$		
pt		$\log \beta^+$	$\log \epsilon^-$	$\log \nu$	$\log \beta^-$	$\log \epsilon^+$	$\log \bar{\nu}$	$\log \beta^+$	$\log \epsilon^-$	$\log \nu$	$\log \beta^-$	$\log \epsilon^+$	$\log \bar{\nu}$
1		-70.281	-39.505	-40.082	-0.366	-6.498	0.138	-3.727	-6.599	-3.543	-28.066	-25.987	-26.525
2		-22.575	-14.310	-14.390	-0.298	-3.397	0.214	-3.207	-3.504	-2.767	-9.924	-9.744	-9.523
3		-6.238	-4.355	-3.858	0.379	-1.190	1.150	-1.691	-0.193	0.432	-3.991	-1.955	-1.246
4		-1.990	-4.686	-6.331	2.867	4.979	6.645	2.693	5.340	7.021	-2.390	4.692	6.303
5		-20.281	-33.686	-34.262	-0.386	-12.318	0.105	-3.727	-2.782	-2.316	-29.392	-31.807	-29.984
6		-22.574	-12.594	-12.674	-0.314	-5.101	0.187	-3.204	-1.938	-1.599	-10.405	-11.457	-10.652
7		-6.235	-4.256	-3.761	0.377	-1.283	1.144	-1.688	-0.096	0.528	-4.022	-2.050	-1.343
8		-1.990	-4.686	-6.331	2.867	4.979	6.645	2.693	5.340	7.021	-2.390	4.692	6.303
9		-70.281	-4.157	5.120	-86.926	-99.999	-87.519	-3.727	5.197	6.469	-99.999	-99.999	-99.999
10		-22.574	-4.159	5.125	-28.991	-43.579	-29.120	-3.204	5.203	6.476	-48.653	-49.935	-48.979
11		-6.222	-4.183	5.172	-7.379	-13.173	-7.036	-1.673	5.216	6.498	-15.447	-13.948	-13.245
12		-2.092	-5.384	7.040	2.489	4.258	5.921	2.797	6.025	7.722	-2.881	3.967	5.575

		$^{55}\text{V} \rightarrow ^{55}\text{Ti}$			$^{55}\text{Ti} \rightarrow ^{55}\text{V}$			$^{56}\text{Mn} \rightarrow ^{56}\text{Fe}$			$^{56}\text{Fe} \rightarrow ^{56}\text{Mn}$		
pt		$\log \beta^+$	$\log \epsilon^-$	$\log \nu$	$\log \beta^-$	$\log \epsilon^+$	$\log \bar{\nu}$	$\log \beta^+$	$\log \epsilon^-$	$\log \nu$	$\log \beta^-$	$\log \epsilon^+$	$\log \bar{\nu}$
1		-79.743	-50.613	-51.192	0.130	-6.320	0.745	-55.626	-24.968	-25.507	-2.482	-7.331	-2.252
2		-26.474	-18.615	-18.702	0.317	-3.209	0.983	-16.931	-8.973	-8.986	-2.300	-4.038	-2.049
3		-7.765	-4.565	-4.099	2.161	0.292	2.918	-3.845	-2.086	-1.510	-0.860	-1.527	-0.140
4		-2.137	-4.583	-6.229	2.558	4.956	6.622	2.633	5.101	6.771	-1.628	4.728	6.364
5		-79.743	-44.793	-45.372	0.121	-12.139	0.727	-55.626	-19.237	-19.773	-2.589	-13.150	-2.404
6		-26.473	-16.899	-16.987	0.310	-4.914	0.971	-16.930	-7.281	-7.285	-2.381	-5.745	-2.167
7		-7.764	-4.466	-4.000	2.159	0.199	2.913	-3.842	-1.988	-1.413	-0.864	-1.622	-0.168
8		-2.137	-4.583	-6.229	2.558	4.956	6.622	2.633	5.101	6.771	-1.628	4.728	6.364
9		-79.743	-4.146	5.156	-75.931	-99.999	-76.526	-55.626	4.727	5.836	-99.999	-99.999	-99.999
10		-26.473	-4.149	5.161	-24.791	-43.391	-24.923	-16.930	4.733	5.845	-35.240	-44.222	-35.381
11		-7.749	-4.171	5.202	-6.006	-11.689	-5.676	-3.829	4.766	5.897	-10.299	-13.519	-10.009
12		-2.225	-5.281	6.938	2.164	4.236	5.897	2.728	5.791	7.474	-1.201	4.006	5.638

TABLE 3—Continued

$^{56}\text{Mn} \rightarrow ^{56}\text{Cr}$		$^{56}\text{Cr} \rightarrow ^{56}\text{Mn}$		$^{56}\text{Ti} \rightarrow ^{56}\text{Sc}$		$^{56}\text{Sc} \rightarrow ^{56}\text{Ti}$	
pt	$\log \beta^+$	$\log \epsilon^-$	$\log \nu$	$\log \beta^-$	$\log \epsilon^+$	$\log \nu$	$\log \bar{\nu}$
1	-45.809	-16.343	-17.094	-2.678	-7.031	-84.917	85.500
2	-15.695	-8.098	-8.129	-2.319	-3.815	-28.983	-29.080
3	-4.782	-2.553	-2.042	0.301	-0.879	-7.474	-7.474
4	2.289	5.000	6.662	1.753	4.914	4.878	6.593
5	-45.809	-10.747	-11.289	-3.076	-12.851	-79.098	-79.681
6	-15.695	-6.383	-6.411	-2.470	-5.521	-27.267	-27.365
7	-4.779	-2.454	-1.944	0.298	-0.973	-7.885	-7.380
8	2.269	5.000	6.662	1.753	4.914	4.878	6.593
9	-45.809	4.683	5.807	-99.999	-99.999	-41.959	-99.999
10	-15.695	4.682	5.807	-36.022	-43.998	-14.887	-43.944
11	-4.765	4.697	5.835	-9.313	-12.865	-4.028	-13.282
12	2.376	5.691	7.367	1.320	4.191	2.820	5.557

$^{56}\text{Cr} \rightarrow ^{56}\text{V}$		$^{56}\text{V} \rightarrow ^{56}\text{Cr}$		$^{57}\text{Zn} \rightarrow ^{57}\text{Cu}$		$^{57}\text{Cu} \rightarrow ^{57}\text{Zn}$	
pt	$\log \beta^+$	$\log \epsilon^-$	$\log \nu$	$\log \beta^-$	$\log \epsilon^+$	$\log \nu$	$\log \bar{\nu}$
1	-87.412	-58.878	-59.457	0.505	-6.140	1.869	-76.636
2	-28.119	-20.349	-20.436	0.515	-3.103	1.870	-25.732
3	-7.964	-5.253	-4.789	1.879	-0.234	2.655	-6.803
4	1.591	4.516	6.122	3.509	5.448	7.294	5.982
5	-87.412	-53.058	-53.637	0.498	-11.959	1.947	-82.442
6	-28.118	-18.609	-18.697	0.510	-4.807	1.947	-27.534
7	-7.960	-3.154	-4.691	1.878	-0.327	2.669	-6.901
8	1.591	4.516	6.122	3.509	5.448	7.295	5.982
9	-87.412	4.072	5.002	-67.204	-99.999	6.731	-99.999
10	-28.118	4.073	5.008	-22.667	-43.284	6.729	-64.970
11	-7.946	4.108	5.068	-5.507	-12.214	6.705	-18.813
12	1.681	5.224	6.839	3.136	4.730	7.994	5.254

$^{56}\text{V} \rightarrow ^{56}\text{Ti}$		$^{56}\text{Ti} \rightarrow ^{56}\text{V}$		$^{57}\text{Ni} \rightarrow ^{57}\text{Cu}$		$^{57}\text{Cu} \rightarrow ^{57}\text{Ni}$	
pt	$\log \beta^+$	$\log \epsilon^-$	$\log \nu$	$\log \beta^-$	$\log \epsilon^+$	$\log \nu$	$\log \bar{\nu}$
1	-65.366	-44.464	-45.042	-5.579	-12.011	1.044	-44.462
2	-21.629	-15.620	-15.707	-0.787	-4.290	1.053	-15.447
3	-5.937	-3.605	-3.126	1.089	-0.425	1.676	-3.586
4	2.667	5.116	6.817	1.327	4.696	7.295	6.217
5	-65.366	-38.644	-39.223	-5.589	-17.830	1.194	-50.281
6	-21.629	-13.904	-13.992	-0.795	-5.994	1.206	-17.142
7	-5.934	-3.506	-3.027	1.087	-0.518	1.729	-3.682
8	2.667	5.117	6.817	1.327	4.696	7.295	6.217
9	-65.366	4.268	5.356	-88.075	-99.999	6.672	-99.999
10	-21.629	4.270	5.359	-29.158	-44.472	6.672	-55.091
11	-5.917	4.286	5.390	-8.014	-12.407	6.699	-16.136
12	2.773	5.798	7.515	0.908	3.963	7.996	3.883

TABLE 3—Continued

$^{57}\text{Ni} \rightarrow ^{57}\text{Co}$		$^{57}\text{Co} \rightarrow ^{57}\text{Ni}$		$^{57}\text{Mn} \rightarrow ^{57}\text{Cr}$		$^{57}\text{Cr} \rightarrow ^{57}\text{Mn}$	
pt	$\log \beta^+$	$\log \epsilon^-$	$\log \nu$	$\log \beta^-$	$\log \epsilon^+$	$\log \nu$	$\log \epsilon^+$
1	-5.524	-6.990	5.668	-27.557	-21.199	-21.729	0.063
2	-3.764	-4.137	3.312	-9.541	-9.487	-9.169	0.260
3	-1.420	-0.479	0.200	-3.387	-2.790	-2.013	2.089
4	2.964	5.402	7.090	-0.932	4.548	6.158	6.729
5	-5.524	-3.185	-2.830	-27.766	-27.018	-27.347	0.030
6	-3.761	-2.669	-2.165	-9.688	-11.203	-9.641	0.237
7	-1.417	-0.381	0.289	-3.406	-2.886	-2.105	0.279
8	2.964	5.402	7.090	-0.932	4.548	6.158	6.729
9	-5.524	5.206	6.453	-99.999	-99.999	-99.999	-89.911
10	-3.761	5.208	6.456	-46.841	-49.680	-47.064	-29.764
11	-1.403	5.225	6.483	-14.565	-14.785	-13.921	-7.479
12	3.060	6.086	7.789	-1.412	3.823	5.430	6.004

$^{57}\text{Fe} \rightarrow ^{57}\text{Co}$		$^{57}\text{Co} \rightarrow ^{57}\text{Fe}$		$^{57}\text{Cr} \rightarrow ^{57}\text{V}$		$^{57}\text{V} \rightarrow ^{57}\text{Cr}$	
pt	$\log \beta^+$	$\log \epsilon^-$	$\log \nu$	$\log \beta^-$	$\log \epsilon^+$	$\log \nu$	$\log \epsilon^+$
1	-11.176	-8.769	-8.896	-11.236	-11.311	-11.360	0.073
2	-6.008	-5.092	-4.893	-6.027	-6.384	-5.676	0.193
3	-2.943	-0.846	-0.283	-1.772	-1.756	-0.853	1.916
4	2.773	5.243	6.921	-0.043	4.718	6.340	6.298
5	-11.176	-4.197	-4.385	-13.725	-17.131	-14.289	0.053
6	-6.000	-3.484	-3.318	-6.138	-8.095	-5.958	0.179
7	-2.940	-0.748	-0.186	-1.784	-1.851	-0.932	1.909
8	2.773	5.244	6.921	-0.043	4.718	6.339	6.298
9	-11.176	5.087	6.313	-99.999	-99.999	-99.999	-81.221
10	-6.000	5.088	6.315	-42.348	-46.572	-42.534	-27.221
11	-2.928	5.100	6.336	-12.738	-13.749	-12.458	-6.958
12	2.867	5.930	7.623	-0.516	3.995	5.612	3.960

$^{57}\text{Fe} \rightarrow ^{57}\text{Mn}$		$^{57}\text{Mn} \rightarrow ^{57}\text{Fe}$		$^{57}\text{Ti} \rightarrow ^{57}\text{V}$		$^{57}\text{V} \rightarrow ^{57}\text{Ti}$	
pt	$\log \beta^+$	$\log \epsilon^-$	$\log \nu$	$\log \beta^-$	$\log \epsilon^+$	$\log \nu$	$\log \epsilon^+$
1	-51.326	-20.585	-21.146	-2.131	-7.121	-1.968	1.431
2	-16.482	-8.474	-8.517	-1.879	-3.925	-1.585	1.456
3	-4.381	-1.689	-1.181	-0.160	-0.565	0.776	2.667
4	2.482	5.103	6.767	0.964	4.885	6.518	6.517
5	-51.326	-14.774	-15.332	-2.281	-12.941	-2.186	1.422
6	-16.481	-6.760	-6.802	-1.953	-5.631	-1.679	1.448
7	-4.378	-1.590	-1.082	0.153	-0.659	0.736	2.664
8	2.482	5.104	6.767	0.964	4.885	6.518	6.517
9	-51.326	4.923	6.110	-99.999	-99.999	-99.999	-66.650
10	-16.481	4.924	6.112	-36.007	-44.108	-36.166	-22.109
11	-4.365	4.935	6.133	-10.251	-12.551	-10.028	-5.141
12	2.581	5.794	7.472	0.509	4.162	5.791	5.791

TABLE 3—Continued

$^{58}\text{Cu} \rightarrow ^{58}\text{Ni}$				$^{58}\text{Ni} \rightarrow ^{58}\text{Co}$				$^{58}\text{Co} \rightarrow ^{58}\text{Fe}$						
pt	$\log \beta^+$	$\log \epsilon^-$	$\log \nu$	$\log \beta^-$	$\log \epsilon^+$	$\log \bar{\nu}$		pt	$\log \beta^+$	$\log \epsilon^-$	$\log \nu$	$\log \beta^-$	$\log \epsilon^+$	$\log \bar{\nu}$
1	-0.452	-4.414	0.122	-55.539	44.413	44.977		1	-19.421	-15.053	-15.518	-8.404	-9.092	-8.754
2	-0.192	-1.994	0.405	-17.917	-15.285	-15.339		2	-8.396	-6.526	-6.369	-6.069	-5.519	-5.207
3	0.084	0.133	1.198	-4.953	-3.885	-3.293		3	-2.778	-1.356	-0.713	-1.707	-2.230	-1.044
4	2.458	5.594	7.275	0.699	4.617	6.224		4	2.912	5.355	7.039	0.773	4.586	6.204
5	-0.452	-0.686	0.367	-55.675	-50.233	-50.797		5	-19.421	-10.425	-10.608	-10.675	-14.911	-11.179
6	0.191	-0.564	0.609	-18.018	-17.001	-16.996		6	-8.383	-4.940	-4.779	-6.234	-7.229	-5.882
7	0.086	0.226	1.260	-4.969	-3.983	-3.388		7	-2.775	-1.259	-0.619	-1.713	-2.326	-1.085
8	2.458	5.594	7.275	0.699	4.617	6.224		8	2.912	5.355	7.039	0.773	4.586	6.204
9	-0.452	5.321	6.587	-99.999	-99.999	-99.999		9	-19.421	5.028	6.200	-99.999	-99.999	-99.999
10	-0.191	5.328	6.599	-54.581	-55.478	-54.712		10	-8.383	5.030	6.203	-39.452	-45.707	-39.607
11	0.094	5.338	6.617	-16.002	-15.892	-15.222		11	-2.763	5.053	6.241	-11.968	-14.226	-11.729
12	2.589	6.277	7.976	-1.175	3.891	5.495		12	3.009	6.041	7.739	0.321	3.862	5.477

$^{58}\text{Ni} \rightarrow ^{58}\text{Mn}$				$^{58}\text{Mn} \rightarrow ^{58}\text{Fe}$				$^{58}\text{Mn} \rightarrow ^{58}\text{Cr}$				$^{58}\text{Cr} \rightarrow ^{58}\text{V}$			
pt	$\log \beta^+$	$\log \epsilon^-$	$\log \nu$	$\log \beta^-$	$\log \epsilon^+$	$\log \bar{\nu}$		pt	$\log \beta^+$	$\log \epsilon^-$	$\log \nu$	$\log \beta^-$	$\log \epsilon^+$	$\log \bar{\nu}$	
1	-68.327	-37.413	-37.983	-0.908	-6.727	-0.456		1	-59.963	-30.776	-31.349	-0.904	-6.729	-0.505	
2	-21.184	-12.916	-12.983	-0.836	-3.560	-0.397		2	-20.340	-12.432	-12.511	-0.227	-3.328	-0.296	
3	-5.258	-3.054	-2.561	0.430	-1.001	1.101		3	-6.532	-2.639	-2.153	2.141	0.929	2.757	
4	2.628	4.998	6.659	1.983	4.813	6.462		4	1.333	4.697	6.312	2.555	5.708	7.379	
5	-68.327	-31.595	-32.165	-0.943	-12.547	-0.505		5	-59.963	-24.956	-25.530	-0.941	-12.549	-0.567	
6	-21.184	-11.201	-11.267	-0.866	-5.265	-0.440		6	-20.340	-10.717	-10.795	-0.243	-5.032	-0.270	
7	-5.255	-2.955	-2.462	0.427	-1.095	1.090		7	-6.529	-2.540	-2.055	2.138	0.835	2.739	
8	2.628	4.998	6.659	1.983	4.813	6.461		8	1.333	4.697	6.312	2.555	5.708	7.379	
9	-68.327	4.673	5.760	-89.367	-99.999	-89.963		9	-59.963	4.622	5.757	-96.382	-99.999	-96.981	
10	-21.184	4.675	5.763	-30.695	-43.743	-30.833		10	-20.340	4.623	5.759	-31.323	-43.510	-31.468	
11	-5.242	4.691	5.794	-8.675	-12.985	-8.372		11	-6.515	4.637	5.785	-7.618	-11.054	-7.346	
12	2.714	5.691	7.364	1.564	4.091	5.736		12	1.433	5.399	7.027	2.118	4.984	6.651	

$^{58}\text{Co} \rightarrow ^{58}\text{Fe}$				$^{58}\text{Fe} \rightarrow ^{58}\text{Cr}$				$^{58}\text{Cr} \rightarrow ^{58}\text{V}$						
pt	$\log \beta^+$	$\log \epsilon^-$	$\log \nu$	$\log \beta^-$	$\log \epsilon^+$	$\log \bar{\nu}$		pt	$\log \beta^+$	$\log \epsilon^-$	$\log \nu$	$\log \beta^-$	$\log \epsilon^+$	$\log \bar{\nu}$
1	-4.909	-6.683	4.947	-22.767	-19.585	-20.092		1	-95.758	-68.968	-69.550	-0.409	-7.503	0.406
2	-4.450	-3.997	3.593	-7.910	-7.738	-7.454		2	-30.497	-24.322	-24.416	-0.443	-4.532	0.378
3	-2.381	-0.594	-0.019	-2.162	-1.568	-0.770		3	-7.733	-6.281	-5.781	0.939	-1.404	1.820
4	2.594	5.285	6.960	-0.661	4.814	6.432		4	3.118	5.199	6.918	2.069	4.511	6.098
5	-4.909	-2.784	-2.511	-24.999	-25.405	-25.397		5	-95.758	-63.149	-63.730	-0.411	-13.323	0.401
6	-4.443	-2.500	-2.134	-8.062	-9.452	-8.019		6	-30.496	-22.607	-22.700	-0.445	-6.236	0.374
7	-2.378	-0.495	0.079	-2.181	-1.663	-0.862		7	-7.730	-6.182	-5.685	0.938	-1.497	1.818
8	2.594	5.285	6.961	-0.661	4.814	6.432		8	3.118	5.199	6.918	2.069	4.511	6.098
9	-4.909	5.129	6.377	-99.999	-99.999	-99.999		9	-95.758	3.676	4.526	-58.532	-99.999	-59.124
10	-4.443	5.130	6.379	-45.305	-47.930	-45.529		10	-30.496	3.681	4.533	-20.175	-44.713	-20.301
11	-2.366	5.139	6.395	-13.360	-13.559	-12.685		11	-7.714	3.720	4.608	-5.680	-13.384	-5.327
12	2.699	5.971	7.662	-1.139	4.090	5.704		12	3.207	5.877	7.612	1.716	3.783	5.370

TABLE 3—Continued

$^{58}\text{V} \rightarrow$		$^{58}\text{Ti} \rightarrow$		$^{58}\text{Ti} \rightarrow$		$^{58}\text{V} \rightarrow$		$^{59}\text{Co} \rightarrow$		$^{59}\text{Fe} \rightarrow$		$^{59}\text{Co} \rightarrow$	
pt	$\log \beta^+$	$\log \epsilon^-$	$\log \nu$	$\log \beta^-$	$\log \epsilon^+$	$\log \nu$	$\log \bar{\nu}$	$\log \beta^+$	$\log \epsilon^-$	$\log \nu$	$\log \beta^-$	$\log \epsilon^+$	$\log \bar{\nu}$
1	-74.447	-48.195	-48.774	0.239	-6.290	0.875	0.875	-47.247	-17.107	-17.603	-4.829	-8.547	-4.784
2	-24.966	-18.017	-18.105	0.370	-3.186	1.032	1.032	-15.021	-7.244	-7.260	-2.578	-4.482	-2.298
3	-7.608	-4.626	-4.158	2.107	0.313	2.846	2.846	-3.645	-1.178	-0.653	0.272	-0.833	0.217
4	1.649	-4.340	5.991	2.486	5.035	6.691	6.691	-2.835	5.254	6.932	0.272	4.754	6.375
5	-74.447	-42.375	-42.955	0.231	-12.109	0.860	0.860	-47.247	-11.496	-11.977	-5.106	-14.367	-5.124
6	-24.965	-16.301	-16.389	0.364	-4.890	1.020	1.020	-15.021	-5.547	-5.557	-2.647	-6.189	-2.399
7	-7.604	-4.527	-4.060	2.106	0.220	2.840	2.840	-3.643	-1.080	-0.555	-0.557	-0.927	0.151
8	1.649	-4.340	5.991	2.486	5.035	6.691	6.691	-2.835	5.254	6.932	0.272	4.753	6.375
9	-74.447	3.886	4.914	-78.656	-99.999	-79.251	-79.251	-47.247	5.054	6.265	-99.999	-99.999	-99.999
10	-24.965	3.888	4.918	-25.710	-43.368	-25.843	-25.843	-15.021	5.055	6.267	-37.984	-44.666	-38.160
11	-7.587	3.908	4.956	-6.278	-11.668	-5.954	-5.954	-3.631	5.066	6.287	-11.310	-12.820	-11.098
12	1.752	5.036	6.698	2.086	4.314	5.966	5.966	2.926	5.941	7.634	-0.195	4.030	5.648

$^{59}\text{Cu} \rightarrow$		$^{59}\text{Ni} \rightarrow$		$^{59}\text{Ni} \rightarrow$		$^{59}\text{Cu} \rightarrow$		$^{59}\text{Mn} \rightarrow$		$^{59}\text{Mn} \rightarrow$		$^{59}\text{Fe} \rightarrow$	
pt	$\log \beta^+$	$\log \epsilon^-$	$\log \nu$	$\log \beta^-$	$\log \epsilon^+$	$\log \nu$	$\log \bar{\nu}$	$\log \beta^+$	$\log \epsilon^-$	$\log \nu$	$\log \beta^-$	$\log \epsilon^+$	$\log \bar{\nu}$
1	-2.001	-5.364	-1.718	-54.008	-26.912	-27.478	-27.478	-63.209	-32.536	-33.108	-1.012	-6.727	-0.645
2	-1.904	-2.921	-1.528	-16.877	-10.742	-10.755	-10.755	-20.455	-12.345	-12.414	-0.884	-3.626	-0.447
3	-0.972	-0.453	0.408	-3.914	-3.388	-2.683	-2.683	-5.978	-2.814	-2.329	1.425	0.033	2.059
4	2.451	5.487	7.164	1.056	4.653	6.268	6.268	1.812	4.797	6.419	2.478	5.404	7.072
5	-2.001	-1.581	-0.923	-54.024	-32.731	-33.297	-33.297	-63.209	-26.716	-27.288	-1.058	-12.546	-0.720
6	-1.902	-1.452	-0.789	-16.890	-12.457	-12.469	-12.469	-20.454	-10.629	-10.698	-0.915	-5.331	-0.491
7	-0.969	-0.358	0.488	-3.918	-3.485	-2.761	-2.761	-5.975	-2.715	-2.231	1.422	-0.060	2.046
8	2.451	5.487	7.164	1.055	4.653	6.267	6.267	1.812	4.797	6.419	2.478	5.404	7.072
9	-2.001	5.102	6.293	-99.999	-99.999	-99.999	-99.999	-63.209	4.665	5.781	-94.405	-99.999	-95.002
10	-1.902	5.105	6.297	-48.258	-50.934	-48.403	-48.403	-20.454	4.667	5.785	-31.493	-43.808	-31.633
11	-0.955	5.121	6.326	-13.774	-15.392	-13.484	-13.484	-5.962	4.683	5.813	-8.095	-11.950	-7.804
12	2.578	6.172	7.866	0.615	3.929	5.540	5.540	1.905	5.498	7.132	2.060	4.685	6.348

$^{59}\text{Ni} \rightarrow$		$^{59}\text{Co} \rightarrow$		$^{59}\text{Co} \rightarrow$		$^{59}\text{Ni} \rightarrow$		$^{59}\text{Cr} \rightarrow$		$^{59}\text{Cr} \rightarrow$		$^{59}\text{Mn} \rightarrow$	
pt	$\log \beta^+$	$\log \epsilon^-$	$\log \nu$	$\log \beta^-$	$\log \epsilon^+$	$\log \nu$	$\log \bar{\nu}$	$\log \beta^+$	$\log \epsilon^-$	$\log \nu$	$\log \beta^-$	$\log \epsilon^+$	$\log \bar{\nu}$
1	-8.044	-8.261	-8.079	-12.713	-11.645	-12.126	-12.126	-78.742	-49.573	-50.153	-0.088	-6.723	0.566
2	-5.710	-4.591	-4.348	-7.348	-6.218	-6.076	-6.076	-25.655	-18.012	-18.100	-0.136	-3.761	0.532
3	-2.686	-1.150	-0.548	-1.544	-2.019	-0.884	-0.884	-7.112	-4.442	-3.971	1.309	-0.574	2.060
4	2.827	5.292	6.967	0.686	4.715	6.339	6.339	2.695	4.899	6.598	1.977	4.670	6.286
5	-8.044	3.845	-3.935	-15.308	-17.464	-15.947	-15.947	-78.742	-43.754	-44.333	-0.096	-12.542	0.552
6	-5.701	-3.037	-2.796	-7.664	-7.930	-7.315	-7.315	-25.654	-16.296	-16.385	-0.143	-5.465	0.521
7	2.827	-1.052	-0.453	-1.552	-2.114	-0.933	-0.933	-7.109	-4.343	-3.873	1.308	-0.667	2.055
8	-8.044	5.088	6.286	-99.999	-99.999	-99.999	-99.999	2.695	4.899	6.598	1.977	4.670	6.286
9	-5.701	5.090	6.290	-42.317	-46.408	-42.478	-42.478	-78.742	4.222	5.236	-77.257	-99.999	-77.852
10	-2.680	5.102	6.311	-12.126	-14.012	-11.900	-11.900	-25.654	4.225	5.268	-25.847	-43.943	-25.979
12	2.920	5.979	7.669	0.225	3.991	5.612	5.612	2.788	5.583	7.295	1.581	3.950	5.562

TABLE 3—Continued

$^{59}\text{Cr} \rightarrow ^{59}\text{V}$				$^{59}\text{V} \rightarrow ^{59}\text{Cr}$				$^{60}\text{Ni} \rightarrow ^{60}\text{Co}$				$^{60}\text{Co} \rightarrow ^{60}\text{Ni}$			
pt	$\log \beta^+$	$\log \epsilon^-$	$\log \nu$	$\log \beta^-$	$\log \epsilon^+$	$\log \bar{\nu}$		pt	$\log \beta^+$	$\log \epsilon^-$	$\log \nu$	$\log \beta^-$	$\log \epsilon^+$	$\log \bar{\nu}$	
1	-82.554	-55.369	-55.950	0.005	-6.774	0.713		1	-26.954	-21.762	-22.231	-4.766	-8.365	-4.753	
2	-26.995	-20.066	-20.156	0.063	-3.709	0.781		2	-12.307	-8.013	-7.985	-3.151	-4.561	-2.793	
3	-7.557	-5.165	-4.639	1.583	-0.429	2.374		3	-3.429	-1.428	-0.888	-0.759	-1.484	-0.146	
4	2.261	4.629	4.609	2.355	4.820	6.450		4	2.916	5.253	6.926	0.954	4.717	6.347	
5	-82.654	-49.550	-50.130	0.000	-12.594	0.704		5	-26.954	-16.314	-16.769	-5.092	-14.184	-5.165	
6	-26.994	-18.350	-18.441	0.058	-5.414	0.773		6	-12.280	-6.348	-6.307	-3.221	-6.268	-2.875	
7	-7.553	-5.066	-4.600	1.582	-0.522	2.370		7	-3.426	-1.330	-0.790	-0.765	-1.578	-0.182	
8	2.261	4.629	6.310	2.355	4.820	6.450		8	2.916	5.253	6.926	0.954	4.717	6.347	
9	-82.654	3.885	4.859	-71.685	-99.999	-72.279		9	-26.954	5.052	6.234	-99.999	-99.999	-99.999	
10	-26.994	3.886	4.862	-23.903	-43.891	-24.033		10	-12.280	5.054	6.237	-36.937	-44.746	-37.092	
11	-7.537	3.910	4.906	-6.177	-12.410	-5.839		11	-3.415	5.074	6.269	-11.146	-13.473	-10.909	
12	2.356	5.317	7.011	1.972	4.096	5.723		12	3.001	5.944	7.631	0.499	3.994	5.620	
$^{60}\text{Zn} \rightarrow ^{60}\text{Cu}$				$^{60}\text{Cu} \rightarrow ^{60}\text{Zn}$				$^{60}\text{Fe} \rightarrow ^{60}\text{Mn}$				$^{60}\text{Mn} \rightarrow ^{60}\text{Fe}$			
pt	$\log \beta^+$	$\log \epsilon^-$	$\log \nu$	$\log \beta^-$	$\log \epsilon^+$	$\log \bar{\nu}$		pt	$\log \beta^+$	$\log \epsilon^-$	$\log \nu$	$\log \beta^-$	$\log \epsilon^+$	$\log \bar{\nu}$	
1	-2.290	-5.313	-2.132	-27.583	-24.510	-25.074		1	-41.074	-12.026	-12.194	-7.364	-8.542	-7.586	
2	-2.086	-2.919	-1.716	-12.084	-10.692	-10.713		2	-13.943	-5.838	-5.863	-2.269	-4.067	-2.126	
3	-0.552	-0.302	0.634	-4.290	-3.841	-3.095		3	-4.237	-0.777	-0.235	-0.151	0.206	1.049	
4	2.846	5.650	7.340	0.510	4.564	6.168		4	2.115	5.022	6.665	0.154	5.269	6.912	
5	-2.290	-1.585	-0.956	-29.727	-30.329	-30.292		5	-41.074	-7.390	-7.682	-8.458	-14.362	-8.840	
6	-2.084	-1.455	-0.813	-12.696	-12.407	-12.362		6	-13.943	-4.136	-4.160	-2.388	-5.773	-2.311	
7	-0.550	-0.207	0.705	-4.296	-3.938	-3.175		7	-4.234	-0.679	-0.137	-0.169	0.112	0.960	
8	2.846	5.651	7.341	0.510	4.564	6.168		8	2.115	5.022	6.665	0.154	5.269	6.912	
9	-2.290	5.250	6.466	-99.999	-99.999	-99.999		9	-41.074	5.048	6.289	-99.999	-99.999	-99.999	
10	-2.084	5.251	6.469	-48.349	-50.885	-48.502		10	-13.943	5.049	6.292	-39.448	-44.251	-39.659	
11	-0.540	5.265	6.495	-14.480	-15.842	-14.199		11	-4.222	5.059	6.310	-11.311	-11.783	-10.805	
12	2.964	6.333	8.040	0.060	3.838	5.440		12	2.207	5.715	7.374	-0.326	4.547	6.185	
$^{60}\text{Ni} \rightarrow ^{60}\text{Cu}$				$^{60}\text{Cu} \rightarrow ^{60}\text{Ni}$				$^{60}\text{Fe} \rightarrow ^{60}\text{Mn}$				$^{60}\text{Mn} \rightarrow ^{60}\text{Fe}$			
pt	$\log \beta^+$	$\log \epsilon^-$	$\log \nu$	$\log \beta^-$	$\log \epsilon^+$	$\log \bar{\nu}$		pt	$\log \beta^+$	$\log \epsilon^-$	$\log \nu$	$\log \beta^-$	$\log \epsilon^+$	$\log \bar{\nu}$	
1	-2.107	-5.501	-1.733	-36.142	-32.856	-33.418		1	-84.932	-54.800	-55.380	-0.447	-7.089	0.211	
2	-1.942	-2.968	-1.512	-14.848	-11.678	-11.700		2	-26.735	-19.005	-19.093	-0.316	-3.935	0.353	
3	-1.029	-0.553	0.308	-3.536	-3.099	-2.359		3	-6.831	-4.815	-4.339	0.970	-1.074	1.762	
4	2.536	5.651	7.336	0.966	4.660	6.267		4	2.745	4.952	6.641	2.291	4.645	6.273	
5	-2.107	-1.725	-1.059	-39.416	-38.676	-39.213		5	-84.932	-48.981	-49.560	-0.455	-12.908	0.197	
6	-1.940	-1.504	-0.831	-15.658	-13.393	-13.415		6	-26.735	-17.290	-17.377	-0.322	-5.639	0.342	
7	-1.027	-0.458	0.386	-3.540	-3.196	-2.434		7	-6.828	-4.716	-4.242	0.969	-1.167	1.758	
8	2.536	5.651	7.336	0.966	4.660	6.267		8	2.745	4.952	6.641	2.291	4.645	6.272	
9	-2.107	5.085	6.270	-99.999	-99.999	-99.999		9	-84.932	4.189	5.156	-72.177	-99.999	-72.770	
10	-1.940	5.091	6.279	-49.144	-51.871	-49.289		10	-26.735	4.194	5.163	-24.804	-44.117	-24.934	
11	-1.016	5.104	6.303	-13.329	-15.102	-13.044		11	-6.815	4.222	5.215	-6.792	-13.055	-6.452	
12	2.668	6.334	8.036	0.528	3.935	5.539		12	2.832	5.639	7.340	1.909	3.921	5.546	

TABLE 3—Continued

		$^{60}\text{Mn} \rightarrow ^{60}\text{Cr}$				$^{60}\text{Cr} \rightarrow ^{60}\text{Mn}$			
pt		$\log \beta^+$	$\log \epsilon^-$	$\log \nu$	$\log \beta^-$	$\log \epsilon^+$	$\log \bar{\nu}$		
1		-63.191	-34.452	-35.025	-0.802	-6.697	-0.383		
2		-21.293	-13.660	-13.738	-0.236	-3.412	0.320		
3		-6.234	-3.138	-2.660	1.593	0.193	2.230		
4		2.189	4.758	6.429	1.688	4.848	6.480		
5		-63.191	-28.632	-29.206	-0.834	-12.516	-0.437		
6		-21.292	-11.944	-12.023	-0.250	-5.116	0.298		
7		-6.230	-3.039	-2.561	1.590	0.100	2.217		
8		2.189	4.758	6.429	1.688	4.848	6.480		
9		-63.191	4.363	5.481	-92.827	-99.999	-93.424		
10		-21.292	4.365	5.484	-30.295	-43.594	-30.436		
11		-6.217	4.380	5.512	-7.913	-11.789	-7.623		
12		2.290	5.447	7.132	1.258	4.125	5.754		

		$^{60}\text{Cr} \rightarrow ^{60}\text{V}$				$^{60}\text{V} \rightarrow ^{60}\text{Cr}$			
pt		$\log \beta^+$	$\log \epsilon^-$	$\log \nu$	$\log \beta^-$	$\log \epsilon^+$	$\log \bar{\nu}$		
1		-99.999	-78.364	-78.846	0.187	-6.968	1.022		
2		-33.477	-26.792	-26.886	0.306	-3.843	1.147		
3		-8.792	-7.349	-6.848	1.130	-1.324	2.053		
4		2.670	4.798	6.511	2.420	4.589	6.185		
5		-99.999	-72.544	-73.126	0.185	-12.787	1.017		
6		-33.476	-25.076	-25.171	0.304	-5.547	1.143		
7		-8.788	-7.250	-6.753	1.129	-1.417	2.051		
8		2.670	4.798	6.512	2.420	4.588	6.184		
9		-99.999	3.086	3.826	-48.787	-99.999	-49.379		
10		-33.476	3.093	3.840	-17.203	-44.024	-17.327		
11		-8.771	3.164	3.970	-4.724	-13.304	-4.362		
12		2.759	5.477	7.206	2.089	3.862	5.457		

		$^{60}\text{V} \rightarrow ^{60}\text{Ti}$				$^{60}\text{Ti} \rightarrow ^{60}\text{V}$			
pt		$\log \beta^+$	$\log \epsilon^-$	$\log \nu$	$\log \beta^-$	$\log \epsilon^+$	$\log \bar{\nu}$		
1		-84.885	-58.806	-59.387	0.601	-6.150	1.310		
2		-28.583	-21.649	-21.741	0.681	-3.084	1.409		
3		-8.654	-6.030	-5.567	2.082	0.021	2.892		
4		1.770	4.228	5.920	2.221	4.746	6.359		
5		-84.885	-52.987	-53.568	0.595	-11.969	1.300		
6		-28.583	-19.934	-20.026	0.677	-4.788	1.401		
7		-8.650	-5.931	-5.469	2.081	-0.072	2.889		
8		1.770	4.228	5.921	2.221	4.746	6.359		
9		-84.885	3.213	4.164	-68.193	-99.999	-68.786		
10		-28.583	3.217	4.170	-22.261	-43.266	-22.390		
11		-8.633	3.245	4.222	-5.443	-11.959	-5.101		
12		1.874	4.912	6.619	1.843	4.021	5.632		

NOTE.—Rates β^+ , ϵ^- , β^- , ϵ^+ are in s^{-1} . Neutrino energy loss rates ν and $\bar{\nu}$ are in MeV s^{-1} . Base 10 logarithms are presented.

energies and the Coulomb correction factors (cf. eqs. [I-3a], [I-3b], [I-5b] and Gove and Martin 1971, p. 208) which require approximations in actual calculations. Some authors use the tables of $\log f$ by Gove and Martin (1971), others use approximate f -factor formulae; some authors use f -factors appropriate for first forbidden transitions (denoted with subscript 1 in Lederer *et al.* 1978), while others use only allowed phase space factors. In short, the $(\log ft)$ -values tabulated in Endt and van der Leun (1978) and Lederer *et al.* (1978) are in some cases calculated by methods unknown to us. The f -factors in our stellar rate program are calculated as accurately as possible, using detailed numerical integrations, but these are not applicable if the published $(\log ft)$ -values have been calculated using an unknown approximation to f .

In order to resolve this problem insofar as possible, $(\log ft)$ -values were recalculated for cases where the appropriate lowest temperature-density point stellar rate differed from the terrestrial rate by more than 30% ($\Delta \log \gtrsim 0.1$). The lowest temperature-density point stellar rates presented on the magnetic tape and in this paper differ from the terrestrial decay rates, where known, by no more than 30%, except, as noted, in the case of electron capture.

An example of a reaction where the $(\log ft)$ -values were adjusted in this manner is the $^{51}\text{Sc} \rightarrow ^{51}\text{Ti}$ electron emission transition. Several $(\log ft)$ -values were measured for this and presented in Lederer *et al.* (1980): from the ^{51}Sc ground state ($J^\pi = 7/2^-$) to state 3 ($7/2^-$) of ^{51}Ti , $\log ft = 5.5$; to state 5 ($5/2^-$), $\log ft = 5.0$. In addition, the ground state to state 4 ($5/2^-$) transition is clearly allowed, yet no branch was observed, so that this transition was assigned $\log ft = 99.9$. When the lowest temperature-density point stellar rate calculation was performed, the electron emission result was $\log \beta^- = 1.059$, $\sim 50\%$ faster than the known terrestrial decay rate (from the lifetime), namely, $\log \beta^- = 1.2536$. The rate for the ground state to state 3 transition was adjusted to $\log ft = 5.9$, while the rate for the ground state to state 5 was adjusted to $\log ft = 5.3$. When the

stellar rates were recalculated, the lowest temperature-density point result became $\log \beta^- = -1.261$, in agreement with the terrestrial rate to better than 2%. This type of procedure was repeated whenever the calculated rate differed from the terrestrial value by 30% or more. This procedure guaranteed that the input data used in the calculations described in this paper are consistent with measurements of terrestrial decay rates.

Table 3 presents the results of the stellar weak rate calculations for free nucleons and the nuclei in Table 1 on an abbreviated temperature and density grid (Table 2) for $\log(\rho/\mu_e) = 3, 7, 11$ and for $T_9 = 1, 3, 10, 100$. The notation and format of these rate tables are similar to those in F²NI, but the entries presenting the temperature and density are replaced with a single entry (1 to 12) describing a temperature-density combination listed in Table 2.

The remaining columns in Table 3 are the logarithm of the positron emission rate, $\log \beta^+$, the logarithm of the continuum electron capture rate, $\log \epsilon^-$, the logarithm of the total ν -energy loss rate (in MeV s^{-1}), $\log \nu$, the logarithm of the electron emission rate, $\log \beta^-$, the logarithm of the continuum positron capture rate, $\log \epsilon^+$, and finally the logarithm of the total $\bar{\nu}$ energy loss rate (in MeV s^{-1}), $\log \bar{\nu}$. It is again emphasized that this rate table is reproduced on a wide mesh temperature and density grid designed only to provide active investigators with a readily accessible means for estimating stellar nuclear weak rates. For accurate calculations involving stellar evolution or nucleosynthesis problems readers are urged to write MJN and request the stellar weak rate magnetic tape.

We would like to thank W. D. Arnett, H. A. Bethe, G. E. Brown, S. E. Koonin, T. A. Weaver, and S. E. Woosley for encouragement and useful discussions. G. Bertsch and S. D. Bloom provided helpful advice on Gamow-Teller collective phenomenon. The hospitality of A. N. Cox, the Los Alamos National Scientific Laboratory, and the Lawrence Livermore National Laboratory is gratefully acknowledged.

REFERENCES

- Arnett, W. D., and Thielemann, F. K. 1981, in preparation.
 Baym, G., Bethe, H. A., and Brown, G. E. 1981, preprint.
 Cosner, K., and Truran, J. W. 1981, University of Illinois preprint.
 Endt, P. M., and van der Leun, C. 1973, *Nucl. Phys.*, **A214**, 1.
 Fowler, W. A., and Hoyle, F. 1964, *Ap. J. Suppl.*, **9**, 201.
 Fuller, G. M. 1982, *Ap. J.*, **252**, 741.
 Fuller, G. M., Fowler, W. A., and Newman, M. J. 1980, *Ap. J. Suppl.*, **42**, 447.
 ———. 1982, *Ap. J.*, **252**, 715.
 Gleit, C. E., Tang, C. W., and Coryell, C. D. 1968, *Nucl. Data Sheets*, **13**, 5.
 Gove, N. B., and Martin, M. J. 1971, *Nucl. Data Tables*, **10**, 205.
 Iben, I., Jr., Kalata, K., and Schwarz, J. 1967, *Ap. J.*, **150**, 1001.
 Lederer, D. M., *et al.* 1978, *Tables of Isotopes*, ed. C. M. Lederer and V. S. Shirley (New York: Wiley and Sons).
 Salpeter, E. E., and Van Horn, H. M. 1969, *Ap. J.*, **155**, 183.
 Seeger, P. A., and Howard, W. M. 1975, *Nucl. Phys.*, **A238**, 491.
 Van Riper, K. A., and Lattimer, J. M. 1981, preprint.
 Weaver, T. A., and Woosley, S. E. 1981, in preparation.

Note added in proof.—We have neglected changes in Q_n due to Coulomb plasma effects. In the plasma a nucleus has its binding energy increased due to interactions with the dense electron gas. In the standard strong—screening, Wigner-Seitz approximation this extra binding is given by (see Salpeter and Van Horn 1969)

$$Q_{\text{Coul}} = (1.764 \times 10^{-5}) Z^{5/3} (\rho/\mu_e)^{1/3} \text{MeV},$$

where Z is the nuclear charge and ρ/μ_e (in g cm^{-3}) is defined in the text. Because of the charge dependence of this binding, the effective nuclear Q -value, Q_n , changes at high density. In general, the electron capture Q -value will increase by

$$\Delta Q_n \approx (2.940 \times 10^{-5}) Z^{2/3} (\rho/\mu_e)^{1/3} \text{ MeV},$$

where Z is the charge of the parent nucleus. This is to be compared with the electron Fermi energy (for $\rho/\mu_e \gtrsim 10^8 \text{ g cm}^{-3}$)

$$W_F \approx 5.155 \times 10^{-3} (\rho/\mu_e)^{1/3} \text{ MeV}.$$

The ratio of ΔQ_n to the electron Fermi energy W_F is independent of density in the strong-screening approximation and is given by

$$\frac{\Delta Q_n}{W_F} \approx 5.703 \times 10^{-3} Z^{2/3} \text{ MeV}.$$

This ratio is at most 0.06 for the largest nuclear charge considered in this paper, $Z = 30$. We conclude that Coulomb plasma changes in the nuclear masses represent negligible effects in the nuclear weak interaction rates in comparison to other uncertainties in the problem. These uncertainties include the total strength and excitation energy of the Gamow-Teller resonances which dominate the rates at high W_F where ΔQ_n is largest and the low-lying discrete Gamow-Teller strength distributions which dominate the rates for low W_F where ΔQ_n is smallest.

We have also neglected the change in energy of highly excited nuclear states relative to the ground state due to Coulomb plasma effects. At low densities where the experimentally determined discrete states dominate the reaction rates these effects are small. At high densities the Gamow-Teller resonances dominate the reaction rates. Because of the collective nature of these resonances, the Coulomb plasma effects will be small.

WILLIAM A. FOWLER: W. K. Kellogg Radiation Laboratory 106-38, California Institute of Technology, Pasadena, CA 91125

GEORGE M. FULLER: W. K. Kellogg Radiation Laboratory 106-38, California Institute of Technology, Pasadena, CA 91125

MICHAEL J. NEWMAN: Applied Theoretical Physics Division, MS 220, Los Alamos National Laboratory, PO Box 1663, Los Alamos, NM 87545